Synthesis and bioactivity of novel histone acetylation inhibitors

Ghizzoni, Massimo

SYNTHESIS AND BIOACTIVITY OF NOVEL HISTONE ACETYLATION INHIBITORS

Potential new drugs for treatment of cancer and inflammation

MASSIMO GHIZZONI

The research project described in this thesis was carried out in the Department of Pharmaceutical Gene Modulation, Groningen Research Institute of Pharmacy, according to the requirements of the Graduate School of Science (Faculty of Mathematics and Natural Sciences, University of Groningen).

Publication of this thesis was financially supported by the University of Groningen.

Layout and cover design: Massimo Ghizzoni

Printing: Off Page, Amsterdam

ISBN: 978-90-367-5191-9

ISBN: 978-90-367-5190-2 (electronic version)

RIJKSUNIVERSITEIT GRONINGEN

SYNTHESIS AND BIOACTIVITY OF NOVEL HISTONE ACETYLATION INHIBITORS

Potential new drugs for treatment of cancer and inflammation

Proefschrift

ter verkrijging van het doctoraat in de
Wiskunde en Natuurwetenschappen
aan de Rijksuniversiteit Groningen
op gezag van de
Rector Magnificus, dr. E. Sterken,
in het openbaar te verdedigen op
vrijdag 9 december 2011
om 16:15 uur

door

Massimo Ghizzoni
geboren op 25 september 1981
te Lagonegro (PZ), Italië

Promotor:	Prof. dr. H.J. Haisma
Copromotor	Dr. F.J. Dekker

Beoordelingscommissie:	Prof. dr. R.P.H. Bischoff
	Prof. dr. R.M.J. Liskamp
	Prof. dr. A.J. Minnaard

Contents

CHAPTER 1

INTRODUCTION AND SCOPE OF THE THESIS

Based on: Ghizzoni M, Haisma HJ, Maarsingh H, Dekker FJ;

Drug Discovery Today (2011) 16: 504-511

EPIGENETICS

Although most of the cells in an organism have the same genome, they clearly present different gene expression patterns according to their functions. This is an evidence of the fact that cell function depends not only on genetic properties, but also on mechanisms of regulation of gene expression. Gene regulation is of critical importance, not only for cell differentiation, but also for normal cellular homeostasis and survival. Cells can indeed adapt to environmental changes by turning on and off the expression of specific genes in response to certain stimuli. Regulation of gene expression occurs at different levels, from DNA to transcription and translation, and involves various mechanisms including chemical and structural alternation of DNA, recruitment of transcription factors and mRNA processing.

Epigenetic modifications have been recognized as an important factor in controlling gene transcription. The term epigenetics was originally coined by C.H. Waddington in 1940s.[1] Over the years, several definitions have been proposed and the term epigenetic has been used in various senses. Today, epigenetics can be defined as the study of reversible heritable changes in gene function that occur without a change in the sequence of nuclear DNA.[2] Epigenetic modifications control gene expression in a potentially heritable but still reversible way. This allows cells to perpetuate information and at the same time be responsive to environmental changes. The two major epigenetic mechanisms are methylation of DNA and posttranslational modifications of chromatin-associated proteins, specifically, histones (figure 1.1). DNA methylation is generally associated with gene repression, whereas histone modifications can have both repressive and activating functions.[3] The importance of epigenetics for cellular development and homeostasis is reflected by the observation that alterations of epigenetic events play a key role in the pathogenesis of human diseases. Proteins controlling epigenetic events are therefore of increasing interest in drug discovery.

HISTONE ACETYLTRANSFERASES

The organization of the eukaryotic DNA into chromatin allows its packaging into the cell nucleus and plays an important role in regulation of gene expression. The fundamental repeating unit of chromatin is the nucleosome (figure 1.1), which consists of 147 base pairs of DNA wrapped around an octameric histone core containing two copies of each of the four histone proteins (H2A, H2B, H3 and H4).[4]

Histones are subject to a wide variety of posttranslational modifications, such as methylation, acetylation, phosphorylation and ubiquitination.[5] These posttranslational modifications modify histones-DNA interactions and change the chromatin structure to expose promoter regions for binding of transcription factors. Furthermore, they mediate specific interactions with multiprotein complexes, which initiate or inhibit gene transcription.[6]

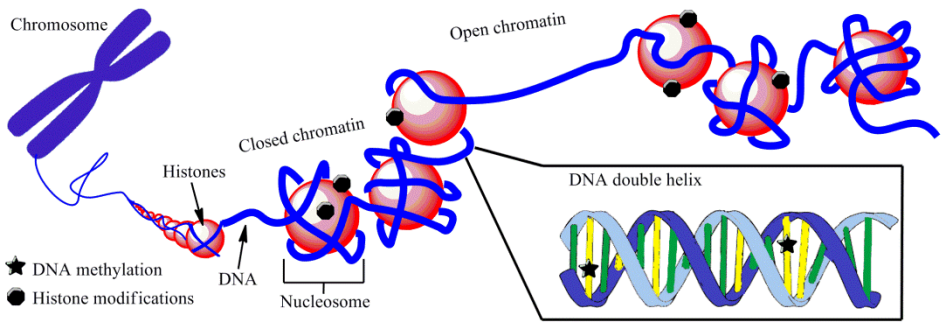

Figure 1.1: *epigenetic modifications and chromatin packing.*

Histone acetylation has been recognized as an important epigenetic control mechanism in gene expression. Reversible acetylation of histones is modulated by the activity of histone acetyltransferases (HATs) and histone deacetylases (HDACs). These enzymes catalyze the introduction or removal of acetyl groups from ε-amino functionalities of specific lysine residues, respectively. Interestingly, many HATs and HDACs are also active on non-histone protein substrates.

HATs are classified based on their cellular localization in nuclear HATs (type A) and cytoplasmic HATs (type B).[7] Whereas little is known about cytoplasmic HATs, several nuclear HATs have been identified and divided into three major families based on their primary structure homology: the GNAT (GCN5-related N-acetyltransferase) family, represented by GCN5 (general control nonderepressible 5) and PCAF (p300/CBP associated factor); the p300/CBP family, including p300 and CBP (CREB binding protein); the MYST family, which includes Tip60 (TAT interacting protein 60) and MOZ (monocytic leukemia zinc finger protein). Although other nuclear HAT families have been identified, they have not been studied extensively.

ROLE OF HATS IN INFLAMMATION

Inflammation is a physiological response, triggered by physical, biological or chemical stimuli, that is necessary for cell survival. Under certain circumstances, however, the inflammatory response is inappropriate or excessive, which leads to a pathological state. Abnormal and chronic inflammatory responses have been associated with various diseases including asthma, cancer, diabetes and neurodegenerative diseases. It has been demonstrated clearly that post-translational modifications of proteins play a crucial role in regulating the intensity, the duration and the specificity of inflammatory responses.

Role of acetylation in NF-κB-mediated inflammation

The nuclear factor κB (NF-κB) transcription factors encompass a family of inducible transcription factors that play a critical role in the expression of numerous genes that are involved in immune and inflammatory responses and in cell survival.[8]

NF-κB transcription factors exist in homo- or heterodimeric complexes consisting of different members of the Rel family proteins. The most prevalent and best studied of these complexes is the p50-p65 heterodimer. In resting cells, p50-p65 is present in the cytoplasm in an inactive form, bound to inhibitory proteins, known as IκBs (figure 1.2). Upon stimulation by specific inducers such as inflammatory cytokines (tumor necrosis factor, interleukin-1), bacterial products (lipopolysaccharide) or oxidative stress (H_2O_2), the IκBs are phosphorylated, ubiquitinated, and degraded. Degradation of IκBs results in the release of the p50-p65 dimer, which is free to translocate into the nucleus. Subsequently, the transcription factor p50-p65 binds to κB target promoters and activates expression of specific genes. Due to the central role of NF-κB in inflammation, the NF-κB pathway has been recognized as a target for therapeutic intervention.

Acetylation of NF-κB complex

Several regulatory mechanisms control the NF-κB response to specific stimuli. Among these, post-translational modifications play an important role and regulate different functions of NF-κB. Post-translational modifications mutually influence each other, which results in a complex pattern of modifications that determine the output and the duration of responses upon specific stimulations of NF-κB. Recently, it has been described that acetylations of specific lysine residues of NF-κB subunits play distinct roles in the regulation of its transcriptional capacity, its DNA-binding ability and duration of its action (figure 1.2).

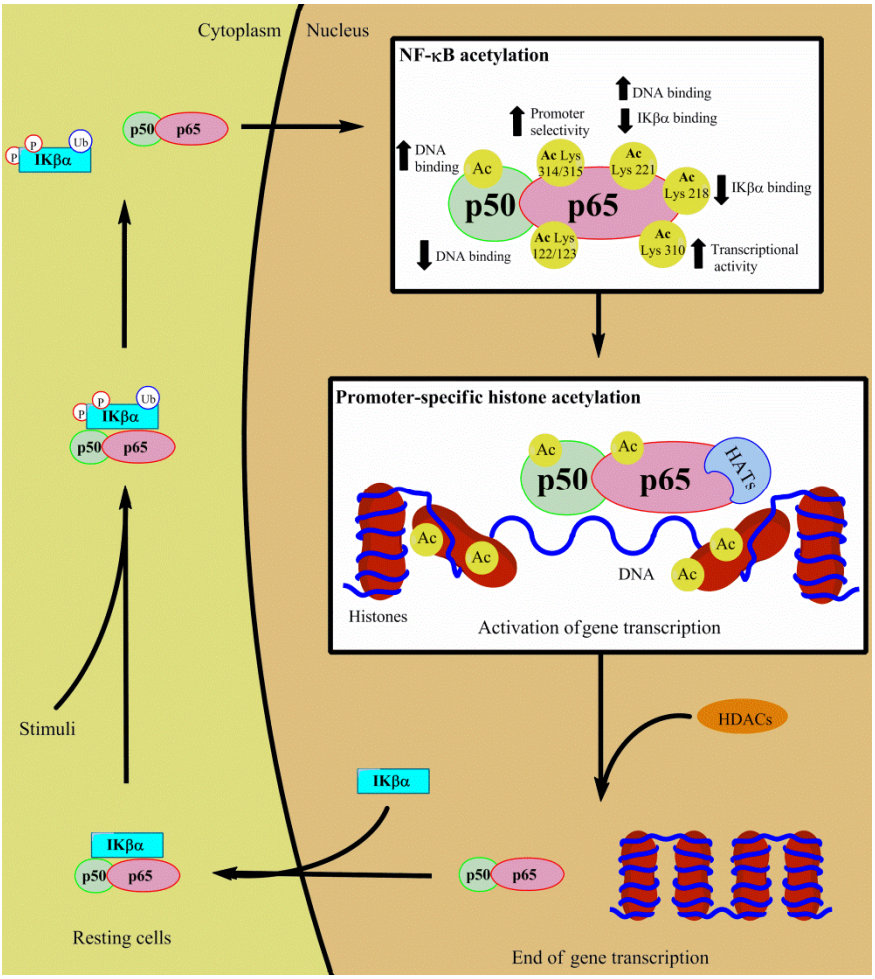

Figure 1.2: *acetylation plays an important role in NF-κB mediated inflammation. In resting cells, the p50-p65 subunits are present in the cytoplasm in an inactive form, bound to the inhibitory protein Ikβα. Upon stimulation Ikβα is phosphorylated, ubiquitinated, and degraded. The p50-p65 dimer is released and translocates into the nucleus, where both subunits are acetylated at different positions. Acetylations of the p50-p65 dimer regulate its transcriptional capacity, its DNA-binding ability and the duration of its action. The p50-p65 subunits recruit HATs to the target genes. Gene-specific histone acetylations by HATs change the chromatin structure to expose promoter regions for binding of p50-p65.*

It has been shown that the p65 NF-κB subunit (also known as RelA) is acetylated at specific sites by different HATs. Chen *et al.* reported acetylation at lysine residues 218, 221 and 310 by the HATs p300 and CBP.[9] Acetylation at Lys 221 increases the binding affinity of the NF-κB complex to the DNA κB enhancer. Furthermore, acetylation at Lys 221, alone or in combination with Lys 218, impairs

assembly of NF-κB with newly synthesized IκBα, which extends the duration of the NF-κB activity. On the contrary, deacetylation by HDAC3 stimulates IκBα binding, which promotes NF-κB export from the nucleus to the cytoplasm.[10] Acetylation at Lys 310 is required for full transcriptional activity of p65, but does not affect the DNA binding or its assembly with IκBα. In a subsequent study, it was shown that acetylation on this position provides a binding site for binding of the bromodomain of the transcriptional coactivator Brd4.[11] Recent work by Yang *et al.* showed that acetylation at Lys 310 enhances the transcriptional activity of p65 by impairing the methylation of lysine residues 314 and 315, which is important for the ubiquitination and degradation of chromatin-associated p65.[12] The HDAC SIRT1 deacetylates p65 at Lys 310 and thus terminates NF-κB dependent gene expression.[13] Thus, acetylations of NF-κB on residues 218, 221 and 310 increase its transcriptional activity.

In contrast, acetylation at other positions decreases the NF-κB transcriptional activity. Acetylation on the lysine residues 122 and 123 by both p300 and PCAF reduce binding of NF-κB to the DNA κB enhancer and facilitate binding to IκBα and subsequent export from the cytoplasm.[14] Others acetylations have no direct effect on transcriptional activity. Acetylation at lysine residues 314 and 315 by p300 do not affect the general transcriptional activity of the NF-κB complex.[15,16] Nevertheless, these acetylations modulate the expression of specific sets of genes, which indicate that site-specific acetylations of p65 regulate the specificity of the NF-κB dependent gene expression.

The p50 subunit of NF-κB is also subject to stimulus-induced acetylation. *In vitro*, p50 is acetylated at lysine residues 431, 440 and 441.[17] It has been shown that acetylation by p300 increases binding of p50 to the DNA and enhances the transcriptional activation by NF-κB.[18]

Further evidence for the importance of direct acetylations of NF-κB subunits as regulatory mechanisms is the observation that diverse cofactors are able to regulate NF-κB transactivation by modulating p50/p65 acetylation levels. For example, the transcriptional repressor Daxx impairs the transcriptional activity of NF-κB by binding to p65 and interferes with its acetylation.[19] In contrast, the transcription coactivator Stat3 maintains constitutive NF-κB activity in inflammation-induced cancers by promoting p300-mediated acetylation of the p65 subunit.[20]

Taking these data together it is concluded that direct acetylation and deacetylation of specific lysine residues in the p50 and p65 subunits of NF-κB play a crucial role in the regulation of different NF-κB functions. Acetylations on different

sites have different effects on NF-κB transcriptional activity and NF-κB dependent gene expression. Several studies show that inhibition of deacetylation extents NF-κB transcriptional activity in response to specific stimuli, whereas other studies demonstrate that inhibition of deacetylation decreases NF-κB transcriptional activity.[8,21,22] This indicates that the resulting effect of both HAT and HDAC inhibition depends on the selectivity for specific NF-κB acetylation sites. The critical role of NF-κB acetylation and deacetylation in the regulation of NF-κB mediated gene expression raises the idea to modulate inflammatory responses by modulating NF-κB acetylation levels with HAT and HDAC inhibitors. It has been shown that NF-κB acetylations are mediated by the HATs such as p300, CBP and PCAF, which indicates that small molecule inhibitors of these HATs will modulate NF-κB signaling via direct inhibition of NF-κB acetylation as well as via modulation of histone acetylation.

Acetylation of co-activators of NF-κB

Several cofactors that are involved in the regulation of the NF-κB transactivation are subject to direct acetylations by HATs. These acetylations modulate their interactions with the NF-κB subunits. Such acetylations have been described for Poly(ADP-ribose) polymerase-1 (PARP-1), Stat1 and the glucocorticoid receptors. PARP1 is a coactivator of NF-κB that has been demonstrated to play a role in inflammatory disorders. PARP-1 is acetylated upon inflammatory stimulation on specific lysine residues by p300 and CBP and deacetylated by HDACs 1-3.[22] Acetylation of PARP-1 is required for the interaction with p50, which results in coactivation of NF-κB in response to inflammatory stimuli. Stat1 is a transcription factor that is able to modulate NF-κB activity. Acetylation of Stat1 by HATs, such as CBP, results in binding to the p65 subunit of NF-κB and consequently reduction of NF-κB signalling.[23] The action of glucocorticoids involves acetylation of the glucocorticoid receptor. The deacetylated form of the glucocorticoid bound glucocorticoid receptor is able to suppress NF-κB activity.[24]

Acetylation of histones in NF-κB mediated gene transcription

Dynamic acetylation and deacetylation of histones play an important role in the regulation of gene transcription resulting from activation of the NF-κB pathway. Upon DNA binding the NF-κB subunits are able to recruit HATs and HDACs to the target gene promoter in order to change the acetylation profiles of the histones. It has been shown that the transcriptional activation domain of p65 interacts with both the N-terminal and C-terminal domain of the HATs CBP and p300.[25] These HATs function as co-activator for gene transcription. It has been demonstrated that the

presence of HATs, such as CBP, p300 and PCAF, at the gene promoter is essential for NF-κB-mediated gene expression.[26] In contrast, it has also been shown that p65 interacts with HDACs, such as HDAC-1 and SIRT6, which function as repressors of gene transcription by deacetylating histones at promoters of NF-κB target genes.[27,28]

The importance of promoter-specific histone acetylation by HATs has been demonstrated for many NF-κB target genes (table 1.1). HATs are involved in gene transcription of granulocyte-macrophage colony-stimulating factor (GM-CSF), which is a protein that is involved in physiological and pathological inflammatory processes. IL-1β stimulates GM-CSF production through activation of the NF-κB pathway. The GM-CSF production is associated with increased acetylation at Lys 8 and 12 of histone H4 connected to the GM-CSF promoter.[29] Another example is CCL11 (also known as eotaxin-1), which is an eosinophil chemo-attractant with relevance in allergic diseases such as asthma. CCL11 transcription is increased upon stimulation with TNF-α. NF-κB is the key transcription factor for CCL11. In the TNF-α-induced CCL11 transcription, PCAF is recruited, upon phosphorylation, to the CCL11 promoter. PCAF increases histone H4 acetylation at Lys 5 and 12, which promotes the p65 association with the DNA and the transcription of CCL11 gene. Histone H4 acetylation is markedly reduced after treatment with β_2-agonists and glucocorticoids. This suggests that one of the mechanisms of actions of these medicines is indirect decrease of histone acetylation, which inhibits inflammatory gene transcription.[30,31]

IL-6 is another important mediator of inflammatory responses. Overexpression of CBP and p300 potentiate basal and TNF-α induced IL-6 promoter activation via interactions with the NF-κB subunit p65. A similar mechanism is proposed for the endothelial leukocyte adhesion molecule (ELAM), which is another NF-κB-dependent promoter.[32] Interferon-γ-inducible protein-10 (CXCL10) is a chemokine implicated in the pathophysiology of asthma and COPD. Stimulation of asthmatic airway smooth muscle cells with TNF-α or IFN-γ induces recruitment of CBP and acetylation of histone H4, but not H3 at the CXCL10 promoter, which consequently increases its transcriptional activity.[33] Another gene that is expressed upon inflammatory stimulation is E-selectin. E-selectin is an adhesion molecule that is rapidly expressed by endothelial cells activated upon inflammatory stimulation. Induction of E-selectin gene expression by TNF-α is associated with hyperacetylation of histones H3 and H4 connected to the E-selectin promoter by the HATs PCAF and p300.[34] Another gene whose expression is induced in response to inflammation is cyclooxygenase 2 (COX-2). Transactivation of COX-2 gene expression involves selective hyperacetylation of histone H4 connected to the COX-2 promoter in a stimulus-specific manner. Stimulation with bradykinin causes acetylation at Lys 5,

8, and 16 whereas stimulation with IL-1ß causes only acetylation at Lys 8.[35] This demonstrates that specific stimuli induce a distinct histone acetylation pattern, which regulates distinct gene transcription patterns in response to specific inflammatory stimuli.

Table1.1: *promoter-specific hyperacetylation of NF-κB-dependent genes.*

Gene	*Stimulus*	*Cell type*	*Acetylation site*	*HAT involved*	*Ref.*
GM-CSF	IL-1ß	A549	Histone H4 Lys 8, 12	unknown	26
Eotaxin-1	TNF-α	HASMC	Histone H4 Lys 5, 12	PCAF	28
Interleukin-8	Legionella	Human lung epithelial	Histone H3 Lys 14 Histone H4	p300/CBP	33
	Listeria	HUVEC	Histone H3 Lys 14, Histone H4 Lys 8	CBP	34
	LPS	HUT-78, Jurkat, monocytes	Histone H4	unknown	35
	H_2O_2, PM_{10}	A549	Histone H4	unknown	36
Interleukin-6	TNF-α	L929sA HEK293T	Global histone acetylation	p300/CBP	29
ELAM	TNF-α	L929sA HEK293T	Global histone acetylation	p300/CBP	29
CXCL10	TNF-α, INF-γ	ASM	Histone H4	CBP	30
E-selectine	TNF-α	HUVECs	Histone H3 Lys 9, 14 Histone H4 Lys 5, 8, 12	PCAF, p300	31
Cox-2	Bradykinin	ASM	Histone H4 Lys 5, 8, 16	unknown	32
	IL-1ß	ASM	Histone H4 Lys 8	unknown	32

Histone acetylation in IL-8 gene expression

Histone acetylation plays an important role in the activation of interleukin 8 (IL-8) gene expression in immune responses triggered by bacterial infections. For example, IL-8 expression in *Legionella pneumophila* infected lung cells involves increased recruitment of p300 and CBP, as well as enhanced acetylation of histones H3 and H4

at the IL-8 gene promoter.[36] The same is observed upon infection by intracellular *Listeria monocytogenes*, which also induces acetylation of histone H3 and H4 at the IL-8 promoter, which consequently increases IL-8 expression. In contrast, *Listeria*-induced IFN-γ gene expression does not require changes in the histone acetylation at the IFN-γ promoter. Furthermore, the HDAC inhibitor Trichostatin A increases *Listeria*-induced expression of IL-8, but not of IFN-γ induced IL-8 expression. This demonstrates that histone acetylation regulates the gene expression patterns in response to specific stimuli.[37] Another stimulus that increases IL-8 expression is LPS. LPS-induced IL-8 gene transcription is associated with acetylation of histone H4 at the IL-8 promoter. Interestingly, glucocorticoids suppress IL-8 expression, which is accompanied by reduction of histone acetylation of the IL-8 promoter.[38] In contrast, IL-8 expression and release is also increased upon oxidative stress induced by H_2O_2 and environmental particulate matter (PM_{10}). It has been shown that H_2O_2 and PM_{10} augment the intrinsic HAT activity in alveolar epithelial cells leading to increased histone H4 acetylation at the IL-8 gene promoter.[39] These findings demonstrate that IL-8 expression is positively correlated with histone acetylation and that the importance of histone acetylation for IL-8 expression depends on the input stimulus.

Role of acetylation in inflammatory diseases

Asthma and COPD

Inflammatory lung diseases, like asthma and COPD (chronic obstructive pulmonary disease) are associated with the expression of multiple inflammatory genes in the lungs. Increasing evidence demonstrates that the balance between HAT and HDAC activity is altered in these diseases. A recent study showed significant reduction of HDAC activity and increased HAT activity in peripheral blood mononuclear cells of children with allergic asthma. The intensity of these alterations was positively correlated to bronchial hyperresponsiveness.[40] In another study, it has been shown that bronchial biopsies from subjects with asthma contain reduced HDAC 1 and 2 expression and decreased HDAC activity. In contrast, HAT activity was increased, although no difference in expression of HATs (PCAF and CBP) was found.[41] Furthermore, it has been found that HAT activity is increased and HDAC activity is decreased in alveolar macrophages of subjects with asthma compared to healthy subjects.[42] The HAT activity was reduced to normal levels in patient that were treated with glucocorticoids, which indicates that glucocorticoids regulate inflammatory responses indirectly by reduction of HAT activity.

The inflammatory lung disease COPD is also characterized by a disturbed HAT/HDAC balance. A study with lung tissue samples of COPD patients showed reduced HDAC activity and expression, and increased histone H4 acetylation at the IL-8 promoter. In contrast to asthma, HAT activity in COPD patients was not increased in comparison with healthy subjects.[43] The reduced HDAC expression and activity measured in COPD are also responsible for the steroid resistance associated with this disease.[24] Taken together, these findings indicate that a shift of the HAT/HDAC balance towards HAT activity may underlie the increased expression of inflammatory genes in inflammatory lung diseases, which is a mechanism that has been described in several review articles.[44-46] This demonstrates that inhibition of HAT activity has potential for treatment of such inflammatory diseases.

Diabetes

Inflammatory processes play a role in the pathogenesis of diabetes. This has been shown in experiments with high glucose conditions, which mimic diabetes. These experiments demonstrated activation of NF-κB-dependent gene transcription of inflammatory genes in monocytes *in vitro*. This activation proceeds through recruitment of p65 and HATs to the TNF-α and COX-2 promoters, with concomitant increases in histone H3 and H4 acetylation. Furthermore, increased histone H3 acetylation at TNF-α and COX-2 promoters has been found in human blood monocytes from type 1 and type 2 diabetic subjects in comparison with non-diabetic subjects.[47] A study in endothelial cells and vascular tissue demonstrated that glucose causes upregulation of p300 accompanied by increased histone acetylation and expression of extracellular matrix proteins and vasoactive factors. These proteins are responsible for alterations of endothelial and vascular structure and function in organs, which are affected by chronic diabetic complications.[48] These results suggest that inhibition of histone acetylation might be a valuable strategy to suppress inflammatory responses in diabetes.

Neurodegenerative diseases

Neurodegenerative diseases, such as Alzheimer's and Parkinson's disease and amyotrophic lateral sclerosis, are characterized by slow and progressive dysfunction and loss of neurons in the central nervous system. Several findings support the theory that inflammation contributes to the development of the neurodegeneration by activating chronic immune responses, in particular by microglia and astroglia. Highly activated glial cells express pro-inflammatory cytokines and chemokines that increase excito-toxicity on neurons and are responsible for neuronal apoptosis.[49,50] The inflammatory response of glial cells involves the activation of different signaling

pathways, including NF-κB, which is accompanied by histone hyperacetylation.[51-53] There are many examples in the literature of small molecules that provide protection against glial cell induced neurodegeneration by blocking the NF-κB pathway.[54,55] These findings raise the idea that HAT inhibitors could find a therapeutic application also in this field.

ROLE OF HATS IN CANCER

Epigenetic events are crucial in the onset and progression of numerous cancer types. The aberrant gene expression observed in cancer has been often connected to alterations of histone acetylation; however, the detailed roles of HATs are unclear. Several studies indicate that HATs act as tumor suppressors. On the contrary, increasing evidences suggest a role as tumor promoters. For example, it has been shown that p300 plays a major role in prostatic cancer cell proliferation. High levels of p300 in biopsies from patients with prostatic cancer are predictive for larger tumor volumes and aggressive cancer progression.[56] A marked increase in p300 mRNA levels has been detected in patient with colorectal cancer and correlated with poor prognosis.[57] Bandyopadhyay *et al.* showed that downregulation of p300 activity resulted in activation of a senescence checkpoint in human melanocytes, which suggests that p300 could be a potential target for novel approaches in the treatment of melanoma.[58]

Other HAT family enzymes have also been described to play a role in cancer manifestation. The HAT MOZ forms fusion genes by chromosome translocation with p300 in acute myeloid leukemia. The fusion transcript has two acetyltransferase domains and could be involved in leukemogenesis through aberrant regulation of histone acetylation.[59] It has been described that Tip60 and PCAF are overexpressed in cisplatin-resistant cells and that knockdown of Tip60 expression renders cells sensitive to cisplatin.[60] Cancer cells overexpressing PCAF showed resistance also to other chemotherapeutic agents. Downregulation of PCAF sensitized cells to chemotherapeutic agents and induced cell cycle arrest and apoptosis.[61] These results suggest that PCAF and Tip60 are critical for cancer cells and represent potential targets for cancer treatment.

In addition, HATs are linked to cancer through their crucial functions in cell cycle progression. For example, CBP and p300 have an essential function during the G1/S transition and are required for cell proliferation.[62,63] It has been shown that acetylation of cyclin A by PCAF is essential in order to allow mitosis progression.[64]

Acetylation of the cell-division cycle (CDC)-6 protein by GCN5 seems to be crucial for proper S-phase progression during the cell cycle.[65]

Changes in global levels of histone acetylation are often associated with different type of cancer. Seligson *et al.* described high levels of acetylation at Lys 18 of histone H3 and Lys 12 of histone H4 in tissue samples from patients with prostate cancer.[66] It has been shown that histones H3 and H4 are hyperacetylated in hepatocellular carcinoma cells compared with cirrhotic and normal livers cells.[67] Histone H3 has been described to be highly acetylated in oral squamous cell carcinoma patient samples.[68] The commonly observed hyperacetylation in cancer suggests that small molecule inhibitors of HATs have potential to suppress cancer development.

Acetylations of non-histone target proteins play an important role in cancer development. The transcription factor c-MYC is one of the most frequently overexpressed oncogenes in human cancer. Acetylation of c-MYC by either GCN5/PCAF or Tip60 increases protein stability, contributing to cancer progression.[69] In a similar way, acetylation of androgen receptor by p300, PCAF or Tip60 is critical for prostate cancer cell growth.[70,71]

Taken together, these studies indicate that, in certain circumstances, increased HAT activity is associated with cancer development. HATs inhibitors could serve as tools to unravel the detailed functions of HATs in cancer and might ultimately lead to therapeutic applications.

HAT INHIBITORS

Small molecule HAT inhibitors that are subtype selective and cell-permeable are essential tools to evaluate the role of HATs in inflammation and cancer. Several classes of HAT inhibitors have been described. The most potent and selective HAT inhibitors are the so-called bisubstrate inhibitors, which include both the histone peptide and CoA (figure 1.3). These inhibitors are remarkably selective and potent but their lack of cell-permeability limits their applicability.[72,73] High-throughput screening led to the identification of isothiazolones as potent HAT inhibitors.[74] It has been suggested that the chemical reactivity of these compounds might be important for their mechanism of action. It is likely that isothiazolone covalently capture a cysteine thiol group in the HAT active site. This property could be employed for the development of probes for activity-based protein profiling (ABBP). However, a better knowledge of isothiazolone structure-activity relationship is necessary to develop them as ABPP probes for HATs.

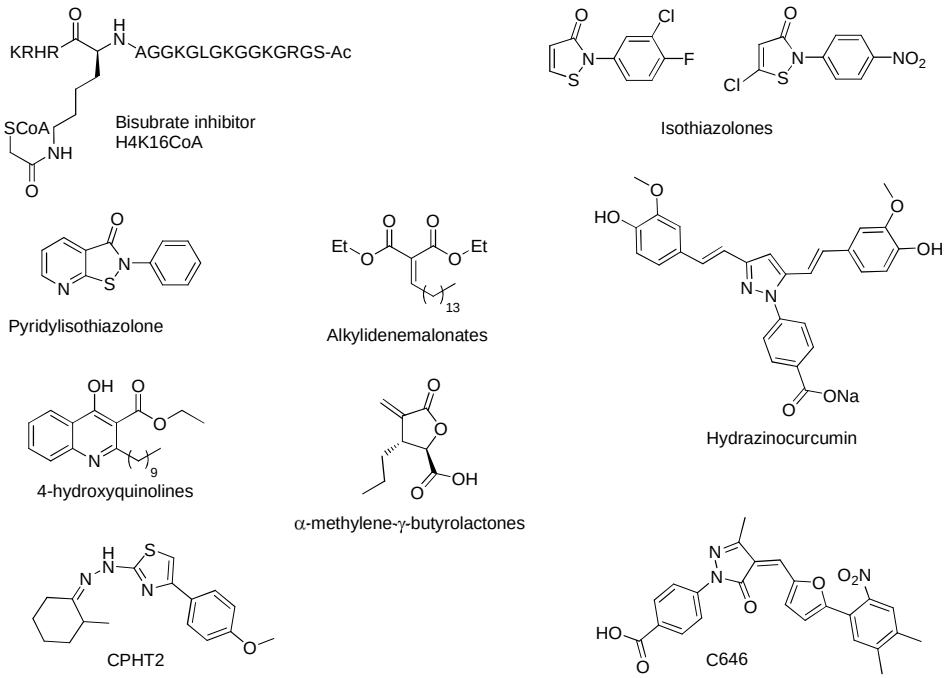

Figure 1.3: *synthetic inhibitors of histone acetyltransferases.*

Recently, a promising HAT inhibitor (C646) was discovered using a virtual ligand screening.[75] This compound is a potent and selective inhibitor of p300 and it is able to reduce histone acetylation and cancer cell growth. Alkylidenemalonates, 4-hydroxyquinolines and α-methylene-γ-butyrolactones have also been described to inhibit HAT activity. Unfortunately, the low potency and specificity has limited their applications in cell-based studies.[76,77]

The screening of natural products has led to the identification of several HAT inhibitors (figure 1.4). Interestingly, these compounds originate from plants known in the traditional medicine to have anti-inflammatory effects. For example, anacardic acid (AA) has been described as inhibitor of the HATs p300/CBP and PCAF.[78] AA is also known to possess anti-inflammatory properties. Sung *et al.* reported that AA inhibits acetylation of p65, and suppresses both inducible and constitutive NF-κB activation with consequent reduction of NF-κB-dependent gene expression. The down-regulation of p300 by siRNA abrogated the effects of AA on the NF-κB pathway, which suggests that the HAT inhibitory effect is essential for the anti-inflammatory properties of this compound.[79]

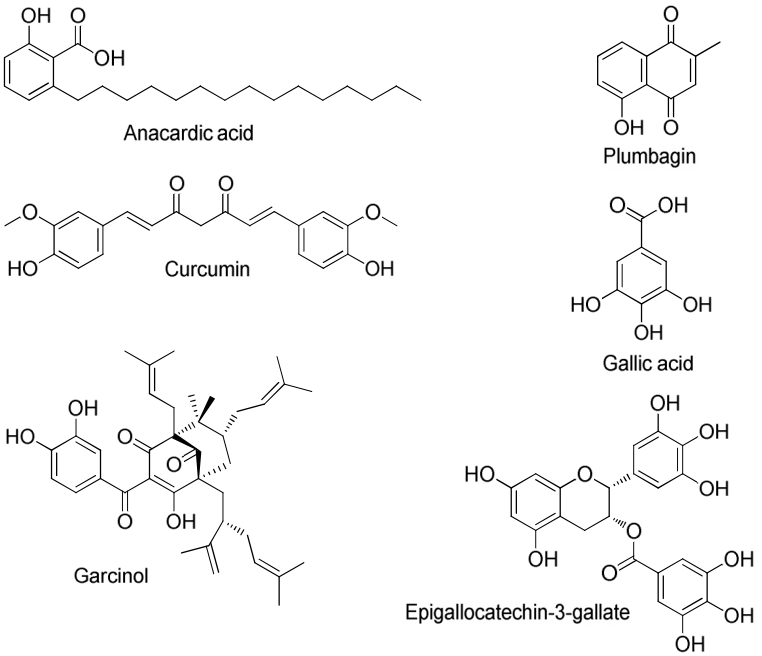

Figure 1.4: *natural product inhibitors of histone acetyltransferases.*

Another natural product, which has recently been described to inhibit the HAT p300, is Plumbagin.[80] Plumbagin also suppresses NF-κB activation induced by different inflammatory stimuli and down-regulates NF-κB-dependent gene expression.[81] Interestingly, the intensively investigated natural product Curcumin is an inhibitor of p300/CBP.[82] Its synthetic derivative hydrazinocurcumin (figure 1.3), inhibits HATs also.[68] Curcumin reduces NF-κB activation induced by a variety of stimuli and down-regulates NF-κB dependent expression of many inflammatory genes via suppression of TNF-α-induced p65 acetylation.[83] Furthermore, the natural products Gallic acid and Epigallocatechin-3-gallate also possess anti-inflammatory properties. Recently, these compounds were described as non-selective inhibitors of HATs.[84,85] They suppress p65 acetylation and abrogate NF-κB activation in response to different inflammatory stimuli. It should, however, be noted that Epigallocatechin-3-gallate also inhibits phosphorylation of several proteins like for example MAP kinases.[86] Finally, the natural product Garcinol is a potent inhibitor of p300 and PCAF and also possesses anti-inflammatory properties.[87] It has been showed that Garcinol inhibits constitutive and induced NF-κB activity and down-regulates NF-κB-dependent genes.[88] Microarray analysis showed that Garcinol inhibited the expression of many disease related genes.[89] Taking these data together

it is tempting to speculate that the anti-inflammatory and HAT inhibitory properties of these natural products are directly connected. However, the development of selective inhibitors for HAT isoenzymes that could specifically downregulate expression of distinct genes, remain a major challenge.

SCOPE OF THE THESIS

HATs have been extensively studied in recent years and an increasing number of functions in cell physiology and pathology have been identified. Nevertheless, the detailed roles and interactions of HAT isoenzymes remain to be elucidated. Small molecule modulators of HAT activity are effective tools to investigate cellular HAT functions and their implications for pathology. Furthermore, these molecules represent starting points for the design of new drugs. For example, the commonly observed hyperacetylation in inflammation demonstrates that small molecule inhibitors of HATs have potential to suppress inflammation. Moreover, several studies suggest that HAT hyperactivity may be associated with tumorigenesis and therefore it is expected that HAT inhibitors may serve as potential anticancer agents.

The currently described HAT inhibitors, however, suffer from low potency, lack of specificity or low cell-permeability, which hampers their use in pharmacological studies. The development of novel HAT inhibitors therefore is urgently required. The aim of the studies described in this thesis is to develop potent and selective small molecule inhibitors of HATs that can effectively inhibit histone acetylation in cells. Ultimately, the aim is to provide novel probes for pharmacological and ABPP studies on HATs.

The studies described in **chapter 2** aim at the design of new covalent isothiazolone-based HAT inhibitors, which could be used as ABPP probes. In this chapter we aim to resolve the structure-activity relationships (SAR) for inhibition of HATs by isothiazolones in order to clarify the structural requirements for biological activity. For this purpose, we investigate the *in vitro* inhibitory activities of different isothiazolone derivatives on the recombinant HAT PCAF. To assess the toxicity of these compounds, we explore the growth inhibition of different cancer cell lines upon treatment with isothiazolones.

In **chapter 3** we continue our studies on isothiazolones as HAT inhibitors. We investigate new synthetic modifications of the isothiazolone ring in order to modulate its reactivity and establish whether changes in chemical reactivity are

correlated to changes in the biological properties. Furthermore, we analyze the reactivity of 5-chloroisothiazolones and 5-chloroisothiazolone-1-oxides towards thiols and thiolates to elucidate the reaction mechanism of these compounds.

The work described in **chapter 4** aims at the design on new non-covalent HAT inhibitors based on the natural product AA, which could be used as tools for pharmacological studies. Using a combination of molecular modeling and organic synthesis, new AA derivatives are developed. We investigate the *in vitro* inhibitory potency of these compounds for the recombinant HAT PCAF activity in order to resolve the SAR. Furthermore, we study the inhibition of histone acetylation in HEP G2 cells upon treatment with AA derivatives to prove their efficacy in cell-based studies.

Chapter 5 extends our investigation on AA derivatives as HAT inhibitors. We aim to develop compounds that are selective towards different recombinant HAT isoenzymes. For this purpose, we synthesized several salicylate derivatives and screen them for the *in vitro* inhibition of three different recombinant HATs. Furthermore, we aim to elucidate the HAT inhibitory mechanism of this class of compounds using enzyme kinetics studies. We also evaluate the inhibitory properties of salicylate derivatives on HAT activity of nuclear extract from cell cultures and tissue samples in order to prove their efficacy in biological samples.

In **chapter 6** the results from the studies described in this thesis are summarized and discussed, together with future perspectives.

CHAPTER 2

INHIBITION OF THE PCAF HISTONE ACETYLTRANSFERASE AND CELL PROLIFERATION BY ISOTHIAZOLONES

Dekker FJ, Ghizzoni M, van der Meer N, Wisastra R, Haisma HJ;

Bioorganic & Medicinal Chemistry (2009) 17: 460–466

Abstract

Small molecule HAT inhibitors are useful tools to unravel the role of histone acetyl transferases (HATs) in the cell and have relevance for oncology. We present a systematic investigation of the inhibition of the HAT p300/CBP Associated Factor (PCAF) by isothiazolones with different substitutions. 5-chloroisothiazolones proved to be the most potent inhibitors of PCAF. The growth inhibition of 4 different cell lines was studied and the growth of two cell lines (A2780 and HEK 293) was inhibited at micromolar concentrations by 5-chloroisothiazolones. Furthermore, the 5-chloroisothiazolone preservative Kathon™ CG that is used in cosmetics inhibited PCAF and the growth of cell lines A2780 and HEK 293, which indicates that this preservative should be applied with care.

INTRODUCTION

Posttranslational modifications of histone proteins play a crucial role in gene-specific transcription regulation in eukaryotes.[90] These histone modifications occur in distinct patterns that mediate specific interactions with multiprotein complexes, which initiate or inhibit gene transcription via the so-called 'histone-code'.[91-93] There is increasing evidence that the histone code plays a crucial role in normal and aberrant cell function and differentiation. Small molecule modulators of histone modifying enzymes are useful tools to unravel the functions of these enzymes and might ultimately lead to therapeutic applications.

The histone acetyltransferases (HATs) form a disparate group of enzymes that mediate acetyl transfer to histones or other proteins.[7,94] The GNAT (Gcn5 related N-acetyltransferase) family HATs include the closely related enzymes PCAF (p300/CBP associated factor) and GCN5 (general control of amino-acid synthesis 5).[95] PCAF acetylates histone H3 on lysine 14 and less efficiently histone H4 on lysine 8.[96] The GNAT family HATs have been recognized as potential anticancer and antiviral targets.[94,97] The HAT GCN5 plays a key role in EGF mediated gene transcription, which is relevant for cancer therapy.[98] Furthermore, GCN5 is crucial for cell cycle progression [99].Deregulation of the activity of GNAT and p300 family HATs plays an important role in a number of human cancers.[100,101]

Despite the potential therapeutic relevance of the GNAT family HATs, very few small molecule inhibitors for GCN5 and PCAF have been described so far. Lau *et al.* described bisubstrate inhibitors for p300 and PCAF by coupling the histone H3 peptide to CoA.[72] However, this provided compounds with poor membrane permeability. The natural products Curcumin, Garcinol and Anacardic acid show HAT inhibitory activity, however their potency is low.[78,82,87] GCN5 and PCAF are inhibited by α-methylene-γ-butyrolactones and isothiazolones, which covalently capture the active site thiol of these enzymes.[74,102]

The isothiazolones provide an interesting starting point for structure based design of PCAF and GCN5 inhibitors. The isothiazolone functionality is readily available via organic synthesis and can easily be decorated with diverse substitutions to enhance binding to the enzyme active site.[103] The crystal structure and the catalytic mechanism of GCN5 and PCAF provide inspiration for inhibitor design.[104-107] The crystal structure of the enzyme GCN5 in complex with a bisubstrate inhibitor shows that the pyrophosphate and the pantothenic acid moiety make extensive hydrogen bonding interactions with the enzyme.[108] The same is

observed in the crystal structure of the enzyme PCAF in complex with CoA (PDB entry 1CM0).[104] This suggests that hydrogen bonding interactions are relevant for binding to the enzyme active site. Thus, inhibitors with hydrogen bond donor/acceptors may show improved binding to the enzyme active site.

In this study we investigated structure activity relationships for inhibition of the enzyme PCAF by isothiazolones. The (5-chloro)isothiazolone scaffold was used to target the active site thiol and the substitution was explored to enhance binding by providing specific interactions with the enzyme. A series of 19 compounds was synthesized and tested for inhibition of PCAF activity. 5-Chloroisothiazolones showed the most potent inhibition of PCAF. 5-Chloroisothiazolone **2e** showed a slightly increased potency compared to the other 5-chloroisothiazolones. Cell lines A2780 and HEK 293 showed growth inhibition upon treatment with micromolar concentrations N-aliphatic substituted 5-chloroisothiazolones, whereas the cell lines WiDr and HEP G2 were much less affected.

RESULTS AND DISCUSSION

Chemistry

A collection of N-functionalized isothiazolones was synthesized using procedures shown in Scheme 2.1.[103,109-111] Different amines were reacted with 3,3′-dithiodipropanoyl chloride **1** to give the dithiodipropionic amides in moderate to high yields. The dithiodipropionic amides were treated with sulfuryl chloride (3 equiv) at 0 ºC in dichloromethane to give the 5-chloroisothiazolones **2** and isothiazolones **3** in ratios between 3:1 and 2:1, which were readily separated using column chromatography. 5-chloroisothiazolones were obtained in yields between 50% and 70% and isothiazolones were obtained in yields around 20% from the same reaction mixture. Surprisingly, **2d** yielded only 23% of the 5-chloroisothiazolone and the corresponding isothiazolone could not be isolated from the same reaction mixture. 5-Chloroisothiazolone **2e** was oxidized by mCPBA to yield 5-chloroisothiazolone-1-oxide **4e**.[109] Treatment of 5-chloroisothiazolone **2e** with $POCl_3$ and ammonia provided 5-chloroisothiazol-3-amine **5e**.[103] 4-acylamino-isothiazolone **7e** was obtained using a modified procedure published by Nádel *et al.*[111] Cbz protected L-Cystin **6** was coupled to an amine HCl-salt using DCC, HOBt and triethylamine as a base followed by treatment with sulfuryl chloride to yield the 4-carbamoyl-5-chloroisothiazolone **7e**.

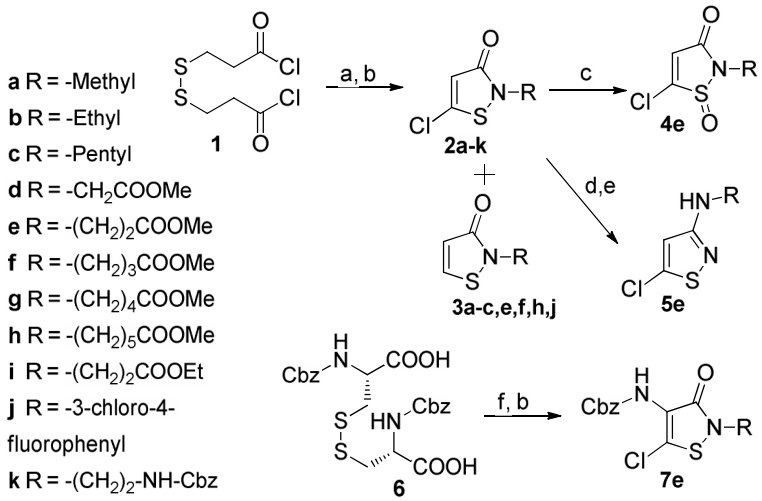

***Scheme 2.1**: synthesis of a focused compound collection. Reagents and conditions: (a) R-NH_2, Et_3N, CH_2Cl_2, (b) SO_2Cl_2, CH_2Cl_2, (c) mCPBA, CH_2Cl_2, (d) $POCl_3$, (e) NH_3, CH_3CN, (f) DCC, HOBt, Et_3N, R-$NH_3^+Cl^-$, CH_2Cl_2.*

Structure–activity relationships for PCAF inhibition

Structure–activity relationships for inhibition of the HAT PCAF by a series of (5-chloro)isothiazolones were investigated in order to explore the binding properties of these compounds (table 1.1). Binding studies were performed using a procedure published by Trievel *et al.*[112] The enzyme activity was measured by detection of CoA-SH by the fluorescent dye 7-(diethylamino)-3-(4'-maleimidylphenyl)-4-methylcoumarin (CPM). The CoA-SH concentrations measured with no inhibitor present were around 50 µM. Enzyme inhibition was measured by determination of the residual enzyme activity after 15 min incubation with the inhibitor. The inhibitor concentrations were maximal 10 µM, so inhibitory effects of more than 20% at 10 µM inhibitor concentration cannot be explained by direct reaction of the inhibitors with CoA-SH, but result from inhibition of the enzyme. Compounds that showed more than 50% inhibition at 10 µM (n = 3) were subjected to IC_{50} determination (n = 3). A representative example is shown in figure 2.1A.

Table 2.1: *inhibition of the HAT PCAF and proliferation of cell lines by (5-chloro)isothiazolones. Inhibition concentration 50% (IC_{50}) determination n = 3, growth inhibition 50% (GI_{50}) determinations n = 8, standard deviations from the non-linear curve fitting are reported.*

	PCAF IC_{50} (μM)	*A2780 GI_{50} (μM)*	*WiDr GI_{50} (μM)*	*HEPG2 GI_{50} (μM)*	*HEK 293 GI_{50} (μM)*
2a/3a 3:1	3.0 ± 0.6	2.0 ± 0.2	5.0 ± 0.4	6.0 ± 1.2	1.4 ± 0.1
2b	3.0 ± 0.3	>10	>10	>10	5.6 ± 0.4
2c	2.9 ± 0.3	2.3 ± 0.2	>10	6.4 ± 0.2	1.7 ± 0.1
2d	2.9 ± 0.7	>10	>10	>10	>10
2e	1.8 ± 0.2	3.3 ± 0.3	7.5 ± 0.3	10 ± 1	2.8 ± 0.3
2f	2.5 ± 0.3	3.0 ± 0.4	>10	7.0 ± 0.8	1.5 ± 0.6
2g	2.8 ± 0.3	5.2 ± 0.1	>10	8.0 ± 0.4	0.7 ± 0.1
2h	3.2 ± 0.2	7.0 ± 0.8	5.6 ± 0.5	9.4 ± 0.3	2.9 ± 0.8
2i	2.0 ± 0.2	3.0 ± 0.1	>10	>10	>10
2j	2.5 ± 0.1	>10	>10	>10	>10
2k	2.6 ± 0.1	8.1 ± 0.7	>10	>10	3.0 ± 0.4
3b	>10	>10	>10	>10	>10
3c	>10	>10	>10	>10	>10
3e	>10	>10	>10	>10	>10
3f	>10	>10	>10	>10	>10
3h	>10	>10	>10	>10	>10
3j	4.2 ± 0.6	>10	>10	>10	>10
4e	5.6 ± 0.2	>10	>10	>10	>10
5e	>10	>10	8.6 ± 1.0	2.0 ± ± 0.3	4.7 ± 0.4
7e	4.9 ± 0.9	5.8 ± 0.6	>10	>10	10

The compounds were designed to evaluate the PCAF inhibition of 5-chloroisothiazolones and isothiazolones with different N-substitutions. The 5-chloroisothiazolone core with only an N-ethyl substitution **2b** shows a potent PCAF inhibition. The PCAF inhibition of **2b** is equal to the commercially available preservative Kathon™ CG **2a/3a**, which is a mixture of N-methyl-5-chloroisothiazolone and N-methylisothiazolone 3:1. An N-pentyl substitution **2c** did not improve binding compared to **2b**. A series of N-substitutions with a methyl ester at different numbers of carbon atoms distance to the (5-chloro-)isothiazolone **2d–h**

was studied. Compound **2e** showed a slightly increased potency compared to the other 5-chloroisothiazolones, which suggests that the N-substitution provides additional interaction with PCAF. Based on compound **2e** a molecular modeling was performed to suggest a binding pose to aid future optimizations of the PCAF inhibition (figure 2.2).

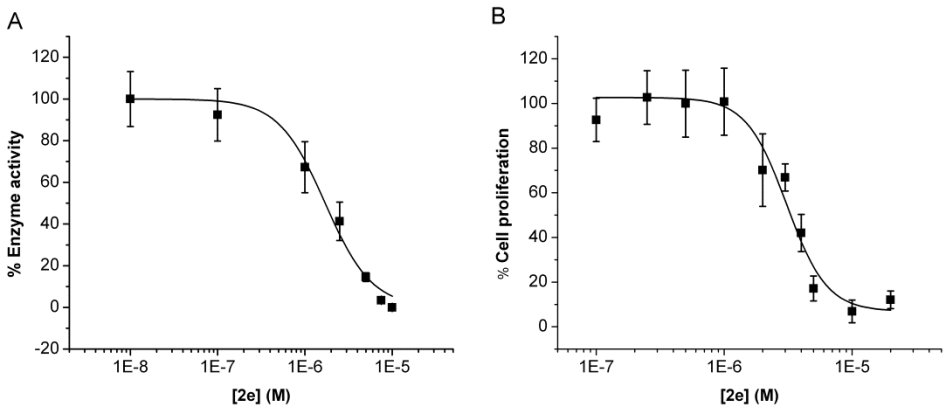

Figure 2.1: *panel A shows the concentration dependence for inhibition of the PCAF enzyme activity by 5-chloroisothiazolone 2e (n = 3, standard deviation shown) and panel B shows the concentration dependence for growth inhibition of the cell line A2780 by 2e (n = 8, standard deviation shown).*

There is a pronounced difference in potency between N-aliphatic substituted 5-chloroisothiazolones **2** and isothiazolones **3**. 5-Chloroisothiazolones **2b–i**,**k** inhibit PCAF with IC_{50} values around 2–3 µM, whereas isothiazolones **3b**,**c**,**e**,**f**,**h**, showed less than 50% inhibition at 10 µM. The difference in potency for the N-aromatic substituted 5-chloroisothiazolone **2j** and isothiazolone **3j** is much less pronounced. The same in observed in the data provided by Stimson *et al.* in which the difference in PCAF inhibitory potency between N-aromatic 5-chloroisothiazolones and isothiazolones is a factor 2 or less.[74]

Compounds with modifications directly on the isothiazolone scaffold were synthesized and the consequences for PCAF inhibition were studied. 5-chloroisothiazolone-1-oxide **4e** inhibited the PCAF activity at micromolar concentrations. The 5-chloroisothiazol-3-amine **5e** did not inhibit PCAF. Substitution of the 5-chloroisothiazolone scaffold in the 4-position with an amino acyl substituent **7e** reduced the PCAF inhibition compared to compound **2e**. Nevertheless, compound **7e** provides an interesting starting point for further optimization of the PCAF inhibition by variation of the 4-amino acyl substituent.

Reports on the reactivity of N-methylisothiazolones and N-methyl-5-chloroisothiazolones indicate a high reactivity of 5-chloroisothiazolones. 5-chloroisothiazolones are prone to nucleophilic substitution in the 5-position and reductive cleavage of the N–S bond.[113] In contrast, for isothiazolones only reductive cleavage of the N–S bond by sulfides is observed and no nucleophilic addition in the 5-position. This study supports the idea that the potent inhibition of 5-chloroisothiazolones is due to their reactivity. Interestingly, isothiazolone **3j** with a N-aromatic substitution shows an IC_{50} of 4.2 µM for PCAF inhibition. This indicates that N-aromatic isothiazolones are either more prone to nucleophilic addition in the 5-position of the isothiazolone or that they are more prone to reductive cleavage of the N–S bond, compared to N-aliphatic substituted isothiazolones.

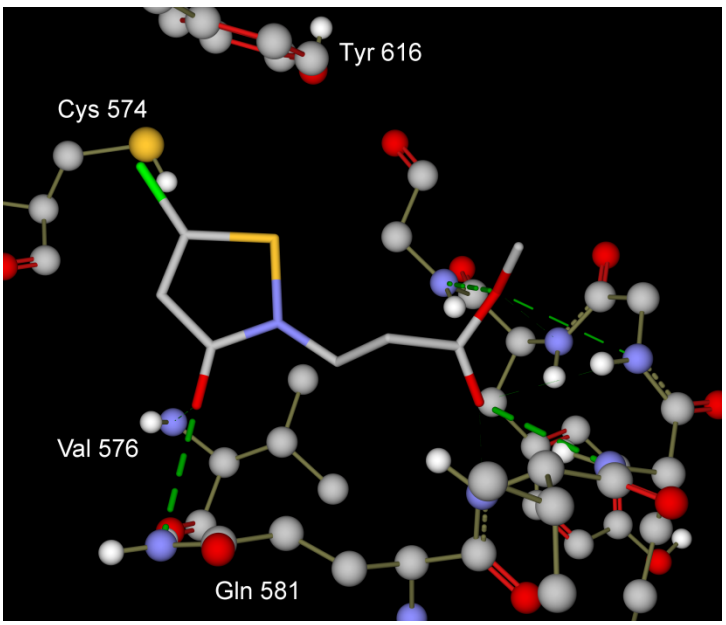

Figure 2.2: *binding pose for* ***2e*** *in the PCAF active site (PDB entry 1CM0) that was proposed by a molecular modeling study. Cys 574 is the active site cysteine. Hydrogen bonds are formed to valine 576 and Glutamine 581 and to the pyrophosphate binding pocket formed by the backbone amides of Glutamine 581,Valine 582, Lysine 583, Glycine 584 and Tyrosine 585.*

Molecular modeling

Modeling studies were performed to propose a binding pose for inhibitor **2e** to aid future optimization of the inhibitors. The crystal structure of PCAF complexed with CoA (PDB entry code 1CM0) was used for docking studies.[104] The molecular modeling study suggested a binding pose in which the methyl ester is hydrogen

bonded to a pocket in which the pyrophosphate is bound in the PCAF crystal structure 1CMO (figure 2.2). The pyrophosphate binding pocket is formed by the backbone of amides of Glutamine 581, Valine 582, Lysine 583, Glycine 584 and Tyrosine 585. The carbonyl from the 5-chloroisothiazolone is hydrogen bonded to Glutamine 581 and Valine 576. Docking of 5-chloroisothiazolone-1-oxide **4e** provided a similar binding pose as observed for **2e**. Docking of **7e** provided also a binding pose comparable to **2e**. These results suggest that the PCAF inhibitory potency of **2e**, **4e** and **7e** might be improved by variations in the substitution in the 4-position of the isothiazolone core. In conclusion, compounds **2e**, **4e** and **7e** provide starting points to design inhibitors with an improved PCAF inhibitory potency.

Growth inhibition of cell lines

Inhibition of cancer cell lines was studied in order to explore the relevance of (5-chloro)isothiazolones as research tools to study the biological mechanisms underlying cell proliferation.[114] The growth inhibition of the human cancer cell lines A2780 (ovarian), WiDr (colon) and HEP G2 (liver) and the human embryonic cell line 293 (kidney) was studied. Growth inhibition was determined using a crystal violet assay. The compounds were screened at 10 µM inhibitor concentration for growth inhibition (n = 8) and compounds with more than 50% growth inhibition were subjected to growth inhibition 50% determination (GI_{50}) (n = 8) (table 2.1). A representative example is shown in figure 2.1B. The N-aliphatic substituted 5-chloroisothiazolones are the most potent compounds for growth inhibition of cell lines A2780 and HEK 293. The growth of cell lines WiDr and HEP G2 were not inhibited or required higher concentrations for inhibition compared to cell lines A2780 and HEK 293, which might be due to differences in the growth rate or differences in cellular biochemistry. Western blots on histone acetylation in cell lines that are treated with optimized inhibitors are required to proof a connection between the PCAF HAT inhibition and the cellular activity.

It is remarkable that compounds **2j** and **3j** do not inhibit the growth of the four cell lines that were studied. This indicates that N-aromatic isothiazolones like **2j** are less potent inhibitors of cell proliferation. Compound **5e** with a 5-chloroisothiazol-3-amine scaffold showed no inhibitory effect on PCAF but shows a potent inhibition of WiDr, HEP G2 and HEK 293 cell lines. This is the first time that a biological effect is described for a compound with a 5-chloroisothiazol-3-amine scaffold.

The commercially available preservative Kathon™ CG **2a/3a** showed a potent PCAF inhibition and a potent growth inhibition of the four cell lines studied (table

2.1). This is remarkable because the mixture has been used as a preservative in rinse-off cosmetics such as shampoos and conditioners for more than 25 years. Kathon™ CG is claimed to be safe and effective, however skin sensitization have been reported.[113,115] The growth inhibition of cell lines shows that Kathon™ CG **2a**/**3a** is cell-permeable and acts on intracellular targets. The inhibition of PCAF indicates that this preservative might modify the epigenetic regulation of gene transcription. Taking these data together we conclude that Kathon™ CG should be applied with care.

CONCLUSION

In conclusion, N-aliphatic substituted 5-chloroisothiazolones inhibit the enzyme PCAF with an IC_{50} around 2–3 µM, whereas N-aliphatic substituted isothiazolones show less than 50% inhibition at 10 µM. The difference in PCAF inhibitory potency between N-aromatic substituted 5-chloroisothiazolones and isothiazolones is much less pronounced. N-Aromatic and N-aliphatic substituted 5-chloroisothiazolones showed a comparable potency for PCAF inhibition. N-Aliphatic substituted 5-chloroisothiazolones inhibited the growth of the cell lines A2780 and HEK 293 in the low micromolar range, whereas growth inhibition of WiDr and HEP G2 required higher concentrations or was not observed. N-Aromatic substituted 5-choroisothiazolones, N-aromatic and N-aliphatic substituted isothiazolones showed less than 50% inhibition of the cell proliferation at 10 µM. Finally, it has been shown that the preservative Kathon™ CG inhibits the HAT PCAF and inhibits the cell growth of A2780, WiDr, HEP G2 and HEK 293 cell lines.

EXPERIMENTAL PROCEDURES

Organic synthesis

General: Chemicals were obtained from commercial sources (Sigma–Aldrich, Acros Organics) and used without previous purification, except dichloromethane that was distilled over CaH_2 before use. Thin-layer chromatography (TLC) was performed on aluminum sheets of Silica Gel 60 F254. Spots were visualized under ultraviolet light, with I_2 vapor, $KMnO_4$ solution or ninhydrin solution. Column chromatography was performed with MP Ecochrom Silica Gel 32–63, 60 Å. ^1H and ^{13}C NMR spectra were recorded on a Varian Gemini-200 (50.32 MHz). Chemical shift values are reported as part per million (δ) relative to residual solvent peaks ($CHCl_3$, ^1H δ = 7.26, ^{13}C δ = 77.16 or CD_3OD, ^1H δ = 3.31, ^{13}C δ = 49.00). The coupling constants (*J*) are reported

in Hertz (Hz). ^{13}C spectra were recorded using the attached proton test (APT) pulse sequence. Electrospray ionization mass spectra (ESI-MS) were recorded on an Applied Biosystems/SCIEX API3000-triple quadrupole mass spectrometer. High-resolution mass spectra (HR-MS) were recorded using a flow injection method on a LTQ-Orbitrap XL mass spectrometer (Thermo Electron, Bremen, Germany) with a resolution of 60,000 at m/z 400. Protonated testosterone (lock mass m/z = 289.2162) was used for internal recalibration in real time. Melting points were determined on an Electrothermal digital melting point apparatus and are uncorrected.

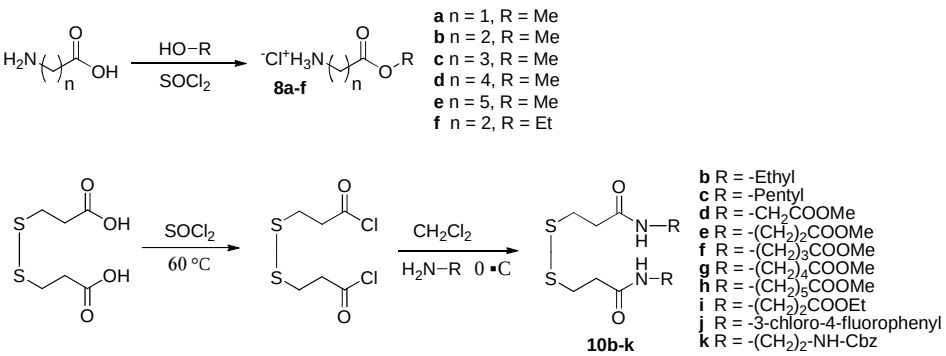

Scheme 2.2: *general procedure 2-3 and chemical structure of compounds* ***8a-f*** *and* ***10b-k****.*

General procedure 1

The dithiobispropanamide (8 mmol) was dissolved in dry CH_2Cl_2 (50 mL) at 0 ºC. SO_2Cl_2 (24 mmol) was added dropwise to the solution, and the mixture was stirred at 0 ºC for 2 h. Subsequently, the mixture was washed with water (2 times 200 mL) and brine (1 time 200 mL), dried with Na_2SO_4 and filtered. The solution was concentrated under reduced pressure and purified using column chromatography.

General procedure 2

$SOCl_2$ (30 mmol) was added dropwise to a suspension of the amino acid (25 mmol) in methanol (25 mL) at 0˚C. The mixture was stirred for 2 hours at 0˚C. The solvent was removed under reduced pressure to give the title compound.

General procedure 3

A mixture of 3,3'-dithiodipropionic acid (15 mmol) was suspended in $SOCl_2$ (10 mL). The suspension was heated to 60 ºC until the starting material dissolved and subsequently the $SOCl_2$ was distilled off leaving 3,3'-dithiodipropanoyl chloride as a dark orange oil behind. The orange oil was dried under vacuum. A mixture of amine·HCl (30 mmol) and triethylamine (66 mmol) in dry CH_2Cl_2 (100 mL) was

cooled to 0˚C and 3,3'-dithiodipropanoyl chloride was added dropwise. After 1 h. the cooling is removed and the mixture was stirred at room temperature overnight. The resulting precipitate was filtered off and the filtrate was extracted with saturated Na_2CO_3 (3 times 50 mL), 1 N HCl (3 times 50 mL), and brine (1 time 50 mL). The organic layer was dried (Na_2SO_4), and concentrated under reduced pressure to give the dithiopropionamide

5-Chloro-2-ethylisothiazol-3(2H)-one (2b)

The product was obtained using procedure 1 starting from **10b**. Purification was performed using column chromatography with hexane/EtOAc 3:1 (v/v) as eluent. Yield 46%. Brown gum. R_f = 0.44 (CH_2Cl_2/MeOH 9:1). ^{1}H NMR (200 MHz, $CDCl_3$): δ 1.32 (t, *J* = 7.2 Hz, 3H), 3.81 (q, *J* = 7.2 Hz, 2H), 6.36 (s, 1H). ^{13}C NMR (50 MHz, $CDCl_3$): δ 15.0, 39.4, 114.8, 146.3, 167.0. HPLC: purity >99%, retention time 6.6 min (column C8 mobile phase H_2O/CH_3CN/TFA 60:40:1). HRMS (*m/z*) 163.9933 $[M+H]^+$, calcd 163.9937 C_5H_7ClNOS.

2-Ethylisothiazol-3(2H)-one (3b)

After elution of **2b** product **3b** was eluted from the column using EtOAc eluent. Yield 10%. Brown gum. R_f = 0.38 (CH_2Cl_2/MeOH 9:1). ^{1}H NMR (200 MHz, $CDCl_3$) δ 1.60 (m, 3H), 3.88 (m, 2H), 6.36 (m, 1H) 8.20 (m, 1H). ^{13}C NMR (50 MHz, $CDCl_3$) δ 15.3, 39.8, 114.9, 140.4, 168.9. GC–MS purity >99%, retention time 2.69 min, (EI) $[M^+]$ *m/z* 129. HRMS (*m/z*) 130.0323 $[M+H]^+$, calcd 130.03266 C_5H_8NOS.

5-Chloro-2-pentylisothiazol-3(2H)-one (2c)

The product was obtained using procedure 1 starting from **10c**. Purification was performed using column chromatography with hexane/EtOAc 8:1 (v/v) as eluent. An extra column chromatography step was required to obtain the pure product. Yield 55%. Orange oil. R_f = 0.53 (CH_2Cl_2/MeOH 94:6). ^{1}H NMR (200 MHz, $CDCl_3$) δ 0.88 (t, *J* = 6.8 Hz, 3H), 1.24-1.38 (m, 4H), 1.59-1.73 (m, 2H), 3.71 (t, *J* = 7.3 Hz, 2H), 6.25 (s, 1H). ^{13}C NMR (50 MHz, $CDCl_3$) δ 14.1, 22.4, 28.8, 29.6, 44.0, 115.0, 145.8, 167.1. GC-MS RT 5.2 min, purity >99%, MS(EI) (*m/z*) 205, calcd 205. HRMS (*m/z*) 206.0402 $[M+H]^+$, calcd 206.04064 $C_8H_{13}ClNOS$.

2-pentylisothiazol-3(2H)-one (3c)

After elution of **2c** product **3c** was eluted from the column using hexane/EtOAc 1:1 (v/v) as eluent. An extra column chromatography step was required to obtain the pure product. Yield 25%. Brown gum. R_f = 0.29 (CH_2Cl_2/MeOH 94:6). ^{1}H NMR (200 MHz, $CDCl_3$) δ 0.89 (t, *J* = 6.5 Hz, 3H), 1.24-1.37 (m, 4H), 1.51-1.79 (m, 2H), 3.79 (t, *J* = 7.3 Hz, 2H), 6.32 (d, *J* = 6.2 Hz, 1H), 8.1 (d, *J* = 6.2 Hz, 1H). ^{13}C NMR (50 MHz,

$CDCl_3$) δ 14.2, 22.6, 28.8, 29.7, 44.5, 114.7, 139.7, 169.1. GC-MS RT 4.8 min, purity >95%, MS(EI) (*m/z*) 171, calcd 171. HRMS (*m/z*) 172.0792 $[M+H]^+$, calcd 172.0796 $C_8H_{14}NOS$.

Methyl 2-(5-chloro-3-oxoisothiazol-2(3H)-yl)ethanoate (2d)

The product was obtained using procedure 1 starting from the **10d**. Purification was performed using column chromatography with hexane/EtOAc 3:2 (v/v) as eluent. Yield 23%. Dark brown gum. R_f = 0.76 (CH_2Cl_2/MeOH 9:1). ^1H NMR (200 MHz, $CDCl_3$) δ 3.78 (s, 3H), 4.48 (s, 2H), 6.32 (s, 1H). ^{13}C NMR (50 MHz, $CDCl_3$) δ 44.1, 53.0, 112.9, 148.2, 167.3, 168.0. GC–MS rt 4.88 min, MS (EI) gave anomalous results. MS (ESI) (*m/z*) 208.0 $[M+H]^+$, calcd 208.0. HRMS (*m/z*) 207.9831 $[M+H]^+$, calcd 207.9835 $C_6H_7ClNO_3S$.

Methyl 3-(5-chloro-3-oxoisothiazol-2(3H)-yl)propanoate (2e)

The product was obtained using procedure 1 starting from **10e**. Purification was performed using column chromatography with hexane/EtOAc 1:2 (v/v) as eluent. Yield 49%. Orange oil. R_f = 0.58 (CH_2Cl_2/MeOH 10:1). ^1H NMR (200 MHz, $CDCl_3$) δ 2.67 (t, J = 6.2 Hz, 2H), 3.66 (s, 3H), 3.95 (t, *J* = 6.2 Hz, 2H), 6.19 (s, 1H). ^{13}C NMR (50 MHz, $CDCl_3$) d 33.9, 39.8, 52.3, 114.3, 147.0, 167.1, 171.8. GC– MS RT 5.97 min, purity >99%, MS(EI) (*m/z*) 221 [M], calcd 221. HRMS (*m/z*) 221.9987 $[M+H]^+$, calcd 221.9992 $C_7H_9ClNO_3S$, (*m/z*) 243.9805 $[M+Na]^+$, calcd 243.9811 $C_7H_8ClNNaO_3S$. HPLC purity >99%%, rt 5.0 min, (column C8 mobile phase H_20/CH_3CN/TFA 60:40:1).

Methyl 3-(3-oxoisothiazol-2(3H)-yl)propanoate (3e)

After elution of **2e** product **3e** was eluted from the column using hexane/EtOAc 1:20 (v/v) as eluent. Yield 23%. Brown oil. R_f = 0.49 (CH_2Cl_2/MeOH 10:1). ^1H NMR (200 MHz, $CDCl_3$) δ 2.76 (t, *J* = 6.5 Hz, 2H), 3.70 (s, 3H), 4.09 (t, *J* = 6.5 Hz, 2H), 6.31 (d, *J* = 6.4 Hz, 1H), 8.10 (d, *J* = 6.2 Hz, 1H). ^{13}C NMR (50 MHz, $CDCl_3$) δ 33.9, 40.2, 52.2, 114.2, 140.4, 169.1, 171.6. GC–MS RT 6.36 min, purity >99%, MS (EI) (*m/z*) 187 [M], calcd 187. HRMS (*m/z*) 188.0378 $[M+H]^+$, calcd 188.0381 $C_7H_9ClNO_3S$, (*m/z*) 210.01961 $[M+Na]^+$, calcd 210.0201 $C_7H_9NNaO_3S$.

Methyl 4-(5-chloro-3-oxoisothiazol-2(3H)-yl)butanoate (2f)

The product was obtained using procedure 1 starting from **10f**. Purification was performed using column chromatography with hexane/EtOAc 1:1 (v/v) as eluent. Yield 67%. Brown solid. Mp = 47.9 °C. R_f = 0.83 (CH_2Cl_2/MeOH 9:1). ^1H NMR (200 MHz, $CDCl_3$) δ 1.92–2.06 (m, 2H), 2.38 (t, *J* = 7.2 Hz, 2H), 3.66 (s, 3H), 3.78 (t, *J* = 7.1 Hz, 2H), 6.19 (s, 1H). ^{13}C NMR (50 MHz, CDCl3): δ 24.9, 30.7, 42.9, 51.9, 114.8, 146.1, 167.1, 173.0. GC–MS RT 6.69 min, purity >99%, MS(EI) (*m/z*) 235 $[M]^+$, calcd

235. HRMS (*m/z*) 236.0143 $[M+H]^+$, calcd 236.0148 $C_8H_{11}ClNO_3S$, (*m/z*) 257.9962 $[M+Na]^+$, calcd 257.9968 $C_8H_{10}ClNNaO_3S$.

Methyl 4-(3-oxoisothiazol-2(3H)-yl)butanoate (3f)

After elution of **2f** product **3f** was eluted from the column using hexane/EtOAc 1:7 (v/v) as eluent. Yield 9%. Brown oil. R_f = 0.78 (CH_2Cl_2/MeOH 9:1). ^1H NMR (200 MHz, $CDCl_3$) δ 2.02 (t, *J* = 7.1 Hz, 2H), 2.37 (t, *J* = 7.2 Hz, 2H), 3.66 (s, 3H), 3.87 (t, *J* = 7.1 Hz, 1H), 6.28 (d, *J* = 6.2 Hz, 1H), 8.1 (d, *J* = 6.2 Hz, 1H). ^{13}C NMR (50 MHz, $CDCl_3$) δ 25.1, 30.8, 43.1, 51.9, 114.8, 139.2, 173.2, 180.3. GC–MS RT time 6.36 min, purity >99%, MS (EI) (*m/z*) 201 $[M]^+$, calcd 201. HRMS (*m/z*) 202.0534 $[M+H]^+$, calcd 202.0538 $C_8H_{12}NO_3S$, (*m/z*) 224.0352 $[M+Na]^+$, calcd 224.03573 $C_8H_{11}NNaO_3S$.

Methyl 4-(5-chloro-3-oxoisothiazol-2(3H)-yl)pentanoate (2g)

The product was obtained using procedure 1 starting from **10g**. Purification was performed using column chromatography with hexane/EtOAc 3:1 (v/v) as eluent. Yield 62%. Brown oil. R_f = 0.52 (CH_2Cl_2/MeOH 94:6). ^1H NMR (200 MHz, $CDCl_3$) δ 1.60–1.90 (m, 4H), 2.35 (t, *J* = 7.2 Hz, 2H), 3.65 (s, 3H), 3.75 (t, *J* = 7.1 Hz, 2H), 6.32 (s, 1H). ^{13}C NMR (50 MHz, $CDCl_3$) δ 21.9, 29.2, 33.5, 43.7, 51.9, 114.9, 146.4, 167.3, 173.6. GC–MS RT 7.58 min, purity >99%, MS (EI) (*m/z*) 249, calcd 249. HRMS (*m/z*) 250.0300 $[M+H]^+$, calcd 250.0305 $C_9H_{13}ClNO_3S$, (*m/z*) 272.0119 $[M+Na]^+$, calcd 272.0124 $C_9H_{12}ClNNaO_3S$.

Methyl 4-(3-oxoisothiazol-2(3H)-yl)pentanoate

After elution of **2g** the product was eluted from the column using hexane/EtOAc 1:8 (v/v) as eluent. Yield 12%. Brown oil. R_f = 0.39 (CH_2Cl_2/MeOH 94:6). The compound was not pure enough for biochemical characterization and was thus excluded from the study.

Methyl 6-(5-chloro-3-oxoisothiazol-2(3H)-yl)hexanoate (2h)

The product was obtained using procedure 1 starting from **10h**. Purification was performed using column chromatography with hexane/EtOAc 3:1 (v/v) as eluent. Yield 61%. Yellow oil. R_f = 0.56 (EtOAc/hexane 6:1). ^1H NMR (200 MHz, $CDCl^3$) δ 1.30–1.42 (m, 2H), 1.56–1.71 (m, 4H), 2.29 (t, *J* = 7.2 Hz, 2H), 3.63 (s, 3H), 3.71 (t, *J* = 7.2 Hz, 2H), 6.24 (s, 1H). ^{13}C NMR (50 MHz, $CDCl_3$) δ 24.4, 26.0, 29.4, 33.8, 43.5, 51.6, 114.8, 145.7, 166.9, 173.9. GC-MS RT 8.36 min, purity >99%, MS (EI) (*m/z*) 263, calcd 263. HRMS (*m/z*) 264.0456 $[M+H]^+$, calcd 264.04612 $C_{10}H_{15}ClNO_3S$.

Methyl 6-(5-chloro-3-oxoisothiazol-2(3H)-yl)hexanoate (3h)

After elution of **2h** product **3h** was eluted from the column using hexane/EtOAc 1:5 (v/v) as eluent. Yield 25%. Yellow oil. R_f = 0.30 (EtOAc/hexane 6:1). ^{1}H NMR (200 MHz, $CDCl_3$) δ 1.30– 1.74 (m, 6H), 2.29 (t, *J* = 7.2 Hz, 2H), 3.63 (s, 3H), 3.76 (t, *J* = 7.2 Hz, 2H), 6.23 (d, *J* = 6.5 Hz, 1H), 8.04 (d, *J* = 6.5 Hz, 1H). ^{13}C NMR (50 MHz, $CDCl_3$) δ 24.5, 26.1, 29.6, 33.9, 43.8, 51.7, 114.8, 139.0, 169.0, 174.0. GC–MS RT 7.98 min, purity >99%, MS (EI) (*m/z*) 229, calcd 229. HRMS (*m/z*) 230.0846 $[M+H]^+$, calcd 230.08509 $C_{10}H_{16}NO_3S$.

Ethyl 3-(5-chloro-3-oxoisothiazol-2(3H)-yl)propanoate (2i)

The product was obtained using procedure 1 starting from **10i**. Purification was performed using column chromatography with hexane/EtOAc 2:1 (v/v) as eluent. Yield 51%. Brown solid. Mp = 73.2 ºC. R_f = 0.67 (CH_2Cl_2/MeOH 9:1). ^{1}H NMR (200 MHz, $CDCl_3$) δ 1.26 (t, *J* = 7.2 Hz, 3H), 2.70 (t, *J* = 6.2 Hz, 2H), 4.00 (t, *J* = 6.2 Hz, 2H), 4.16 (q, *J* = 7.1, 7.3 Hz, 2H), 6.24 (s, 1H). ^{13}C NMR (50 MHz, $CDCl_3$) δ 14.4, 34.2, 39.9, 61.4, 114.3, 147.1, 167.2, 171.4. GC–MS RT 6.43 min, purity >99%, MS (EI) (*m/z*) 235, calcd 235. HRMS (*m/z*) 236.0143 $[M+H]^+$, calcd 236.0148 $C_8H_{11}ClNO_3S$.

5-Chloro-2-(3-chloro-4-fluorophenyl)isothiazol-3(2H)-one (2j)

The product was obtained using procedure 1 starting from **10j**. Purification was performed using column chromatography with EtOAc/hexanes 1:10 (v/v) as eluent. Yield 62%. White solid, Mp = 116.9 °C; R_f = 0.66 (EtOAc/cyclohexane 1:1). ^{1}H NMR (200 MHz, $CDCl_3$) δ 6.36 (s, 1H), 7.10–7.21 (m, 1H), 7.43–7.36 (m, 1H), 7.63 (dd, *J* = 2.6, 6.5 Hz, 1H). ^{13}C NMR (50 MHz, $CDCl_3$) δ 114.8, 117.2, 117.6, 124.9, 125.0, 127.6, 146.5, 154.8, 159.8, 165.4. GC–MS purity >99%, RT 7.8 min, MS (EI) (*m/z*) 263, calcd 263. HRMS (*m/z*) 263.9448 $[M+H]^+$, calcd 263.9453 $C_9H_5Cl_2FNOS$.

2-(3-Chloro-4-fluorophenyl)isothiazol-3(2H)-one (3j)

After elution of **2j** product **3j** was eluted from the column using EtOAc/hexanes 1:2 as eluent. Yield 23%. Orange oil, R_f = 0.18 (EtOAc/cyclohexane 1:1). ^{1}H NMR (200 MHz, $CDCl_3$) δ 6.33 (d, *J* = 6.3 Hz, 1H), 7.10–7.21 (m, 1H), 7.47–7.41 (m, 1H), 7.68 (dd, *J* = 2.6/6.5 Hz, 1H), 8.19 (d, *J* = 6.3 Hz, 1H). ^{13}C NMR (50 MHz, $CDCl_3$) δ 114.8, 117.0, 117.5, 125.0, 127.4, 140.1, 154.7, 159.7, 167.7. GC–MS purity >95%, RT 7.7 min, MS (EI) (*m/z*) 229, calcd 229. HRMS (*m/z*) 229.9838 $[M+H]^+$, calcd 229.98427 $C_9H_6ClFNOS$.

Benzyl [2-(5-chloro-3-oxoisothiazol-2(3H)-yl)ethyl]carbamate (2k)

The product was obtained using procedure 1 starting from **10k**. Purification was performed using column chromatography with EtOAc/hexanes 3:1 (v/v) as eluent. Yield 29%. Yellow gum, R_f = 0.35 (EtOAc/hexane 3:1), ^{1}H NMR (200 MHz, $CDCl_3$) δ 3.45–3.47 (m, 2H), 3.86 (t, *J* = 6 Hz, 2H), 5.01 (s, 2H), 6.25 (s, 1H), 7.35 (m, 5H). ^{13}C NMR (50 MHz, $CDCl_3$) δ 41.1, 43.5, 66.9, 114.3, 128.1, 128.2, 128.6, 136.4, 152.4, 156.9, 160.8. HPLC purity >94%%, RT 12.3 min, (column C8 mobile phase H_20/CH_3CN/TFA 60/40/1). HRMS (*m/z*) 313.0414 $[M+H]^+$, calcd 313.0408 $C1_3H_{14}ClN_2O_3S$. (*m/z*) 335.0233 $[M+Na]^+$, calcd 335.0228 $C_{13}H_{13}ClN_2NaO_3S$.

Methyl 3-(5-chloro-1-oxido-3-oxoisothiazol-2(3H)-yl)propanoate (4e)

Compound **2e** (1 mmol) was dissolved in CH_2Cl_2 (15 mL) and *m*-chloroperbenzoic acid was added in several portions. The mixture was stirred at room temperature for 16 h. Several crystals $Na_2S_2O_3 \cdot 5H_2O$ and H_2O (5 mL) were added and the mixture was stirred for 10 min. A saturated solution of $NaHCO_3$ (50 mL) was added, this mixture was stirred for 5 min and the phases were separated. The organic layer was washed with saturated $NaHCO_3$ (50 mL), brine (50 mL) and dried with Na_2SO_4 and the solvent was evaporated under reduced pressure. The residue was purified by column chromatography with EtOAc/hexanes 1:2 as eluent. Yield 50%, yellow oil, R_f = 0.72 (EtOAc/hexane 10:1). ^{1}H NMR (200 MHz, CD_3OD) δ 2.70–2.77 (m, 2H), 3.68 (s, 3H), 3.99 (t, *J* = 6.8 Hz, 2H), 6.98 (s, 1H). ^{13}C NMR (50 MHz, $CDCl_3$) δ 34.5, 38.3, 52.4, 125.4, 158.6, 166.5, 173.7. GC–MS RT 6.1 min, purity >99%, MS (ESI) (*m/z*) 206, calcd 206 (M-OMe). HRMS (*m/z*) 237.9936 $[M+H]^+$, calcd 237.9941 $C_7H_9ClNO_4S$.

Methyl 3-[(5-chloroisothiazol-3-yl)amino]propanoate (5e)

Compound **2e** (0.74 mmol) was dissolved in $POCl_3$ (1.5 mL) and stirred overnight at room temperature. The next morning an orange-brown precipitate was observed. Isopropylether (20 mL) was added and the precipitate intensified. The suspension was centrifuged (4000 rpm, 10 min), the supernatant was discarded and the residue washed with isopropylether. Subsequently, the residue was suspended in CH_3CN (10 mL), cooled to 0 ºC and NH_3 gas was bubbled through the solution for 30 min. The red-white suspension turned into a brown solution with a white precipitate. The suspension was filtered and the filtrate was concentrated under reduced pressure and purified using column chromatography EtOAc/hexanes 1:6 as eluent. Yield 44%, Yellow solid, Mp = 73.2 °C, R_f = 0.33 (EtOAc/hexane 3:1), ^{1}H NMR (200 MHz, $CDCl_3$) δ 2.64 (t, *J* = 6.2 Hz, 2H), 3.61 (t, *J* = 5.9 Hz, 2H), 3.68 (s, 3H), 6.34 (s, 1H). ^{13}C NMR (50 MHz, $CDCl_3$) δ 33.9, 38.5, 51.9, 112.3, 151.8 163.6, 173.2. GC–MS RT 5.9 min,

purity >99%, MS (EI) (*m/z*) 220, calcd 220. HRMS (*m/z*) 221.0146 $[M+H]^+$, calcd 221.0152 $C_7H_{10}ClN_2O_2S$.

Methyl 3-[4-{[(benzyloxy)carbonyl]amino}-5-chloro-3-oxoisothiazol-2(3H)-yl] propanoate (7e)

The product was obtained using procedure 1 starting from **9**. Purification was performed using column chromatography with EtOAc/hexanes 1:1 (v/v) as eluent. Yield 70%. Off-white gum. R_f = 0.38 (EtOAc/cyclohexane 2:1). ^1H NMR (200 MHz, $CDCl_3$) δ 2.67 (m, 2H), 3.70 (s, 3H), 3.96 (m, 2H), 5.15 (s, 2H), 7.34 (m, 5H). ^{13}C NMR (50 MHz, $CDCl_3$) δ 33.6, 40.5, 52.2, 67.9, 119.1, 128.3, 128.4, 128.6, 135.7 153.2, 163.0 171.6. HPLC purity >99%. HRMS (*m/z*) 371.0463 $[M+H]^+$, calcd 371.0469 $C_{15}H_{16}ClN_2O_5S$.

Methyl 2-aminoethanoate•HCl (8a)

The product was obtained employing procedure 2 in 98% yield. White solid. M.p = 135.4 °C. R_f = 0.59 (CH_2Cl_2/MeOH 9:1). ^1H NMR (200 MHz, D_2O) δ 3.85 (s, 3H), 3.96 (s, 2H). ^{13}C NMR (50 MHz, D_2O) δ 40.2, 53.5, 161.3. ESI-MS (m/z) 90.0 $[M+H]^+$, calc. 90.1.

Methyl 3-aminopropionate•HCl (8b)

The product was obtained employing procedure 2 in quantitative yield. White solid, M.p. = 101.0 °C, R_f = 0.50 (triethylamine/methanol/dichloromethane 1:10:90). ^1H NMR (200 MHz, D_2O) *δ* 2.86 (t, *J* = 6.5 Hz, 2H), 3.30 (t, *J* = 6.4 Hz, 2H), 3.76 (s, 3H). ^{13}C NMR (50 MHz, D_2O) *δ* 31.2, 35.2, 52.7, 162.2. MS(ESI) (m/z) 104.1 $[M+H]^+$, calc. 104.1.

Methyl-4-aminobutanoate•HCl (8c)

The product was obtained employing procedure 2 in quantitative yield. White solid. M.p = 120.0 °C. R_f = 0.26 (CH_2Cl_2/MeOH 9:1). ^1H NMR (200 MHz, D_2O) *δ* 1.85 (m, 2H), 2.42 (t, *J* = 7.2 Hz, 2H), 2.93 (t, *J* = 7.8 Hz, 2H), 3.59 (s, 3H). ^{13}C NMR (50 MHz, D_2O) *δ* 22.2, 30.7, 38.9, 52.5, 175.8. MS(ESI) (m/z) 118.1 $[M+H]^+$, calc. 118.1.

Methyl-4-aminopentanoate•HCl (8d)

The product was obtained employing procedure 2 in quantitative yield. White solid. M.p = 146.3 °C. R_f = 0.19 (CH_2Cl_2/MeOH 9:1). ^1H NMR (200 MHz, D_2O) *δ* 1.65-1.73 (m, 4H), 2.46 (t, *J* = 6.9 Hz, 2H), 3.02 (br.t, 2H), 3.70 (s, 3H). ^{13}C NMR (50 MHz, D_2O) *δ* 21.2, 26.3, 33.1, 39.2, 52.3, 163.2. MS(ESI) (m/z) 132.1 $[M+H]^+$, calc. 132.1.

Methyl-6-aminohexanoate•HCl (8e)

The product was obtained employing procedure 2. Yield 94%. White solid. M.p = 123.1 °C. R_f = 0.38 (CH_2Cl_2/MeOH/Et_3N 90:10:1). ^1H NMR (200 MHz, D_2O) δ 1.33-1.42 (m, 2H), 1.56-1.70 (m, 4H), 2.41 (t, J = 7.4 Hz, 2H), 2.98 (t, J = 7.5 Hz, 2H), 3.68 (s, 3H). ^{13}C NMR (50 MHz, D_2O) δ 23.8, 25.2, 26.5, 33.5, 39.4, 52.3, 170.8. MS(ESI) (m/z) 146.1 $[M+H]^+$, calc. 146.1.

Ethyl 3-aminopropanoate•HCl (8f)

The product was obtained employing procedure 2, in which methanol was replaced for ethanol, in quantitative yield. White solid. M.p = 68.2°C. R_f = 0.38 (CH_2Cl_2/MeOH 9:1). ^1H NMR (200 MHz, D_2O) δ 1.29 (t, J = 7.1 Hz, 3H), 2.84 (t, J = 6.7 Hz, 2H), 3.32 (t, J = 6.5 Hz, 2H), 4.24 (q, J = 7.0 Hz, 2H). ^{13}C NMR (50 MHz, D_2O) δ 13.4, 31.4, 35.2, 62.5, 171.7. MS(ESI) (m/z) 118.1 $[M+H]^+$, calc. 118.1.

Cbz-Cystin-NHC$_2$H$_4$COOMe (9)

Cbz-Cystin (4 mmol) was suspended in dry DMF (5 mL) and stirred at room temperature. HOBt (8 mmol) and DCC (8 mmol) were added subsequently and the mixture is stirred for 15 min at room temperature. HCl salt **8b** (8 mmol) and triethylamine (8 mmol) were added subsequently and the mixture was stirred for 45 min at room temperature. The reaction mixture was diluted with ethylacetate (50 mL) and filtered. The ethylacetate was extracted with 1N aqueous HCl solution (50 mL, 2 times), saturated aqueous Na_2CO_3 (50 mL, 2 times), brine (50 mL) and dried (Na_2SO_4). The organic solvent was evaporated to yield the product with sufficiently high purity (>90%, TLC) for the next reaction step. Yield 75%. Brown-white solid. M.p = 120.9 °C. R_f = 0.38 (CH_2Cl_2/MeOH/acetic acid 90:10:1). ^1H NMR (200 MHz, $CDCl_3$): δ 2.49 (t, J = 6.2 Hz, 4H), 2.92 (d, J = 6.2 Hz, 4H), 3.48 (t, J = 6.5 Hz, 4H), 3.64 (s, 6H), 3.75 (m, 2H), 5.11 (s, 4H), 7.34 (m, 10H). ^{13}C NMR (50 MHz, $CDCl_3$): δ □25.1, 29.8, 35.4, 51.9, 55.0, 67.4, 128.8, 128.3, 136.3, 154.9, 170.2, 172.7. MS(ESI) (m/z) 679.4 $[M+H]^+$, calc. 679.2.

3,3'-dithiobis(N-ethylpropanamide) (10b)

The product was obtained following procedure 3 starting from ethylamine. Yield 37%. Brown gum. R_f = 0.57 (CH_2Cl_2/MeOH 9:1). ^1H NMR (200 MHz, $CDCl_3$) δ 1.16 (t, J = 7.2 Hz, 3H), 2.62-2.71 (m, 2H), 2.96-3.24 (m, 4H).^{13}C NMR (50 MHz, $CDCl_3$) δ 14.8, 34.8, 36.0, 61.9, 172.6. MS(ESI) (m/z) 265.2 $[M+H]^+$, calc. 265.1, (m/z) 287.1 $[M+Na]^+$, calc. 287.1.

3,3'-dithiobis(N-pentylpropanamide) (10c)

The product was obtained following procedure 3 starting from pentan-1-amine. Yield 80%. Brown-white brown solid. M.p = 121.4 °C. R_f = 0.4 (CH_2Cl_2/MeOH 94:6). ^{1}H NMR (200 MHz, $CDCl_3$) δ 0.88 (t, *J* = 6.6 Hz, 3H), 1.25-1.32 (m, 4H), 1.43-1.57 (m, 2H), 2.57 (t, *J* = 7.1 Hz, 2H), 2.97 (t, *J* = 7.1 Hz, 2H), 3.18-3.28 (m, 2H), 6.38 (br. 2H) ^{13}C NMR (50 MHz, $CDCl_3$) δ 14.2, 22.6, 29.3, 29.4, 34.6, 35.9, 40.0 171.3. MS(ESI) (m/z) 349.2 $[M+H]^+$, calc. 349.2, (m/z) 371.2 $[M+Na]^+$, calc. 371.2.

3,3'-dithiobis[N-(methyl 2-aminoethanoate)propanamide] (10d)

The product was obtained following procedure 3 starting from **8a**. Yield 27%. Dark brown solid. M.p = 65.5 °C. R_f = 0.59 (CH_2Cl_2/MeOH 9:1). ^{1}H NMR (200 MHz, $CDCl_3$) δ 2.65-3.28 (m, 4H), 3.76 (s, 3H), 4.06 (d, *J* = 5.0 Hz, 2H). ^{13}C NMR (50 MHz, $CDCl_3$) δ 34.6, 35.4, 41.4, 52.6, 166.0, 171.1. MS(ESI) (*m/z*) 353.2 $[M+H]^+$, calc. 353.1, (*m/z*) 375.1 $[M+Na]^+$, calc. 375.1.

3,3'-dithiobis[N-(methyl 2-aminopropionate)propanamide] (10e)

The product was obtained following procedure 3 starting from **8b**. Yield 42%. Brown gum. R_f = 0.38 (CH_2Cl_2/MeOH 9:1). ^{1}H NMR (200 MHz, $CDCl_3$) δ 2.51-2.58 (m, 8H), 2.90-2.97 (t, *J* = 6.9 Hz, 4H), 3.47-3.56 (m, 4H), 3.68 (s, 3H). ^{13}C NMR (50 MHz, $CDCl_3$) 33.9, 34.0, 35.1, 35.9, 52.0, 171.0, 173.0. MS(ESI) (m/z) 381.2 $[M+H]^+$, calc. 381.1, (m/z) 403.2 $[M+Na]^+$, calc. 403.1.

3,3'-dithiobis[N-(methyl 2-aminobutanoate)propanamide] (10f)

The product was obtained following procedure 3 starting from **8c**. Yield 62%. Brown solid. M.p. = 102.1 °C. R_f = 0.50 (CH_2Cl_2/MeOH 9:1). ^{1}H NMR (200 MHz, $CDCl_3$) δ 1.83 (m, 2H), 2.37 (t, *J* = 7.4 Hz, 2H), 2.56 (t, *J* = 6.9 Hz, 2H), 2.96 (t, *J* = 6.9 Hz, 2H), 3.26 (m, 2H), 3.65 (s, 3H). ^{13}C NMR (50 MHz, $CDCl_3$) 24.7, 31.6, 34.4, 35.8, 39.2, 51.9, 171.4, 174.0. MS(ESI) (m/z) 409.2 $[M+H]^+$, calc. 409.2, (m/z) 431.2 $[M+Na]^+$, calc. 431.2.

3,3'-dithiobis[N-(methyl 2-aminopentanoate)propanamide] (10g)

The product was obtained following procedure 3 starting from **8d**. Yield 45%. Brown solid. M.p. = 60.8 °C. R_f = 0.39 (CH_2Cl_2/MeOH 94:6). ^{1}H NMR (200 MHz, $CDCl_3$) δ 1.50-1.73 (m, 8H), 2.33 (t, *J* = 6.8 Hz, 4H), 2.53-2.69 (m, 4H), 2.97 (t, *J* = 7.1 Hz, 4H), 3.26 (m, 4H), 3.65 (s, 6H). ^{13}C NMR (50 MHz, $CDCl_3$) 22.2, 29.1, 33.7, 34.5, 36.0, 39.4, 51.8, 171.3, 174.2. MS(ESI) (m/z) 437.2 $[M+H]^+$, calc. 437.2, (m/z) 459.3 $[M+Na]^+$, calc. 459.2.

3,3'-dithiobis[N-(methyl 2-aminohexanoate)propanamide] (10h)

The product was obtained following procedure 3 starting from **8e**. Yield 62%. Brown solid. M.p. = 97.3 °C. R_f = 0.63 (CH_2Cl_2/MeOH 9:1). ^{1}H NMR (200 MHz, $CDCl_3$) δ 1.29-1.66 (m, 6H), 2.30 (t, *J* = 7.2 Hz, 2H), 2.57 (t, *J* = 7.0 Hz, 2H), 2.97 (t, *J* = 6.9 Hz, 2H), 3.24 (m, *J* = 6.5 Hz, 2H), 3.64 (s, 3H), 6.44 (br. t). ^{13}C NMR (50 MHz, $CDCl_3$) δ 24.5, 26.4, 29.2, 33.9, 34.4, 35.8, 39.5, 51.7, 171.2, 174.2. MS(ESI) (m/z) 465.3 $[M+H]^+$, calc. 465.2, (m/z) 487.3 $[M+Na]^+$, calc. 487.2.

3,3'-dithiobis[N-(ethyl 2-aminopropionate)propanamide] (10i)

The product was obtained following procedure 3 starting from **8f**. Yield 83%. Brown solid. M.p = 93.3 °C. R_f = 0.64 (CH_2Cl_2/MeOH 9:1). ^{1}H NMR (200 MHz, $CDCl_3$) δ 1.24 (t, *J* = 7.1 Hz, 3H), 2.54 (m, 4H), 2.94 (t, *J* = 7.0 Hz, 2H), 3.51 (m, 2H), 4.31 (q, *J* = 7.1 Hz, 2H), 6.60 (br s, 1H). ^{13}C NMR (50 MHz, $CDCl_3$) δ 14.3, 34.1, 34.4, 35.2, 35.8, 59.9, 171.2, 172.6. MS(ESI) (m/z) 409.2 $[M+H]^+$, calc. 409.2, (m/z) 431.2 $[M+Na]^+$, calc. 431.2.

3,3'-dithiobis[N-(3-chloro-4-fluorophenyl)propanamide] (10j)

The product was obtained following procedure 3 starting from 3-chloro-4-fluoroaniline. Yield 76%. Orange solid, M.p. = 133.7°C; R_f = 0.44 (ethyl acetate/cyclohexane 1:1). ^{1}H NMR (200 MHz, $CDCl_3$/CD_3OD 1:1) δ 2.57 (t, *J* = 4.5 Hz, 4H), 2.79 (t, *J* = 4.5 Hz, 4H), 6.85 (t, *J* = 5.9 Hz, 2H), 7.13 (m, 2H), 7.54 (d, *J* = 4.5 Hz, 2H). ^{13}C NMR (50 MHz, $CDCl_3$/CD_3OD 1:1): δ 33.6, 35.9, 115.9, 116.4, 119.4, 119.5, 121.9, 151.9, 156.8, 170.4. MS(ESI) (m/z) 465.3 $[M+H]^+$, calc. 465.0.

3,3'-dithiobis[N-(benzyl(2-aminoethyl)carbamate)propanamide] (10k)

The product was obtained following procedure 3 starting from benzyl (2-aminoethyl)carbamate. Yield 55%. Brown gum, R_f = 0.51 (CH_2Cl_2/MeOH 9:1), ^{1}H NMR (200 MHz, $CDCl_3$) *δ* 2.50-3.20 (m, 8H), 3.23-3.70 (m, 8H), 5.08 (s, 4H), 7.10-7.40 (m, 10H). ^{13}C NMR (50 MHz, $CDCl_3$) 32.9, 34.1, 41.5, 58.8, 67.0, 128.3, 128.8, 129.1, 129.2, 136.6, 165.0, 171.9.

Modeling

Molecular dockings were performed using the program Molegro Virtural Docker 2007 (MVD) from Molegro ApS, Aarhus, Denmark. The crystal structure from PCAF (PDB entry 1CM0) chain B, was prepared for dockings using the default settings in MVD. The water molecules were removed before docking. The ligands were geometry optimized using HYPERCHEM 7.5 Professional (Hypercube, Inc) using molecular mechanics with the Amber force field and Polar-Ribiere (conjugate gradient) algorithm. The optimized ligands were prepared for docking using the default

settings in MVD.[116] The 5-chloroisothiazolones, isothiazolones and 5-chloro-isothiazolones-1-oxide were docked with a distance constraint of 6 Å between the Cys 574 thiol and the carbon atom 5 in the isothiazolone scaffold. Docking solutions were calculated within a sphere of 15 Å from the Cys 574 thiol. Docking solutions were selected based on the MOLDOCKSCORE and the docking solutions were evaluated manually and the amino acid side chain in a radius of 10 Å from the ligand were energy minimized, followed by energy minimization of the ligand.

Enzyme inhibition studies

A fluorescent histone acetyl transferase assay described by Trievel *et al.* was used for enzyme inhibition studies.[112] The human recombinant histone acetyl transferases PCAF (p300/CREB-binding protein Associated Factor) was purchased from Biomol International. The histone H3 peptide (Ac-QTARKSTGGKAPRKQLATKNH2) was purchased from Pepscan (Lelystad, NL) (purity >98%, m/z 1034.9 $[M+2H]^{2+}$ calcd 1035.2).The other chemicals were purchased from Sigma–Aldrich. The assay buffer contained 100 mM HEPES/NaOH, pH 7.5, 0.8% Triton-X. 10 µL inhibitor solution (variable concentration) in assay buffer and 10 µL of the histone acetyl transferase (0.25 µM) in assay buffer containing 0.1% N-ethylmaleimide (NEM)-treated BSA were mixed in incubated for 15 min. 10 µL AcCoA (400 µM) in assay buffer and 20 µL Histone H3 peptide solution (200 µM) in assay buffer were added. The enzymatic reaction was allowed to proceed for 15 min followed by subsequent addition of 50 µL isopropanol and 100 µL 7-diethylamino-3-(4'-maleimidylphenyl)-4-methylcoumarin (CPM) 25 µM in assay buffer. The mixture was incubated for 15 min and the fluorescence was read with an excitation of 360 nm and an emission of 460 nm. The signal with no inhibitor present was set to 100% and the signal with no Histone H3 peptide present was set to 0%. Inhibitor solutions were prepared as 10 mM stock solution in DMSO and subsequently diluted to the desired final concentration using assay buffer. Calculations were performed using the Excel 2003 and the Microcal Origin 7 software. Screenings were performed at 10 µM inhibitor concentration (n =3, two times) and compounds showing more than 50 % inhibition at 10 µM were subjected to IC_{50} determination. IC_{50} determinations were performed using two-fold dilutions of the inhibitor starting from 10 µM. The IC_{50}'s were derived by non-linear curve fitting of the data.

Cell growth inhibition

Cell culture

The growth inhibition of the human cancer cell lines A2780 (ovarian), WiDr (colon) and HEP G2 (liver) and the human embryonic cell line 293 (kidney) was studied. The

cells were maintained in Dulbecco's modified Eagles Medium with 10% heat-inactivated fetal calf serum, 50 IU/mL penicillin and 50 mg/mL streptomycin at 37 ºC in a humidified 5% CO_2 incubator. All cell culture reagents were purchased from invitrogen.

Cell proliferation

Cell proliferation was measured by a Crystal Violet assay. For this assay, cells were seeded at 5000 cells per well into 96-well plates, grown for 24 h, and treated for an additional 48 h with the different inhibitors. After this, the medium was aspirated and the cells were fixed with 50 µL 1% crystal violet in 70% ethanol for 30 min. Subsequently, the cells were washed with water and the staining was solubilized by addition of 100 µL 1% SDS in water. The plates were read at 550 nm. A blank extinction value in which no cells were seeded was subtracted from all determinations and cell growth with no inhibitor present was set to 100%. All concentrations were tested in 8-fold on one plate and the GI_{50} values of most potent inhibitors were measured again on a new plate.

CHAPTER 3

REACTIVITY OF ISOTHIAZOLONES AND ISOTHIAZOLONE-1-OXIDES IN THE INHIBITION OF THE PCAF HISTONE ACETYLTRANSFERASES

Ghizzoni M, Haisma HJ, Dekker FJ;

European Journal of Medicinal Chemistry (2009) 44: 4855–4861

Abstract

Development of small molecule inhibitors of the histone acetyltransferase p300/CBP associated factor (PCAF) is relevant for oncology. The inhibition of the enzyme PCAF and proliferation of the cancer cell line HEP G2 by a series of 5-chloroisothiazolones was compared to a series of 5-chloroisothiazolone-1-oxides. The PCAF inhibitory potency of 5-chloroisothiazolones and 5-chloroisothiazolone-1-oxides is influenced by substitution in the 4-position. A study on the reactivity of the HAT inhibitors towards thiols and thiolates indicates that 5-chloroisothiazolones reacted quickly with propane-1-thiolate to provide many products, whereas 5-chloroisothiazolone-1-oxides provide only one defined product. Growth inhibition studies indicate that 5-chloroisothiazolones inhibit proliferation of HEP G2 cells at concentrations between 8.6 and 24 μM, whereas 5-chloroisothiazolone-1-oxides required higher concentrations or showed no inhibition.

INTRODUCTION

Histone acetylation and deacetylation play a crucial role in regulation of gene transcription in eukaryotes.[90] These histone modifications are regulated by two classes of enzymes: histone acetyltransferases (HATs) and histone deacetylases (HDACs), which respectively catalyze the addition to and the removal of acetyl groups on specific lysine residues.[7] Small molecule inhibitors are useful tools to study the functions of these enzymes and have potential therapeutic applications.[107,117]

HATs are grouped into different families according to their sequence similarity.[94] The GNAT (Gcn5 related N-acetyltransferase) family HATs include the closely related enzymes PCAF (p300/CBP associated factor) and GCN5 (general control of amino-acid synthesis 5).[95] The members of this family play a key role in endothelial growth factor (EGF) mediated gene transcription and in cell cycle progression and have therefore been recognized as potential anticancer targets.[97-99] Furthermore, deregulation of the activities of GNAT and p300 family HATs plays an important role in human immunodeficiency virus (HIV) and chronic obstructive pulmonary disease (COPD).[89,118]

Despite significant efforts, very few small molecule and cell-permeable inhibitors for GCN5 and PCAF have been described until now. Potent and selective bisubstrate inhibitors for p300 and PCAF have been reported but their lack of cell-permeability limits their application.[72] The natural products curcumin, garcinol and anacardic acid show HAT inhibitory activity, however their potency is low.[78,82,87] A promising class of inhibitors is represented by isothiazolones, which inhibit HATs with IC_{50}'s in the micromolar range.[74,119,120]

The PCAF inhibition of isothiazolones is expected to derive from their reactivity towards the enzyme's active site thiol. The reaction of isothiazolones with a thiolate involves nucleophilic attack at the sulfur atom with concomitant cleavage of the S–N bond to give a ring opened product that can react further.[113] For 5-chloroisothiazolone-1-oxides the reactivity towards thiolates is unknown.

Previously, we have reported a significant difference in PCAF HAT inhibition between N-aliphatic substituted 5-chloroisothiazolones and isothiazolones.[120] The most potent derivative is denoted isothiazolone A (figure 3.1). We also found that PCAF is inhibited by the 5-chloroisothiazolone-1-oxide denoted isothiazolone oxide A (figure 3.1). Furthermore, we have demonstrated that 5-chloroisothiazolones inhibit

the growth of cancer cell lines in the micromolar range, whereas isothiazolones showed no inhibition at 10 μM.

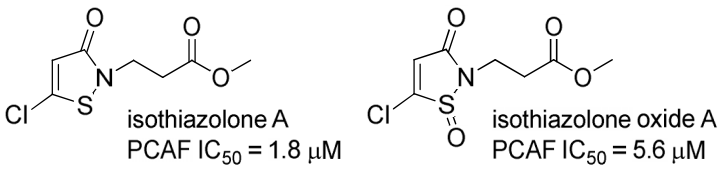

Figure 3.1: *inhibitors of the HAT PCAF with an isothiazolone or isothiazolone-1-oxide core structure.*

In this study we investigated synthetic modifications of 5-chloroisothiazolones and 5-chloroisothiazolone-1-oxides and studied their reactivity to thiols and thiolates using HPLC and NMR. We studied also their inhibition of the enzyme PCAF and inhibition of cell proliferation. Chloro and methyl substituents were introduced in the 4-position of the 5-chloroisothiazolone and 5-chloroisothiazolone-1-oxide core in order to study the effect of substituents on the inhibition of the enzyme PCAF. Finally, the growth inhibition of HEP G2 liver cancer cells upon treatment with 5-chloroisothiazolones and 5-chloroisothiazolone-1-oxides was investigated to explore the toxicity of these molecules.

CHEMISTRY

Synthesis of isothiazolones and isothiazolone-1-oxides

A series of 5-chloroisothiazolones and 5-chloroisothiazolone-1-oxides was synthesized in order to explore synthetic modifications of the isothiazolone ring and their effects on inhibition of the enzyme PCAF and cell proliferation. Synthesis was performed according to previously published procedures.[103] Amines were reacted with 3,3´-dithiobispropionyl chloride to yield the corresponding 3,3´-dithiobispropionic amides. The 3,3´-dithiobispropionic amides were treated with 3 equivalents sulfuryl chloride in dichloromethane. This provided reaction mixtures in which the 5-chloroisothiazolones were the main products (40–60%) and the isothiazolones the minor product (10–20%). According to the literature, 4,5-dichloroisothiazolones **7** and **8** can be obtained in one step from 3,3´-dithiobispropionic amides by treatment with 5 equivalents of sulfuryl chloride in yields between 10% and 40%. We hypothesized that chlorination of the purified 5-chloroisothiazolones in the 4-position would provide the 4,5-dichloroisothiazolones with higher yields. Indeed, treatment of **1** and **3** with sulfuryl chloride gave the 4,5-dichloroisothiazolones **7** and **8** in yields of 55%

and 90%, respectively (Scheme 1). Compound **2** was synthesized according to the procedure described by Yue *et al.*[121] However, product **2** was obtained with a yield of 10% instead of the reported 30–70%. The lower yield may be explained by the steric hindrance for formation of the S–N bond when the N is tert-butyl substituted.

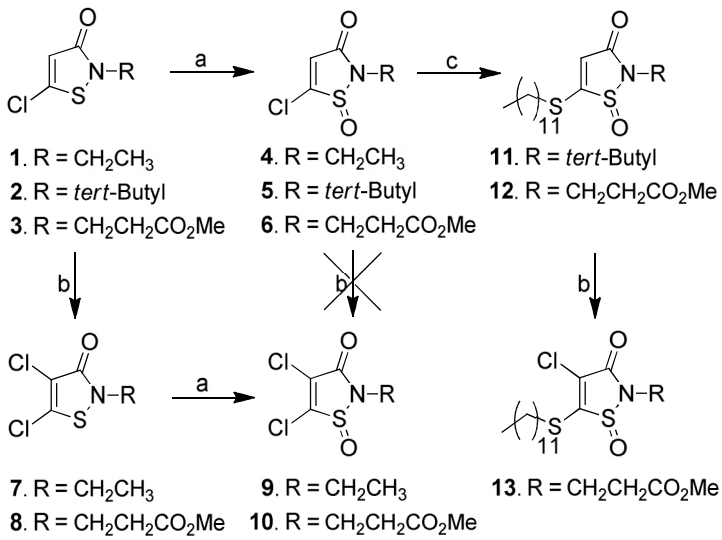

Scheme 3.1: *reagents and conditions: (a) mCPBA, CH_2Cl_2, (b) SO_2Cl_2, CH_2Cl_2, (c) CH_3-$(CH_2)_{11}$-SH, Et_3N, CH_2Cl_2.*

The 5-chloroisothiazolones were oxidized by *m*CPBA to yield the corresponding 5-chloroisothiazolone-1-oxides **4**–**6** as racemic mixtures in yields between 60% and 80% after purification. Combs *et al.* demonstrated that comparable S-oxides can be resolved using chiral HPLC and that the stereochemistry is stable.[122] However, attempts to separate the enantiomers of 5-chloroisothiazolone-1-oxides **6** using chiral HPLC failed.

Attempts were made to chlorinate the 5-chloroisothiazolone-1-oxides **4** and **6** in the 4-position using sulfuryl chloride. However, overnight treatment with 3 equivalents of sulfuryl chloride at room temperature did not show conversion of the starting materials into the desired products **9** and **10**. Apparently, it is not possible to chlorinate 5-chloroisothiazolone-1-oxides in the 4-position under these conditions. Compounds **9** and **10** were obtained via oxidation of **7** and **8** using *m*CPBA in yields around 80%.

Thiol substitution on the 5-chloroisothiazolone-1-oxides **5** and **6** was studied using dodecane-1-thiol as a reagent. The thiol (–SH) did not react with the 5-chloroisothiazolone-1-oxides, whereas a very quick reaction (<30 min) with the

thiolate (–S-) was observed. Products **11** and **12** were obtained by reaction of **5** and **6** with dodecane-1-thiol in the presence of triethylamine in yields around 60% after purification. Compound **12** was chlorinated in the 4-position using sulfuryl chloride as a reagent to give **13** in 58% yield.

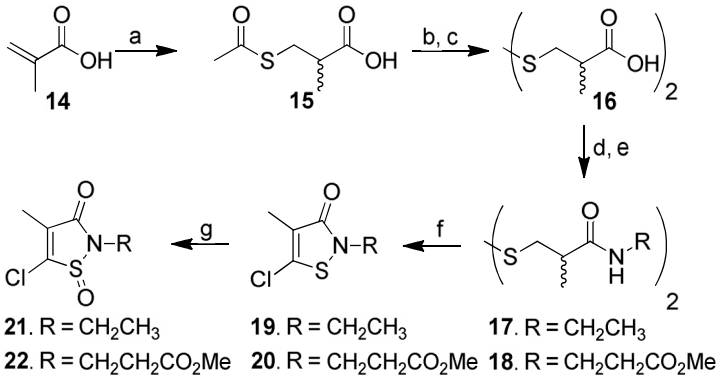

Scheme 3.2: *reagents and conditions: (a) Thioacetic acid, cyclohexane, reflux, (b) 6 N HCl in H_2O, reflux (c) aqueous 35% H_2O_2, (d) $SOCl_2$, reflux, (e) R-NH_2, Et_3N, CH_2Cl_2, (f) SO_2Cl_2, CH_2Cl_2 (g) mCPBA, CH_2Cl_2.*

5-chloro-4-methylisothiazolones **19** and **20** were synthesized using the procedure shown in Scheme 2.[113,123] Methacrylic acid (**14**) was subjected to Michael addition with thioacetic acid to give the 3-(acetylthio)-2-methylpropanoic acid (**15**) as a racemic mixture in 50% yield. Deacetylation was achieved by treatment with 6 N HCl, and the resulting thiol was oxidized using H_2O_2 to yield the 3,3´-dithiobis(2-methylpropanoic acid) (**16**) that was pure enough to continue to the next step. The diacid **16** was converted to the diacylchloride and coupled to different amines to give the crude 3,3´-dithiobispropionic amides **17** and **18** in yields around 30% over 3 steps. The crude 3,3´-dithiobispropionic amides were treated with 3 equivalents of sulfuryl chloride at 0 ºC in dichloromethane to give the 5-chloro-4-methylisothiazolones **19** and **20** in yields of 38% and 52%, respectively. Compounds **19** and **20** were oxidized by mCPBA to the corresponding 1-oxide derivates **21** and **22** in yields around 75%.

Reactivity of isothiazolones and isothiazolone-1-oxides

The biological activity of isothiazolones and their derivatives originates from both their binding to proteins and their reactivity towards thiolates.[124,125] It has been described that isothiazolones react with thiolates on the sulfur atom, with concomitant cleavage of the S–N bond. A study on N-methylisothiazolone **25**, with N-Acetyl-Cys as thiolate, showed formation of intermediate **27** (figure 3.2).[113] The

reaction between 5-chloro-N-methylchloroisothiazolone **23** is expected to proceed through the same mechanism, however intermediate **28** has not been identified. This might be due to the increased reactivity of intermediate **28** due to the presence of the chlorine atom. Another line of evidence for this inhibitory mechanism has been provided by a study on inhibition of $p56^{lck}$ tyrosine kinase by isothiazolones.[125] Morley *et al.* have studied the reactivity of (5-chloro)isothiazolones towards 2-methyl-2-propanethiol at pH 4 in aqueous environment. They have found kinetic rate constants in the order 23 >24> 25> 26 (figure 3.2).[126]

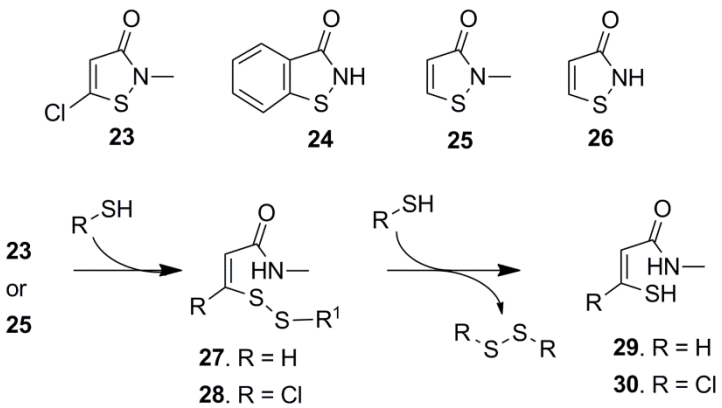

Figure 3.2: *reactivity of the isothiazolone core.*

The reactivity of 5-chloroisothiazolones and 5-chloroisothiazolone-1-oxides towards thiols and thiolates was studied using comparable methods as published previously.[127] HPLC analysis showed that **3** did not react with propane-1-thiol in acetonitrile as a solvent after 24 h treatment at room temperature. In contrast, treatment with sodium propane-1-thiolate in acetonitrile resulted in a quick conversion into many new products. Treatment with 0.1 equivalent thiolate resulted in 10% conversion of the starting material. Treatment with 0.5 equivalents resulted in 50% conversion and many new products were observed. After treatment with 1.0 equivalent thiolate the starting material disappeared and many new peaks were observed. These results show that 5-chloroisothiazolones do not react with thiols, whereas they react quickly with thiolates providing many products that could not be identified.

The thiol reactivity of 5-chloroisothiazolone-1-oxide **6** was investigated. No reaction was observed between **6** and propane-1-thiol after treatment overnight. On the contrary, **6** reacted quickly with sodium propan-1-thiolate in acetonitrile to provide one new product. Treatment with 0.1 equivalent resulted in one new product

with a conversion of about 10%. Treatment with 0.5 equivalent resulted in about 50% conversion into one new product. After treatment with 1.0 equivalent, the starting material was completely converted into one new product. NMR data showed that this product derives from addition-elimination in the 5-position. Treatment of 5-chloroisothiazolon-1-oxide with more than 1.0 equivalent of sodium propan-1-thiolate provided substitution in the 5-position, followed by substitution in the 4-position. These data show that 5-chloroisothiazolone-1-oxides do not react with thiols, whereas they react quickly with thiolates through addition-elimination in the 5-position.

PHARMACOLOGY

Histone acetyltransferase inhibition

Inhibition of the HAT PCAF by 5-chloroisothiazolones and 5-chloroisothiazolone-1-oxides was investigated in order to explore the binding properties of these compounds. The PCAF HAT inhibition studies were performed using a fluorescent assay as described previously.[112,120] 5-Chloroisothiazolones **1** and **3** showed PCAF inhibition with IC_{50} values of 3.0 and 1.8 μM, respectively (table 3.1). The effects of substitutions in the 5-chloroisothiazolone 4-position on PCAF inhibition were studied. Introduction of a chlorine in the 4-position provided compounds 7 and 8 with an IC_{50} of 2.4 and 2.6 μM, whereas introduction of a methyl group in the 4-position provided compounds **19** and **20** with less than 50% inhibition at 10 μM.

The inhibitory properties of these molecules derive both from their binding to the enzyme active site and from their chemical reactivity. Chloro- or methyl-substitution in the 4-position of 5-chloroisothiazolones could change the binding configuration to the active site of the enzyme and thus influence the inhibitory properties.

Substitution of the 5-chloroisothiazolones in their 4-position changes their reactivity. The methyl group is an electron donating group (EDG) due to inductive effects, whereas the chlorine is a net electron-withdrawing group (EWG) due to inductive effects partially counteracted by an electron donating contribution through resonance. Introduction of an EDG like a methyl group (**20**) causes loss of potency, which suggests that an EDG in the 4-position adds electron density to the isothiazolone ring and thus stabilizes it for nucleophilic attack. On the contrary, the introduction of an EWG like a chlorine atom (**8**) does not affect the inhibitory properties. This datum suggests that the isothiazolone reactivity on the 1-position

towards thiolates is already at its maximum and cannot be increased further by an EWG.

The effect of substitution in the 4-position of 5-chloroisothiazolone-1-oxides on inhibition of PCAF activity was studied. The compounds were tested as racemic mixtures. Compound **4**, with an N-ethyl substitution, showed less than 50% inhibition at 10 μM. Introduction of either a chlorine (**9**) or a methyl group (**21**) in the 4-position, provided compounds that did not show any inhibition at 10 μM. Compound **6** with a methyl ester in the N-substitution showed PCAF inhibition with an IC_{50} value of 5.6 μM. Introduction of either a chloro (**10**) or a methyl substituent (**22**) provided compounds that showed less than 50% PCAF inhibition at 10 μM. These differences in binding could derive from changes in binding to the enzyme active site as well as from changes in reactivity.

Table 3.1: *inhibition of HAT PCAF and proliferation of cell lines by 5-chloroisothiazolinone and isothiazolone-1-oxide.*

		R^1	R^2	R^3	PCAF IC_{50} μM[a]	HEP-G2 IC_{50} μM[b]
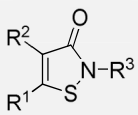	**1**	Cl	H	Ethyl	3.0 ± 0.3	12 ± 0.5
	7	Cl	Cl	Ethyl	2.4 ± 0.1	12 ± 2
	19	Cl	CH_3	Ethyl	> 10	9.1 ± 0.9
	3	Cl	H	$(CH_2)_2CO_2Me$	1.8 ± 0.2	24 ± 3
	8	Cl	Cl	$(CH_2)_2CO_2Me$	2.6 ± 0.6	16 ± 3
	20	Cl	CH_3	$(CH_2)_2CO_2Me$	> 10	8.6 ± 1
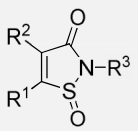	**4**	Cl	H	Ethyl	> 10	> 100
	9	Cl	Cl	Ethyl	> 10	> 100
	21	Cl	CH_3	Ethyl	> 10	> 100
	6	Cl	H	$(CH_2)_2CO_2Me$	5.6 ± 0.2	> 100
	10	Cl	Cl	$(CH_2)_2CO_2Me$	> 10	> 100
	22	Cl	CH_3	$(CH_2)_2CO_2Me$	> 10	> 100
	5	Cl	H	*tert*-Butyl	> 10	27 ± 9
	11	$S(CH)_{11}CH_3$	H	*tert*-Butyl	>10	> 50
	12	$S(CH)_{11}CH_3$	H	$(CH_2)_2CO_2Me$	> 10	> 100
	13	$S(CH)_{11}CH_3$	Cl	$(CH_2)_2CO_2Me$	> 10	> 100

[a] Inhibition concentration 50% (IC_{50}) determination n = 3.

[b] Growth inhibition 50% determinations n = 8.

The 5-dodecylthioisothiazolone-1-oxides **11** and **12** and 5-dodecylthio-4-chloroisothiazolone-1-oxide **13** showed no detectable PCAF inhibition at 10 μM. The lack of activity of these compounds might derive both from their binding properties to the enzyme active site as well as their reactivity towards thiolates.

Growth inhibition

Growth inhibition of cancer cells was studied in order to explore how modifications of the isothiazolone core influence the inhibition of cell proliferation. The growth inhibition of the human cancer cell line HEP G2 (liver cancer) was studied using a crystal violet assay as described previously.[120] The 5-chloroisothiazolones inhibited the growth of HEP G2 cells with IC_{50} values between 8.6 and 24 μM (table 3.1). The differences in PCAF inhibitory potency are not reflected in the inhibition of cell proliferation. Other mechanisms might be involved in the inhibition of cell proliferation by these compounds like for example binding to other proteins or reactions with cellular glutathione. Western blot on inhibition of histone acetylation upon treatment of this cell line with the inhibitors is required to investigate if the molecules inhibit histone acetylation in cell-based assays.

5-Chloroisothiazolone-1-oxides showed less than 50% inhibition of cell proliferation at 100 μM, with the exception of compound **5**. In general, 5-chloroisothiazolone-1-oxides are less lipophilic then 5-chloroisothiazolones, which might hamper their cellular permeability. The partition coefficient (log P) for isothiazolone-1-oxide **6** was determined to be 0.08, whereas for isothiazolone **3** a log P value of 0.69 was measured. The low log P value of isothiazolone-1-oxide **6** might hamper the inhibition of cell proliferation.

CONCLUSION

A series of 5-chloroisothiazolones and 5-chloroisothiazolone-1-oxides with chlorine and methyl substitutions in the 4-position was synthesized. 5-chloroisothiazolones were readily chlorinated in the 4-position by sulfuryl chloride, whereas the 5-chloroisothiazolone-1-oxides could not be chlorinated in the 4-position under the applied conditions. 5-Chloroisothiazolones do not react with thiols whereas they react quickly with thiolates. Upon reaction, multiple products were observed which hampers the elucidation of the reaction mechanism. 5-chloroisothiazolone-1-oxides do not react with thiols, whereas they react quickly with thiolates in the 5-position. The reaction occurs via an addition-elimination mechanism to give 5-

alkylthioisothiazolone-1-oxides. The resulting 5-alkylthioisothiazolone-1-oxide was chlorinated in the 4-position using sulfuryl chloride.

N-aliphatic substituted 5-chloroisothiazolones (**1** and **3**) showed PCAF inhibition at micromolar concentrations (2–3 μM). Chlorine substitution in the 4-position yielded products which retained PCAF inhibition, whereas methyl substitution provided compounds that showed no inhibition at 10 μM. 5-Chloroisothiazolone-1-oxide **6** with a methyl ester in the N-substitution shows an IC_{50} of 5.6 μM whereas **4** shows an IC_{50} higher than 10 μM. These data indicate that the methyl ester contributes to PCAF inhibition. Methyl or chlorine substitution in the 4-position and thiol substitution in the 5-position of 5-chloroisothiazolone-1-oxides provides compounds with IC_{50} values higher than 10 μM. 5-chloroisothiazolones inhibit the growth of HEP G2 cancer cells in concentrations between 8.6 and 24 μM, whereas little or no growth inhibition was observed for 5-chloroisothiazolone-1-oxides.

EXPERIMENTAL PROTOCOLS

General procedures

Chemicals were obtained from commercial suppliers (Sigma–Aldrich, Acros Organics) and in most cases used without further purification. Dichloromethane was dried by distillation over CaH_2 before use. Aluminum sheets of Silica Gel 60 F254 were used for Thin-layer chromatography (TLC). Spots were visualized under ultraviolet light or stained with $KMnO_4$ solution. MP Ecochrom Silica Gel 32–63 60 Å was used for column chromatography. Melting points were determined on an Electrothermal digital melting point apparatus and are uncorrected. ^1H and ^{13}C NMR spectra were recorded on a Varian Gemini-200 (50.32 MHz) spectrometer. Chemical shift values are reported relative to residual solvent peaks (CD_3OD, ^1H δ = 3.31, ^{13}C δ = 49.00 or $CHCl_3$, ^1H δ = 7.26, ^{13}C δ = 77.16). The coupling constants (*J*) are reported in Hertz (Hz). ^{13}C spectra were recorded using the attached proton test (APT) pulse sequence. HPLC analyses were performed with a Waters 510 pump, equipped with an ISCO 2360 gradient programmer and a Waters 486 UV detector (254 nm). The column was a 25 cm x 4.6 mm (5 μm) Discovery C18, with a flow of 0.5 mL/min. Electrospray ionization mass spectra (ESI-MS) were recorded on an Applied Biosystems/SCIEX API3000-triple quadrupole mass spectrometer. High-resolution mass spectra (HR-MS) were recorded using a flow injection method on an LTQ-Orbitrap XL mass spectrometer (Thermo Electron, Bremen, Germany) with a resolution of 60,000 at m/z 400. Internal recalibration in real time was performed with protonated testosterone (lock mass m/z = 289.2162).

Synthetic procedure 1

The starting material (1.0 mmol) was dissolved in dichloromethane (10 mL), and m-chloroperbenzoic acid (70%) (1.2 mmol, 0.29 g) was added in several portions over 20 min. The mixture was stirred for 3 h at room temperature. A few milligrams of sodium metabisulfite were added to quench the excess mCPBA, and the mixture was stirred for 5 min. The solvent was evaporated under reduced pressure, and the residue was dissolved in EtOAc (15 mL), and extracted with saturated $NaHCO_3$ solution (3 x 15 mL) and brine (1 x 15 mL). The organic layer was dried over Na_2SO_4, filtered and the solvent was evaporated under reduced pressure. The crude product was purified by column chromatography.

Synthetic procedure 2

The starting material (1.0 mmol) was dissolved in dichloromethane (10 mL). Sulfuryl chloride (3.0 mmol, 0.24 mL) was added slowly and the solution was stirred overnight at room temperature. H_2O (1.0 mL) was added to the solution, and the mixture was stirred for 5 min. The mixture was extracted with water (3 x 10 mL) and brine (1 x 10 mL), dried over Na_2SO_4, and filtered. The solvent was evaporated under reduced pressure, and the product was purified by column chromatography.

Synthetic procedure 3

The dithiobispropanamide (1.0 mmol) was dissolved in dry dichloromethane (5 mL) and cooled to 0˚C. Sulfuryl chloride (3.0 mmol, 0.24 mL) was added dropwise, and the mixture was stirred for 2h at room temperature. H_2O (1.0 mL) was added, and the mixture was stirred for 5 min. Subsequently, the mixture was extracted with water (3 x 10 mL) and brine (1 x 10 mL), dried over Na_2SO_4, and filtered. The solvent was evaporated under reduced pressure, and the product was purified by column chromatography.

5-chloro-2-ethylisothiazol-3(2H)-one-1-oxide (4)

The product was obtained using procedure 1 starting from **1** and purified using column chromatography with EtOAc/Hex 1:2 (v/v) as eluent. The compound was obtained as a yellow oil (100 mg, 56%): R_f = 0.38 (EtOAc/Hex, 1:2); ^{1}H NMR (200 MHz, $CDCl_3$): δ = 1.33 (t, *J* = 7.1 Hz, 3H), 3.65-3.89 (m, 2H), 6.67 ppm (s, 1H); ^{13}C NMR (50 MHz, $CDCl_3$): δ = 14.8, 36.8, 124.4, 156.9, 169.4 ppm; HPLC: purity > 98%, RT = 9.6 min, mobile phase: H_2O:CH_3CN:TFA 60:40:0.1; HRMS: *m*/*z* $[M+H]^+$ calcd for $C_5H_7{}^{35}ClNO_2S$: 179.9988, found: 179.9876.

2-tert-butyl-5-chloroisothiazol-3(2H)-one 1-oxide (5)

The product was obtained using procedure 1 starting from **2** and purified using column chromatography with EtOAc/Hex 1:2 (v/v) as eluent. The compound was obtained as a colorless oil (62 mg, 30%): R_f = 0.6 (EtOAc/Hex, 1:1); ^{1}H NMR (200 MHz, $CDCl_3$) : δ 1.63 (s, 9H), 6.55 ppm (s, 1H); ^{13}C NMR (50 MHz, $CDCl_3$): δ 29.4, 59.7, 125.8, 136.3, 165.6 ppm; HPLC: purity 98%, RT = 11.1 min, mobile phase: H_2O:CH_3CN:TFA 50:50:0.1; MS (ES, 70 eV): *m/z* 207.9 $[M+H]^+$.

4,5-dichloro-2-ethylisothiazol-3(2H)-one (7)

The product was obtained using procedure 2 starting from **1** and purified using column chromatography with EtOAc/Hex 1:1 (v/v) as eluent. The compound was obtained as a yellow oil (109 mg, 55%): R_f = 0.51(EtOAc/Hex 1:2); ^{1}H NMR (200 MHz, $CDCl_3$): δ = 1.32 (t, *J* = 7.2 Hz, 3H), 3.86 ppm (q, *J* = 7.0 Hz, 2H); ^{13}C NMR (50 MHz, $CDCl_3$): δ = 14.7, 40.4, 138.4, 161.8, 168.0 ppm; HPLC: purity 99%, RT = 12.2 min, mobile phase: H_2O:CH_3CN:TFA 60:40:0.1; HRMS: *m/z* $[M+H]^+$ calcd for $C_5H_6{}^{35}Cl_2NOS$: 197.9542, found: 197.9543.

Methyl 3-(4,5-dichloro-3-oxoisothiazol-2(3H)-yl)propanoate (8)

The product was obtained using procedure 2 starting from **3** and was purified using column chromatography with EtOAc/Hex 1:1 (v/v) as eluent. The compound was obtained as a yellow oil (233 mg, 91 %): R_f = 0.40 (EtOAc/Hex 1:1); ^{1}H NMR (200 MHz, $CDCl_3$): δ = 2.75 (t, *J* = 6.1 Hz, 2H), 3.71 (s, 3H), 4.07 ppm (t, *J* = 6.0, Hz 2H); ^{13}C NMR (50 MHz, $CDCl_3$): δ = 33.6, 41.0, 52.3, 114.5, 139.7, 162.1, 171.7 ppm; HPLC: purity > 98%, RT = 10.5 min, mobile phase: H_2O:CH_3CN:TFA 50:50:0.1; HRMS: *m/z* $[M+H]^+$ cald for $C_7H_8{}^{35}Cl_2NO_3S$: 255.9597, found: 255.9596.

4,5-dichloro-2-ethylisothiazol-3(2H)-one-1-oxide (9)

The product was obtained using procedure 1 starting from **7** and purified using column chromatography with EtOAc/Hexane 1:3 (v/v) as eluent. The compound was obtained as a pale yellow solid (165 mg, 77 %): R_f = 0.58 (EtOAc/Hex, 1:2); ^{1}H NMR (200 MHz, $CDCl_3$): δ = 1.32-1.40 (m, 3H), 3.72-3.91 (m, 2H) ppm. ^{13}C NMR (50 MHz, $CDCl_3$): δ = 14.7, 38.0, 131.0, 148.7, 159.8 ppm; HPLC: purity 98%, RT = 12.2 min, mobile phase: H_2O:CH_3CN:TFA 50:50:0.1; HRMS: *m/z* $[M+H]^+$ calcd for $C_5H_6{}^{35}Cl_2NO_2S$: 213.9491, found: 213.9491.

Methyl 3-(4,5-dichloro-1-oxido-3-oxoisothiazol-2(3H)-yl)propanoate (10)

The product was obtained using procedure 1 starting from **8** and purified using column chromatography with EtOAc/Hex 1:2 (v/v) as eluent. The compound was obtained as a yellow oil (212 mg, 78 %): R_f = 0.48 (EtOAc/Hex, 1:1); ^{1}H NMR (200

MHz, $CDCl_3$): δ = 2.71-2.81 (m, 2H), 3.70 (s, 3H), 4.05 ppm (t, *J* = 6.5 Hz, 2H); ^{13}C NMR (50 MHz, $CDCl_3$): δ = 33.4, 38.2, 52.3, 130.6, 149.4, 160.3, 171.1 ppm; HPLC: purity 98%, RT = 11.5 min, mobile phase: H_2O:CH_3CN:TFA 50:50:0.1; HRMS: *m/z* $[M+H]^+$ calcd for $C_7H_8{}^{35}Cl_2NO_4S$: 271.9546, found: 271.9544.

2-tert-butyl-5-(dodecylthio)isothiazol-3(2H)-one-1-oxide (11)

Dodecane-1-thiol (1.2 mmol, 0.28 mL,) was added to a solution of 2-*tert*-butyl-5-chloroisothiazol-3(2H)-one-1-oxide (1.2 mmol, 0.25 mg) in dry dichloromethane at room temperature. Triethylamine (1.2 mmol, 0.15 mL) was added dropwise, and the mixture was stirred for 3 h at room temperature. Dichloromethane (50.0 mL) was added, and the organic layer was extracted with H_2O (3 x 50 mL) and brine (1 x 50 mL), and dried with Na_2SO_4. The solvent was evaporated under reduced pressure, and the residue was purified by column chromatography using EtOAc/Hex 1:25 (v/v) as eluent. The compound was obtained as a white solid (241 mg, 57%): R_f = 0.42 (EtOAc/Hex, 1:4); mp: 62 °C; ^1H NMR (200 MHz, $CDCl_3$): δ = 0.87 (t, *J* = 6.5 Hz, 3H), 1.20-1.50 (m, 18H), 1.62 (s, 9H), 1.65-1.85 (m, 2H), 2.98 (t, *J* = 7.3 Hz, 2H), 6.07 ppm (s, 1H). ^{13}C NMR (50 MHz, $CDCl_3$): δ = 14.3, 22.8, 28.3, 28.9, 29.1, 29.3, 29.5, 29.6, 29.7, 32.0, 33.6, 58.9, 118.0, 165.5, 167.2 ppm. MS (ESI): *m/z* 374.1 $[M+H]^+$.

Methyl 3-[5-(dodecylthio)-1-oxido-3-oxoisothiazol-2(3H)-yl] propanoate (12)

The product was obtained using the same procedure as for compound **11** starting from dodecane-1-thiol and methyl 3-(5-chloro-1-oxido-3-oxoisothiazol-2(3H)-yl)propanoate (**6**). The compound was purified using column chromatography with EtOAc/Hex (v/v) 1:10 as eluent and was obtained as a white solid (335 mg, 69%): R_f = 0.39 (EtOAc/Hex, 1:2); mp: 55.7 °C;. ^1H NMR (200 MHz, $CDCl_3$): δ = 0.86 (t, *J* = 6.5 Hz, 3H), 1.20-1.50 (m, 18H), 1.65-1.85 (m, 2H), 2.72 (dt, *J* = 4.0, 7.1 Hz, 2H), 3.01 (t, *J* = 7.3 Hz, 2H), 3.69 (s, 3H), 3.98 (t, *J* = 6.8 Hz, 2H) 6.15 ppm (s, 1H). ^{13}C NMR (50 MHz, $CDCl_3$): δ = 14.23, 22.8, 28.2, 28.8, 29.1, 29.4, 29.5, 29.6, 29.7, 32.0, 33.8, 33.9, 37.2, 52.1, 115.8, 166.4, 168.3, 171.4 ppm; HRMS: *m/z* $[M+H]^+$ calcd for $C_{19}H_{34}NO_4S_2$: 404.1924, found: 404.1925.

Methyl 3-[4-chloro-5-(dodecylthio)-1-oxido-3-oxoisothiazol-2(3H)-yl]propanoate (13)

The product was obtained using procedure 1 starting from **12** and was purified using column chromatography with EtOAc/Hex 1:10 (v/v) as eluent. The compound was obtained as a colorless oil (254 mg ,58%): R_f = 0.49 (EtOAc/Hex, 1:2); ^1H NMR (200 MHz, $CDCl_3$): δ = 0.86 (t, *J* = 6.5 Hz, 3H), 1.20-1.80 (m, 20H), 1.65-1.85 (m, 2H), 2.65-2.80 (m, 2H), 2.85-3.00 (m, 2H), 3.69 (s, 3H), 3.95-4.10 ppm (m, 2H). ^{13}C NMR (50 MHz, $CDCl_3$): δ =14.4, 28.8, 29.0, 29.2, 29.3, 29.6, 29.7, 29.8, 30.9, 32.1, 33.2, 38.4,

39.9, 40.7, 52.4, 95.8, 167.8, 169.5, 171.2 ppm; HRMS: *m/z* $[M+H]^+$ calcd for $C_{19}H_{33}{}^{35}ClNO_4S_2$: 438.1534, found: 438.1532.

3-(acetylthio)-2-methylpropanoic acid (15)

Methacrylic acid (40 mmol, 3.39 mL) was dissolved in 50 mL cyclohexane. Thioacetic acid (120 mmol, 8.58 mL) was slowly added, and the reaction mixture was stirred at reflux overnight. The reaction mixture was cooled to room temperature, and the solvent was evaporated under reduced pressure. The residue was dissolved in 50 mL ethylacetate, and extracted with HCl 1N (3 x 50 mL) and brine (1 x 30 mL). The organic layer was dried with Na_2SO_4, and the solvent evaporated under reduced pressure. The product was purified by column chromatography with ethylacetate:hexane 1:4 (v/v) as eluent to give a colorless oil (3.24 g, 50%). R_f = 0.60 (EtOAc/Hex 2:1); ^{1}H NMR (200 MHz, CD_3OD): δ = 1.21 (d, *J* = 7 Hz, 3H), 2.32 (s, 3H), 2.61-2.67 (m, 1H), 3.03-3.09 ppm (m, 2H); ^{13}C NMR (50 MHz, CD_3OD): δ = 17.1, 30.4, 32.6, 41.0, 178.2, 196.9; MS (ESI): *m/z* 161.2 $[M+H]^+$.

3,3'-dithiobis(2-methylpropanoic acid) (16)

3-(acetylthio)-2-methylpropanoic acid (**15**) (15 mmol, 2.40 g) was suspended in 20 mL HCl 6N and refluxed for 4h. The mixture was cooled to room temperature, hydrogen peroxide sol 35% (15 mmol, 1.28 mL) was added at 0 ˚C and the mixture stirred for 15 min. The H_2O_2 was quenched with few milligrams of sodium bisulfite and the mixture extracted with ethylacetate (3 x 30 mL). The organic layers were collected, extracted with brine (1 x 50mL) and dried over Na_2SO_4. The solvent was evaporated under reduced pressure to give the product that was used for the next step without any further purification. The compound was obtained as a pale yellow oil (1.40 g, 39 %): R_f = 0.44 (EtOAc/Hex 2:1); ^{1}H NMR (200 MHz, CD_3OD): δ = 1.22-1.36 (m, 6H), 2.78-3.03 (m, 4H), 3.53-3.56 (m, 1H), 3.88-3.92 ppm (m, 1H).

3,3'-dithiobis(N-ethyl-2-methylpropanamide) (17)

The 3,3'-dithiobis(2-methylpropanoic acid) (**16**) (19 mmol, 4.0 g) was suspended in 15 mL $SOCl_2$ and the resulting mixture was heated to reflux until complete dissolution of the acid. The solvent was evaporated under reduced pressure to furnish the diacidchloride as a pale yellow oil. Triethylamine (76 mmol, 10.5 mL) was added to a solution of Ethylamine*HCl (38 mmol, 3.10 g) in 80 mL of dry dichloromethane and the resulting mixture was cooled to 0 °C. A previously prepared solution of the diacidchloride in dichloromethane was added dropwise and the mixture was stirred at 0 °C overnight. The mixture was extracted with brine (1 x 50 mL), the organic layer was dried with Na_2SO_4 and the solvent evaporated under reduced pressure to

give the product as an orange oil. The crude product was used for the next step without purification.

3,3'-dithiobis[N-(methyl 2-aminoethanoate)-2methylpropanamide] (18)

3,3'-dithiobis(2-methylpropanoic acid) (**16**) (5 mmol, 1.05 g) was suspended in 5 mL $SOCl_2$, and the resulting mixture was heated to reflux until complete dissolution of the acid. The solvent was evaporated under reduced pressure to furnish the diacidchloride as pale yellow oil. Triethylamine (22 mmol, 3.05 mL) was added to a solution of methyl 3-aminopropionate*HCl (10 mmol, 1.40 g) in 25 mL of dry dichloromethane, and the resulting mixture was cooled to 0 ^oC. A previously prepared solution of the diacidchloride in dichloromethane was added dropwise, and the mixture was stirred at 0 ^oC overnight. The mixture was extracted with brine (2 x 30 mL), and the organic layer was dried on Na_2SO_4, and the solvent evaporated under reduced pressure to give the product as a brown gum. The crude product was used for the next step without purification.

5-chloro-2-ethyl-4-methylisothiazol-3(2H)-one (19)

The product was obtained using general procedure 3 starting from 3,3'-dithiobis(N-ethyl-2-methylpropanamide) and was purified using column chromatography with EtOAc/Hex 1:6 (v/v) as eluent. The compound was obtained as a yellow liquid (64 mg, 38%): R_f = 0.34 (EtOAc/Hex, 1:2); ^1H NMR (200 MHz, $CDCl_3$): δ = 1.26 (t, *J* = 7.2, 3H), 1.97 (s, 3H), 3.78 ppm (q, *J* = 7.3, 2H). ^{13}C NMR (50 MHz, $CDCl_3$): δ 10.9, 14.8, 39.0, 122.0, 138.4, 166.5 ppm; HPLC: purity 98%, RT = 9.2, mobile phase: H_2O:CH_3CN:TFA 60:40:0.1; HRMS: *m/z* $[M+H]^+$ calcd for $C_6H_9{}^{35}ClNOS$: 178.0088, found: 178.0088.

Methyl 3-(5-chloro-4-methyl-3-oxoisothiazol-2(3H)-yl)propanoate (20)

The product was obtained using general procedure 3 starting from 3,3'-dithiobis[N-(methyl 2-aminopropionate)-2-methylpropanamide] and purified using column chromatography with EtOAc/Hex 1:4 (v/v) as eluent. The compound was obtained as a yellow gum (122 mg, 52%): R_f = 0.44 (EtOAc/Hex, 1:1); ^1H NMR (200 MHz, $CDCl_3$): δ = 1.98 (s, 3H), 2.71 (t, *J* = 6.2 2H), 3.70 (s, 3H), 4.02 ppm (t, *J* = 6.3 2H). ^{13}C NMR (50 MHz, $CDCl_3$): δ = 10.9, 33.8, 39.8, 52.2, 121.5, 139.6, 166.9, 171.7; HPLC: purity 99%, RT = 11.4 min, mobile phase: H_2O:CH_3CN:TFA 60:40:0.1; HRMS: *m/z* $[M+H]^+$ calcd for $C_8H_{11}{}^{35}ClNO_3S$: 236.0142, found: 236.0141.

5-chloro-2-ethyl-4-methylisothiazol-3(2H)-one-1-oxide (21)

The product was obtained using procedure 1 starting from **19** and purified using column chromatography with EtOAc/Hex 1:2 (v/v) as eluent. The compound was

obtained as a colorless liquid (159 mg, 82%): R_f = 0.72 (EtOAc/Hex, 1:1); ^{1}H NMR (200 MHz, $CDCl_3$): δ = 1.32 (t, *J* = 7.3, 3H), 2.05 (s, 3H), 3.69-3.87 ppm (m, 2H). ^{13}C NMR (50 MHz, $CDCl_3$): δ = 10.9, 14.8, 39.0, 122.0, 138.4, 166.5 ppm; HPLC: 98%, RT = 11.8 min, mobile phase: H_2O:CH_3CN:TFA 60:40:0.1; HRMS: *m/z* $[M+H]^+$ calcd for $C_6H_9{}^{35}ClNO_2S$: 194.0037, found: 194.0032.

Methyl 3-(5-chloro-4-methyl-1-oxido-3-oxoisothiazol-2(3H)-yl)propanoate (22)
The product was obtained using procedure 1 starting from **20** and purified using column chromatography with EtOAc/Hex 1:4 (v/v) as eluent. The compound was obtained as a colorless oil (181 mg, 72%): R_f = 0.56 (EtOAc/Hex, 1:1); ^{1}H NMR (200 MHz, $CDCl_3$): δ = 2.04 (s, 3H), 2.69-2.77 (m, 2H), 3.69 (s, 3H), 4.00 ppm (t, *J* = 6.7, 2H). ^{13}C NMR (50 MHz, $CDCl_3$): δ = 10.8, 33.6, 37.4, 52.2, 133.6, 149.8, 165.6, 171.2 ppm; HPLC: purity 97%, RT = 11.2, mobile phase H_2O:CH_3CN:TFA 60:40:0.1; HRMS: *m/z* $[M+H]^+$ calcd for $C_8H_{11}{}^{35}ClNO_4S$: 252.0092, found 252.0091.

Reaction of isothiazolone with propane-1-thiol

A solution 0.1 M of propane-1-thiol (3 mmol, 271 µL) in CH_3CN (30 mL) was prepared. The concentration of free thiol was quantified using 5,5'-Dithio-bis(2-nitrobenzoic acid) (DTNB). A DTNB standard calibration curve was prepared measuring the UV extinction, starting from 1 mM DTNB with an excess of thiol (10 mM). A sample of propane-1-thiol solution (100 µL) was mixed with 20 mM DTNB solution (100 µL). The UV absorbance was measured and the SH content was then calculated from the calibration curve. No significant differences were observed between the calculated and measured concentration. For the reaction, the compound (50 µmol) was dissolved in CH_3CN (2 mL). The previously prepared solution 0.1 M of propanethiol in CH_3CN (50 µmol, 500 µL) was added, and the progress of the reaction was followed by HPLC. As eluent, a mobile phase composition H_2O:CH_3CN:TFA 50:50:0.1 was used and the compounds were identified on the basis of their retention times.

Reaction of isothiazolone with sodium propane-1-thiolate

A solution of sodium propane-1-thiolate in water (30mL) was prepared from propane-1-thiol (272 µL, 3 mmol) and NaOH (108mg, 2.7 mmol). The concentration of free thiolate was quantified using 5,5'-Dithio-bis(2-nitrobenzoic acid (DTNB) as already described. The compound (50 µmol) was dissolved in CH_3CN (2 mL). The solution 0.1 M of sodium propane-1-thiolate (0.1, 0.5 or 1.0 equiv.) was added, and the progress of the reaction was followed by HPLC. As eluent, a mobile phase composition H_2O:CH_3CN:TFA 50:50:0.1 was used, and the compounds were identified on the basis of their retention times.

LogP measurement

The compound (4 mmol) was dissolved in 1-octanol (1 mL). Water (1 mL) was added and the mixture was vigorously shaken with a vortex mixer (3 x 5 min) and centrifuged (2000g, 10 sec). The two layers were separated and analyzed by HPLC. The logP was calculated comparing the area of the peaks of the two layers.

Enzyme inhibition studies

A fluorescent histone acetyltransferase assay described by Trievel *et al*. was used for enzyme inhibition studies.[112] Enzyme inhibition was measured by determination of the residual enzyme activity after 15 min incubation with the inhibitor. The enzyme activity was measured by detection of CoA-SH by the fluorescent dye 7-(diethylamino)-3-(4'-maleimidylphenyl)-4-methylcoumarin (CPM). The CoA-SH concentrations measured with no inhibitor present were around 50 µM. The inhibitor concentrations were maximal 10 µM, so that inhibitory effects of more than 20% at 10 µM inhibitor concentration cannot be explained by direct reaction of the inhibitors with CoA-SH. Compounds that showed more than 50% inhibition at 10 µM (n = 3) were subjected to IC_{50} determination (n = 3). The human recombinant histone acetyltransferase PCAF (p300/CREB-bindingprotein Associated Factor) was obtained from Biomol International. The histone H3 peptide (Ac-QTARKSTGGKAPRKQLATKNH2) was purchased from Pepscan (Lelystad, NL).

Cell Growth Inhibition

All cell culture reagents were purchased from Invitrogen. The human cancer cells HEP G2 (liver) were maintained in Dulbecco's modified Eagles Medium with 10% heat-inactivated fetal calf serum, 50 IU/mL penicillin, and 50 mg/mL streptomycin at 37 °C in a humidified 5% CO_2 incubator. Cell proliferation was measured by a Crystal Violet assay. The cells were seeded at 5000 cells per well into 96-well plates, grown for 24 h, and treated for an additional 48 h with the different inhibitors. The medium was then aspirated, and the cells were fixed with 50 µL 1% crystal violet in 70% ethanol for 30 min. The cells were washed with water and the staining was solubilized by addition of 100 µL 1% SDS in water. The plates were read at 550 nm. A blank extinction value in which no cells were seeded was subtracted from all determinations and cell growth with no inhibitor present was set to 100%. All concentrations were tested in 8-fold on one plate and the GI_{50} values of most potent inhibitors were measured again on a new plate.

CHAPTER 4

IMPROVED INHIBITION OF THE HISTONE ACETYLTRANSFERASE PCAF BY AN ANACARDIC ACID DERIVATIVE

Ghizzoni M, Boltjes A, de Graaf C, Haisma HJ and Dekker FJ;

Bioorganic & Medicinal Chemistry (2010) 18: 5826–5834

Abstract

Several lines of evidence indicate that histone acetyltransferases (HATs) are novel drug targets for treatment of diseases like cancer and inflammation. The natural product anacardic acid is a starting point for development of small molecule inhibitors of the histone acetyltransferase (HAT) p300/CBP associated factor (PCAF). In order to optimize the inhibitory potency, a binding model for PCAF inhibition by anacardic acid was proposed and new anacardic acid derivatives were designed. Ten new derivatives were synthesized using a novel synthetic route. One compound showed a two-fold improved inhibitory potency for the PCAF HAT activity and a two-fold improved inhibition of histone acetylation in HEP G2 cells.

INTRODUCTION

For several diseases treatment with the currently available drugs is not satisfactory, which demonstrates the need for conceptually new drugs for new therapeutic targets. The epigenetic regulation of gene transcription is an area of research in which new therapeutic targets are being discovered. Gene transcription is, among others, regulated by histone acetyltransferases (HATs) (figure 4.1).[90] Deregulation of histone acetylation has been linked to several diseases, including cancer and inflammation, which suggests that HATs are potential anti-inflammatory targets.[89,94,128]

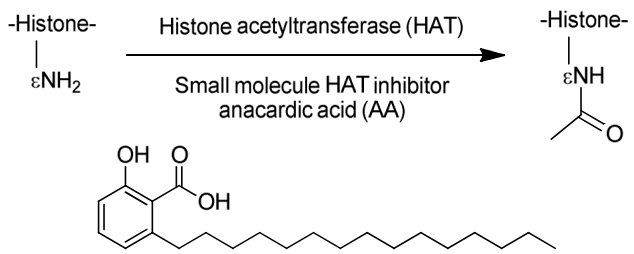

Figure 4.1: *acetylation of histone lysine residues by histone acetyltransferases provides potential anti-inflammatory drug targets. Anacardic acid is a cell-permeable small molecule inhibitor of the histone acetyltransferase PCAF.*

Ultimately, we aim to explore the role of histone acetyltransferases in inflammation by development of small molecule inhibitors. Inflammation involves a variety of inflammatory mediators whose transcription is enhanced during the disease process by global histone acetylation as well as gene specific histone acetylation. Several studies showed a disturbed balance between HAT and HDAC activity in inflammatory diseases. Asthma patients show increased HAT activity in bronchial biopsies, whereas the activity and expression of HDACs are decreased.[29] The same was observed in lung tissue for chronic obstructive pulmonary disease (COPD) patients compared to healthy subjects.[41] Tissue of patients with COPD showed reduced HDAC activity and increased histone H4 acetylation in the interleukin-8 promoter.

Nuclear factor κB (NF-κB) mediated signal transduction plays an important role in inflammation. When activated, NF-κB translocates to the nucleus, where it binds to the κB recognition site of target genes and to cofactors with intrinsic HAT activity such as p300/CBP and PCAF.[32] This leads to global acetylation of lysine residues in histone H4 and opening of the chromatin structure, enabling transcription of

proinflammatory genes, including IL-8.[39] This mechanism is supported by the observation that *Legionella pneumophila*-induced IL-8 release from alveolar epithelial cells is decreased by HAT inhibition and enhanced by HDAC inhibition. These findings suggest that restoring the HAT/HDAC balance by small molecule inhibitors of histone acetylation provides opportunities for treatment of inflammation.[36,41,42,118]

Only a few small molecule inhibitors of HATs are currently available. Potent and selective bisubstrate inhibitors for the HATs p300 and PCAF have been described, however the lack of cell permeability represents a disadvantage.[72] Another well-known class of inhibitors is represented by isothiazolones, which are cell-permeable and potent; however their reactivity limits their specificity.[74,119,120,129] Furthermore, the natural products curcumin, plumbagin, garcinol and anacardic acid (AA, figure 4.1) have been reported as inhibitors of different classes of HATs.[78,80,82,87] Interestingly, it has been demonstrated that anacardic acid suppresses the NF-κB pathway, which shows the potential of this compound to suppress inflammation.[79] Several benzamide derivatives of anacardic acid have been studied for inhibition of p300, however they were either equally potent p300 HAT inhibitors compared to anacardic acid or they activated the p300 HAT.[78,130]

In this study we describe hypothesis-driven optimization of the HAT inhibitory potency of anacardic acid. We proposed a binding model for anacardic acid in the PCAF active site using molecular modeling techniques. Based on this model, a series of new anacardic acid derivatives was designed. A convenient synthetic route was developed to synthesize these derivatives. We varied the 6-alkyl chain of anacardic acid by different substituent in order to improve the potency and the drug likeness of these inhibitors. A series of 10 anacardic acid derivatives was synthesized and their inhibitory potency for the recombinant HAT PCAF enzyme and for histone acetylation in HEP G2 cells was studied.

RESULTS AND DISCUSSION

Molecular docking studies

The crystal structure of PCAF in complex with Coenzyme A (CoA) has been published previously.[104] Using this structure, docking studies were performed in order to propose a possible binding mode for anacardic acid. We hypothesized that the salicylate group of anacardic acid mimics the pyrophosphate group of CoA, which forms an extensive H-bond network with the backbone amide nitrogens of V582,

G584, G586, and T587, with the sidechain hydroxyl of T587, and with the water molecule w6 (figure 4.2a). This active site water molecule is further stabilized by an H-bond network with the backbone of E580, K583, and Y585 (figure 4.2a). Docking simulations including this essential water molecule indeed yielded a (highest ranked) pose of anacardic acid similar to the CoA binding mode (figure 4.2b), in which the carboxylic group accepts H-bonds from the backbone of K583, G584, G586, and w6, the hydroxyl group donates a H-bond to the T587 sidechain in the pyrophosphate binding pocket, and the long alkyl chain of anacardic acid protrudes deep into the hydrophobic pantothenic acid binding pocket between beta strand 4 (ß4) and alpha helix 4 (α4) (figure 4.2b). The anacardic acid binding mode is further stabilized by aromatic edge-to-face stacking between the salicylate ring and Y616.

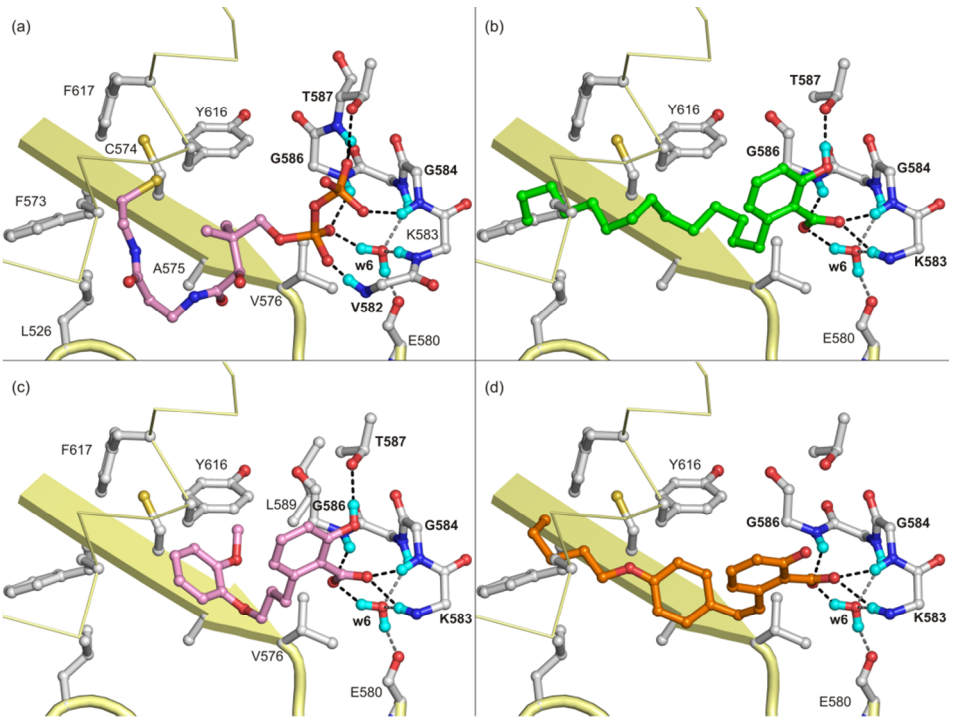

Figure 4.2: *(a) binding mode of the natural substrate CoA bound to the HAT PCAF active site (PDB code 1CM0). Only the pantothenic acid and the pyrophosphate of CoA are shown. The substrate carbon atoms are shown in purple. Docked binding configurations of anacardic acid (b) (carbons atoms in green), compound* ***4e*** *(c) (carbon atoms in pink), and compound* ***6d*** *(d) (carbon atoms in orange). Helix α4 and beta strand β4 are represented by yellow ribbons. Important binding residues are shown as ball-and-sticks with grey carbon atoms. Oxygen, nitrogen sulphur, phosphor, and hydrogen atoms are colored red, blue, yellow, orange, and cyan, respectively. Protein-ligand as well as w6-ligand and protein-w6 H-bonds described in the text are shown as black or grey dotted lines.*

This molecular docking pose was used as starting point for the design of new molecules and to rationalize structure-activity relationships. First of all, the role of the hydrophobic chain in the binding to the pantothenic acid pocket between α4 and β4 was investigated. Secondly, it was hypothesized that incorporation of a second aromatic ring could further stabilize ligand binding via additional aromatic stacking interactions with Y616. Thirdly, the acidity of the carboxyl group was modulated by introduction of substituents on the salicylate ring. In silico predicted binding modes of novel potent anacardic acid-based PCAF ligands (figure 4.2 c-d) will be discussed in the paragraph *"2.3. Enzyme inhibition assay"*.

Chemistry

A convenient synthetic method was developed in order to synthesize a diverse series of compounds with a salicylate functionality. Several syntheses of anacardic acid have been described so far, however these routes require harsh conditions that are not compatible with many functional groups.[131-133] Therefore, a new synthetic route was developed, in which a Sonogashira coupling is the key step (scheme 4.1).

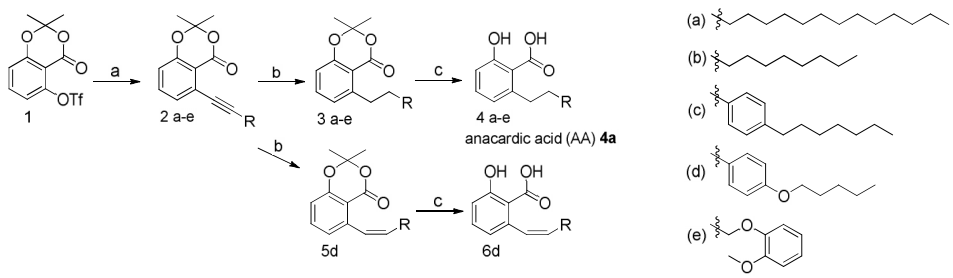

Scheme 4.1: *synthesis of anacardic acid derivatives: reagents and conditions: a) CuI, $PdCl_2(PPh_3)_2$, Et_2NH, HC≡CR, CH_3CN, 70 °C; b) H_2, Pd/C, MeOH, 40 °C; c) KOH 5 N, THF, 55 °C*

Triflate **1** was synthesized according to previously published procedures, starting from the commercially available 2,6-dihydroxybenzoic acid.[134] Different terminal alkynes were coupled in presence of CuI, diethylamine, and $PdCl_2(PPh_3)_2$ to give the correspondent alkynyls **2**. The Sonogashira reaction, performed in acetonitrile at 70 °C on oil bath, required 2 hours to give the product with high yields (80-90%). The same reaction was also performed in acetonitrile at 100 °C with microwave irradiation. In this case, the product was obtained in comparable yields after just 30 min. Hydrogenation, using palladium on activated carbon as catalyst, was used to reduce the akynyl triple bond to a single bond. The best yields (60-80%) were obtained if hydrogenation was performed for 16 h, with 3 atm. H_2-pressure in

methanol at 40 °C. In case of compound **2d**, hydrogenation under the described conditions gave the correspondent cis-alkene **5d** (J = 12.1 Hz). To obtain the alkane **3d**, it was necessary to perform hydrogenation for 40 h. The last step in this synthetic route was the cleavage of the acetonide protecting group. This was achieved by saponification with KOH 5 N at 55 °C with yields between 50% and 80%.

Structures of 4-hydroxy-6-alkyl-salicylates **12a** and **12b** (scheme 4.2) are closely related to another natural compound known as olivetolic acid, an intermediate in the biosynthesis of cannabinoids.[135] A synthetic route towards these compounds has been described by Dushin and Danishefsky.[136] This route implicates a Sonogashira coupling on **7**, followed by hydrogenation to give the correspondent **9**. Cleavage of the acetonide **9** to yield **12** poses a challenge. Saponification by hydroxide (OH^-) can only be performed under forcing conditions due to deprotonation of the 4-hydroxy group and concomitant electron-donation to the carboxylate. Acidic cleavage of the acetonide will result in decarboxylation.[137] We designed another route to avoid these problems (Scheme 2). Building block **10** was employed for Sonogashira coupling to terminal alkenes.[138] The resulting alkynyls gave the desired product upon hydrogenation concomitant with hydrogenolysis of the benzyl group.

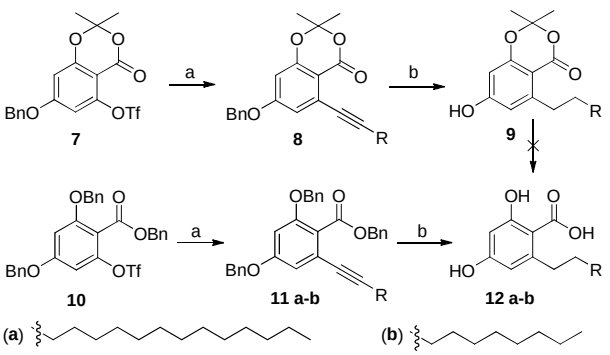

Scheme 4.2: *synthesis of olivetolic acid derivatives: reagents and conditions: a) CuI, $PdCl_2(PPh_3)_2$, Et_2NH, HC≡CR, CH_3CN, 70 °C; b) H_2, Pd/C, MeOH, 40 °C*

Anacardic acid derivatives with an alkoxy function in the 2-position were synthesized starting from **13** (scheme 4.3). Compound **13** was converted to **14** using a Williamson ether synthesis with benzyl bromine (yield 83%). In contrast, reaction of **13** with tetradecylchloride did not give the desired product. Compound **16** was obtained by Mitsunobu coupling between **13** and tetradecanol (yield 29%). Saponification of **14** and **16** provided the corresponding free carboxylic acids **15** and **17** with yields of 49% and 66% respectively. Compound **18** was synthesized from anacardic acid using a catalytic amount of H_2SO_4 in methanol.

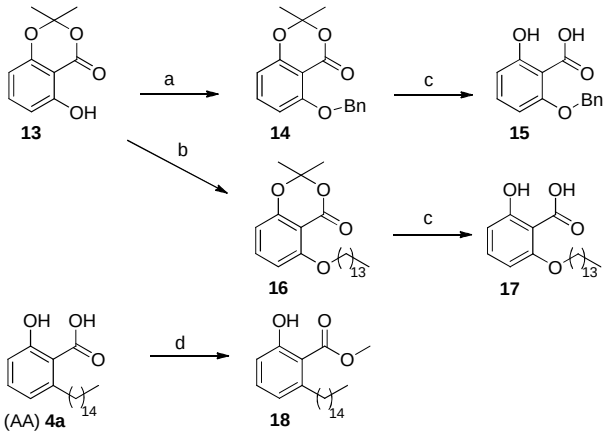

Scheme 4.3: *reagents and conditions: a) Benzylbromide, K_2CO_3, DMF; b) tetradecanol, PPh_3, DIAD, THF; c) KOH 5N, THF, 55 °C; d) H_2SO_4, MeOH, reflux.*

Enzyme inhibition assay

The synthesized compounds were tested for inhibition of the HAT PCAF using an indirect ELISA assay in order to study their binding properties and structure-activity relationship. The ELISA was based on detection of acetylated lysine residues on a histone H4 peptide using an anti-acetyl-lysine antibody. Human recombinant PCAF was used as source of HAT activity. Anacardic acid (AA) **4a** showed around 40% inhibition at 1 mM (figure 4.3), which would give an estimated IC_{50} value between 1 and 2 mM. The potency measured in our assay is 100-fold lower than the estimation by Balsubramanyam *et al.* but in line with the IC_{50} reported by Wu *et al.*[73,78] The differences might be explained by the fact that Wu *et al.* used comparable Ac-CoA concentrations, whereas Balsubramanyam *et al.* used lower Ac-CoA concentrations in the enzyme inhibition assay. Furthermore, differences in assay buffer composition or differences in the enzyme source might cause differences in IC_{50} values.

Several modifications of the salicylate moiety were investigated to slightly modulate the acidity of the carboxyl group. Compounds **12a** and **12b** showed comparable potency as observed for compounds AA **4a** and **4b**, respectively. These data show that the introduction of a hydroxyl group in the 4-position of the salicylate does not influence the inhibitory properties. Introduction of an alkoxy group in the 6-position of the salicylate ring **17** did not lead to significant changes in potency. The methyl ester of anacardic acid was synthesized to study the importance of a free

carboxylic acid for the interaction with PCAF, however the water solubility of **18** is too low for testing at 1 mM concentration in our assay.

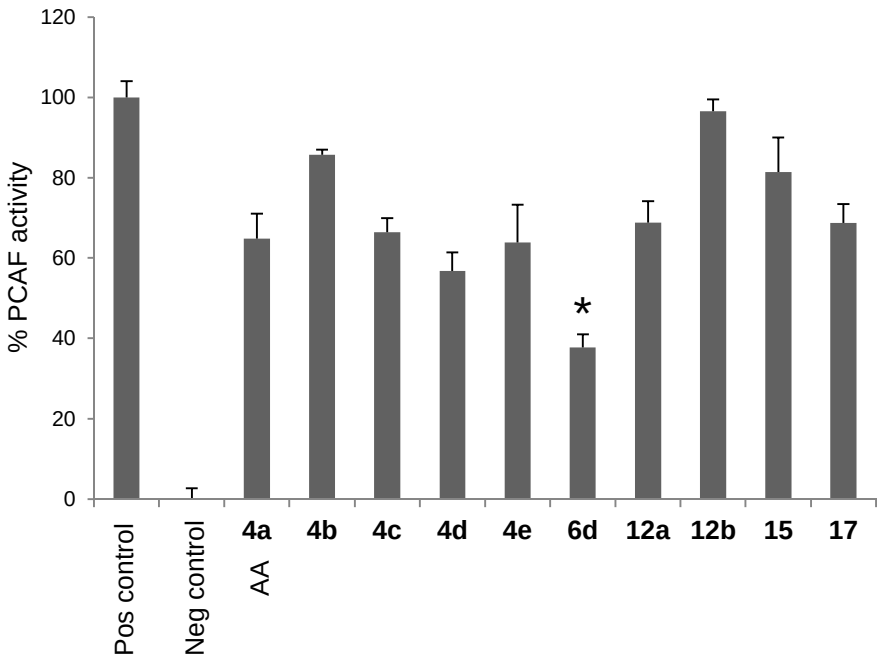

Figure 4.3: *inhibition of the HAT PCAF by different compounds at 1 mM. Data are expressed as percentage of PCAF activity (n=3, *P<0.05 compared to AA **4a**).*

The role of the hydrophobic interactions for the ligand potency was investigated by modifications of the hydrophobic alkyl chain. Compounds **4c** and **4d** showed inhibition comparable to anacardic acid, indicating that introduction of an aromatic ring in the chain did not affect the inhibitory properties. On the other hand, compounds **4b** and **12b** were less potent than the correspondent AA **4a** and **12a**, indicating that one-third reduction of the chain length causes loss of potency. Also compound **15**, with a benzyl group instead of the long alkylic chain, showed less than 20% inhibition at 1mM. These data suggest that hydrophobic interactions at the end of the CoA binding pocket are important for binding. This observation is in line with the proposed binding mode of anacardic acid (figure 4.2b), which is stabilized by hydrophobic interactions deep in the pantothenic acid pocket between α4 and β4 (figure 4.1a).

Interestingly, incorporation of a 3-(2-methoxyphenoxy)propyl moiety **4e** provided equal inhibition to AA **4a**. In the highest ranked docking pose of **4e** (figure 4.2c), the

2-methoxyphenoxy ring stacks between the aromatic rings of Y616 and F617, whereas the 2-methoxy group can be accommodated in a small additional pocket between L589, V576 and Y616. Compound **4e** provides a good platform for further structural variation in order to optimize the inhibitory potency of this compound class.

Compound **6d** is the only compound that proved to be more potent than anacardic acid in our assay. We measured for this compound an IC_{50} of 662 ± 64 µM (figure 4.4). Remarkably, compounds **4c** and **4d**, also including a second benzyl group, but lacking the *cis* double bond, did not show increased potency compared to anacardic acid **4a**. In the highest ranked docking pose of compound **6d**, the salicylate moiety is hydrogen bonded to the pyrophosphate binding pocket as described for anacardic acid **4a** (figure 4.2d). In addition, the geometry of the *cis*-double bond forces the phenoxy ring in an optimal conformation for face-to-edge aromatic stacking with Y616 and orientates the hydrophobic tail of the molecule deep into the hydrophobic binding cleft between α4 and β4 (figure 4.2d) . This conformational restriction could explain the increased potency of **6d** compared to **4d**. Furthermore, compound **6d** has improved druglike properties compared to anacardic acid. In conclusion, compounds **6d** and **4e** provide a starting point for the design of new PCAF inhibitors.

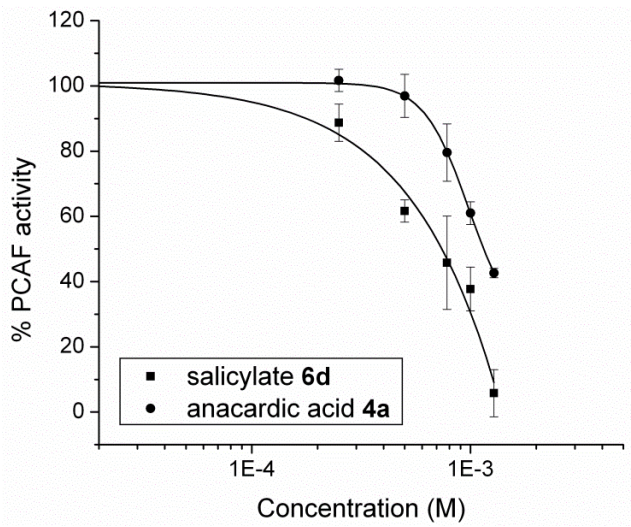

Figure 4.4: *IC_{50}'s for inhibition of PCAF HAT activity by anacardic acid **4a** and salicylate **6d**.*

Cell-based study

Since compound **6d** was more potent than anacardic acid **4a**, we decided to test the effects of **6d** on histone acetylation in a cell-based study. Histone H4 acetylation levels in HEP G2 cells were measured using an anti-acetyl histone H4 antibody. The HDACs inhibitor suberoylanilide hydroxamic acid (SAHA) was used to increase the basal histone acetylation. Cells were treated for 24 h with 5 µM SAHA and co-treated with different concentration of **6d** and anacardic acid **4a**. The cells were treated with subtoxic concentrations of the inhibitors. Figure 4.5a shows that SAHA increased histone H4 acetylation levels significantly. Compound **6d** decreased the acetylation induced by SAHA in HEP G2 cells at 30 µM and 60 µM. The decrease is stronger than observed for a comparable concentration of anacardic acid (AA) **4a**. Quantification of the western blot results (figure 4.5b) showed a significant increased inhibition for compound **6d** compared to AA **4a** ($P<0.01$). These data demonstrate that compound **6d** is a useful tool to inhibit histone acetylation in cell-based studies. Differences between the effective concentrations between the inhibition of the recombinant enzyme and the cell-based studies might originate from factors such as differences in the assay buffer composition, differences in the Ac-CoA concentration or differences in the enzyme source. Furthermore, the fact that higher concentrations of AA **4a** and **6d** were required to inhibit the recombinant enzyme PCAF compared to the cell-based studies could indicate that these compounds target different histone acetyltransferases in the cell-based studies.

CONCLUSION

In this study we describe the development of a salicylate derivative **6d** with improved inhibition of histone acetylation compared to the natural product anacardic acid. A binding configuration of anacardic acid in the HAT PCAF active site was proposed using molecular modeling. In this binding model, the salicylate is bounded in the pyrophosphate binding pocket and the alkyl chain is located in the CoA substrate binding cleft. Based on this model, new anacardic acid derivatives were designed in order to explore the role of the alkyl chain and the importance of the salicylate moiety. A convenient synthetic route towards anacardic acid was developed and 10 derivatives were synthesized. Testing of the inhibitory potency for the PCAF HAT activity showed that one derivative had a 2-fold improved inhibitory potency for the HAT PCAF recombinant enzyme. Moreover, this derivative showed also a 2-fold improved potency for inhibition of histone H4 acetylation in cell-based

studies on HEP G2 cells. This is the first report on hypothesis-driven optimization of the HAT PCAF inhibition.

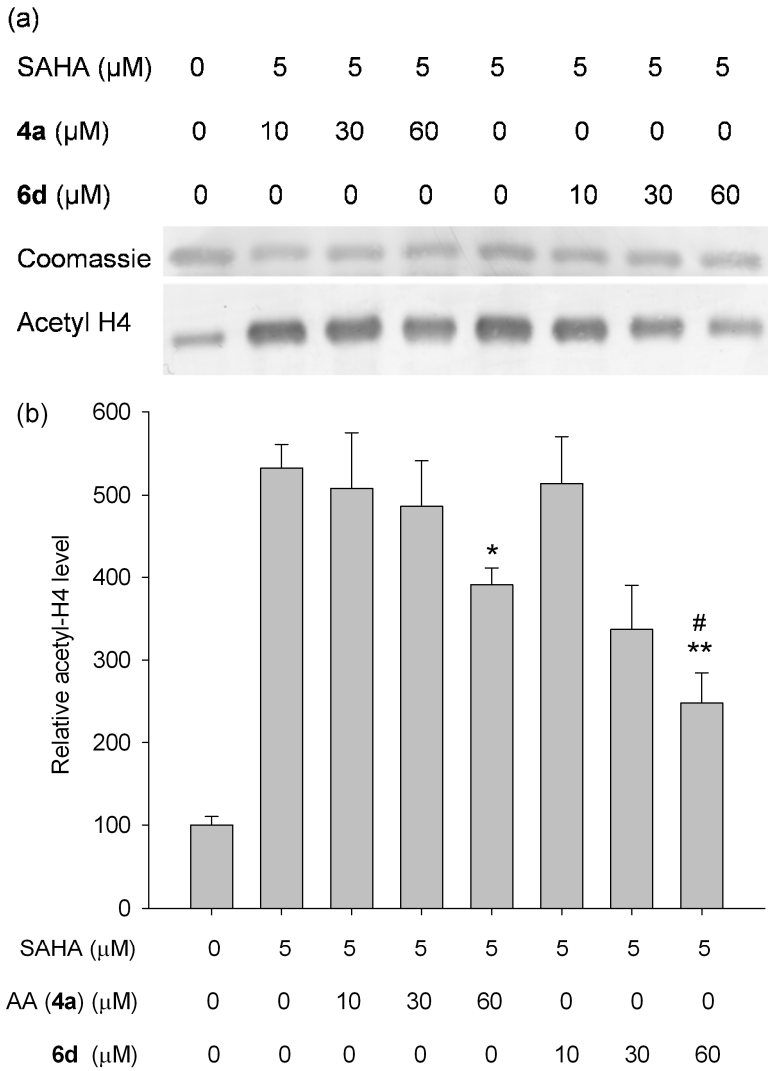

Figure 4.5: *cell-based studies on histone H4 acetylation levels in HEP G2 cells. a) Western blot of histone extracts of HEP G2 cells after 24h treatment with different concentrations of the indicated compounds. Coomassie brilliant blue staining was used to determine equal amount of loading. b) Quantification of Histone H4 acetylation levels: values are shown in comparison to histone acetylation levels of non-treated cells (100%) and expressed as mean ± SEM of three independent experiments. *P<0.05, **P<0.01 compared to SAHA stimulated samples. #P<0.01 compared to SAHA - AA* ***4a*** *(60 µM) treated samples.*

EXPERIMENTAL SECTIONS

Chemistry

Chemicals were purchased from Sigma–Aldrich and Acros Organics, and used without further purification. Solvents were dried before use according to known procedures and all the reactions were carried-out under a nitrogen atmosphere. Analytical thin-layer chromatography (TLC) was performed on aluminum sheets of Silica Gel 60 F254. Ultraviolet light, $KMnO_4$ solution or ninhydrin solution were used to visualize bands. All microwave irradiation reactions were carried out in a Biotage Initiator™ Microwave Synthesizer. Column chromatography was performed with MP Ecochrom Silica Gel 32–63, 60 Å. ^1H and ^{13}C NMR spectra were recorded on a Varian Gemini-200. ^{13}C spectra were recorded using the attached proton test (APT) pulse sequence. Chemical shift values are reported as part per million (δ) relative to residual solvent peaks ($CDCl_3$, ^1H δ = 7.26, ^{13}C δ = 77.16 or CD_3OD, ^1H δ = 3.31, ^{13}C δ = 49.00). The coupling constants (J) are reported in Hertz (Hz). Electrospray ionization mass spectra (ESI-MS) were recorded on an Applied Biosystems/SCIEX API3000-triple quadrupole mass spectrometer. High-resolution mass spectra (HR-MS) were recorded using a flow injection method on a LTQ-Orbitrap XL mass spectrometer (Thermo Electron, Bremen, Germany) with a resolution of 60,000 at m/z 400. Protonated testosterone (lock mass m/z = 289.2162) was used for internal recalibration in real time. Melting points were determined on an Electrothermal digital melting point apparatus and are uncorrected.

Synthetic procedure 1

Freshly distilled diethylamine (3.0 mmol, 0.30 mL) and the alkyne (2.2 mmol) were subsequently added to a solution of the triflate (2.0 mmol), CuI (0.20 mmol, 38 mg), and $PdCl_2(PPh_3)_2$ (0.01 mmol, 70 mg) in degassed anhydrous acetonitrile (6.0 mL). The mixture was either stirred for 2 h at 70 °C on oil bath or subjected to microwave irradiation for 30 min at 100 °C (70W). Water (10 mL) was added and the mixture was extracted with EtOAc (3 x 30 mL). The combined organic phases were washed with brine (1 x 60 mL), dried over Na_2SO_4 and filtered. The solvent was evaporated under reduced pressure and the residue was purified by column chromatography.

Synthetic procedure 2

A suspension of the starting material (1.5 mmol) and Pd/C (10%) (0.15 mmol) in methanol (30 mL) was shaken overnight at 40 °C, with 3 atm. H_2-pressure in a PARR apparatus. The mixture was filtered through Celite, and the filtrate was

concentrated under reduced pressure. The residue was purified by column chromatography.

Synthetic procedure 3

The starting material (1.0 mmol) was dissolved in THF (2.0 mL). KOH 5 N (10 mmol, 2.0 mL) was added and the solution was stirred overnight at 55 °C. The reaction mixture was diluted with EtOAc (10 mL) and acidified with 1 N HCl (20 mL). The mixture was extracted with EtOAc (3 x 30 mL). The organic phases were collected, washed with brine (1 x 50 mL), dried over Na_2SO_4 and filtered. The solvent was evaporated and the product was purified by column chromatography or crystallization.

2,2-dimethyl-5-(pentadec-1-ynyl)-4H-benzo[d][1,3]dioxin-4-one (2a)

The product was obtained using procedure 1 starting from **1** (0.65 g, 2.0 mmol) and 1-pentadecyne (0.46 g, 2.2 mmol), using oil bath heating. The crude product was purified using column chromatography with EtOAc/Hex 1:6 (v/v) as eluent to yield **2a** (0.65 g, 85%) as a brown solid; R_f = 0.60 (EtOAc/Hex 1:2); ^{1}H NMR (200 MHz, $CDCl_3$): δ = 0.87 (3H, t, J = 6.5 Hz), 1.20-1.65 (22H, m), 1.70 (6H, s), 2.50 (2H, t, J = 7.1 Hz), 6.85 (1H, d, J = 8.5Hz), 7.18 (1H, d, J = 7.6Hz), 7.38 ppm (1H, t, J = 7.9Hz); ^{13}C NMR (50 MHz, $CDCl_3$): δ = 14.3, 20.2, 22.9, 25.9, 28.7, 29.2, 29.4, 29.6, 29.7, 29.9, 32.1, 78.9, 98.8, 105.7, 114.2, 116.6, 126.5, 129.1, 134.9, 156.6, 161.6 ppm; MS (ESI): m/z 385.5 $[M+H]^+$.

2,2-dimethyl-5-(dec-1-ynyl)-4H-benzo[d][1,3]dioxin-4-one (2b)

The product was obtained using procedure 1 starting from **1** (0.65 g, 2.0 mmol) and 1-decyne (0.30 mg, 2.2 mmol) using oil bath heating. It was purified by column chromatography using EtOAc/Hex 1:5 (v/v) as eluent. The product was obtained as a brown solid (0.52 g, 86%); R_f = 0.58 (EtOAc/Hex 1:1); ^{1}H NMR (200 MHz, $CDCl_3$): δ = 0.86 (3H, t, J = 6.5 Hz), 1.27-1.65 (12H, m), 1.68 (6H, s), 2.48 (2H, t, J = 6.9 Hz), 6.84 (1H, d, J = 8.2 Hz), 7.17 (1H, d, J = 7.6 Hz), 7.38 ppm (1H, t, J = 8.1 Hz); ^{13}C NMR (50 MHz, $CDCl_3$): δ = 14.2, 20.1, 22.8, 25.8, 28.6, 29.1, 29.2, 29.3, 32.0, 78.8, 98.7, 105.5, 114.2, 116.5, 126.5, 129.0, 134.8, 156.6, 159.1 ppm; MS (ESI): m/z 315.3 $[M+H]^+$.

5-((4-heptylphenyl)ethynyl)-2,2-dimethyl-4H-benzo[d][1,3]dioxin-4-one (2c)

The product was obtained using procedure 1 starting from **1** (0.65 g, 2.0 mmol) and 1-ethynyl-4-heptylbenzene (0.44 g, 2.2 mmol) using oil bath heating. The residue was purified by column chromatography using EtOAc/Hex 1:14 (v/v) as eluent. The product was obtained as a brown solid (0.66 g, 88%); R_f = 0.62 (EtOAc/Hex 1:5); ^{1}H

NMR (200 MHz, $CDCl_3$): δ = 0.88 (3H, t, J = 6.6 Hz), 1.26-1.73 (8H, m), 1.59 (2H, m), 1.73 (6H, m), 2.62 (2H, t, J = 7.65 Hz), 6.89-6.93 (1H, m), 7.17 (2H, d, J = 8.2 Hz), 7.28-7.33 (1H, m), 7.42-7.46 (1H, m), 7.50-7.57 ppm (2H, d, J = 8.2 Hz); ^{13}C NMR (50 MHz, $CDCl_3$): δ = 14.2, 22.8, 25.9, 29.2, 29.3, 31,3, 31.9, 36.1, 87.2, 96.8, 105.7, 114.0, 117.0, 120.2, 125.8, 128.5, 128.6, 132.1, 134.9, 144.2, 156.8, 159.0 ppm; MS (ESI): m/z 377.3 $[M+H]^+$.

2,2-dimethyl-5-((4-(pentyloxy)phenyl)ethynyl)-4H-benzo[d][1,3] dioxin-4-one (2d)

The product was obtained using procedure 1 starting from **1** (0.65 g, 2.0 mmol) and 1-eth-1-ynyl-4-(pentyloxy)benzene (0.41 g, 2.2 mmol) using either oil bath heating or microwave irradiation. The residue was purified by column chromatography using EtOAc/Hex 1:6 (v/v) as eluent. The product was obtained as brown oil. The yield was 80% (0.58 g) after oil bath heating and 84% (0.61 g) after microwave irradiation; R_f = 0.57 (EtOAc/Hex 1:2); ^{1}H NMR (200 MHz, $CDCl_3$): δ = 0.72 (3H, t, J = 6.9 Hz), 1.21-1.17 (4H, m), 1.50-1.52 (8H, m), 3.74 (2H, t, J = 6.6 Hz), 6.62-6.68 (3H, m), 7.03-7.08 (1H, m), 7.20 (1H, d, J = 7.9 Hz), 7.31-7.36 ppm (2H, m); ^{13}C NMR (50 MHz, $CDCl_3$): δ = 14.1, 22.5, 25.8, 28.2, 29.0, 68.1, 86.7, 96.9, 105.7, 113.8, 114.6, 114.9, 116.7, 126.0, 128.2, 133.7, 134.9, 135.3, 156.7, 159.1, 159.8 ppm; MS (ESI): m/z 365.2 $[M+H]^+$.

5-(3-(2-methoxyphenoxy)prop-1-yn-1-yl)-2,2-dimethyl-4H-benzo [d][1,3]dioxin-4-one (2e)

The product was obtained using procedure 1 starting from **1** (0.65 g, 2.0 mmol) and 1-methoxy-2-(prop-2-yn-1-yloxy)benzene (0.36 g, 2.2 mmol) using either oil bath heating or microwave irradiation. The residue was purified by column chromatography using EtOAc/Hex 1:5 (v/v) as eluent. The product was obtained as yellow oil in 88% yield (0.60 g) after bath heating and 86% yield (0.58 g) after microwave irradiation; R_f = 0.43 (EtOAc/Hex 1:2); ^{1}H NMR (200 MHz, $CDCl_3$): δ = 1.79 (6H, s), 3.97 (3H, s), 5.16 (2H, s), 6.98-7.07 (4H, m), 7.29-7.35 (2H, m), 7.46-7.54 ppm (1H, m); ^{13}C NMR (50 MHz, $CDCl_3$): δ = 25.8, 56.0, 57.9, 85.1, 91.2, 105.8, 111.8, 115.0, 117.8, 121.0, 122.2, 124.6, 129.3, 135.0, 147.2, 149.8, 156.6, 158.8 ppm; MS (ESI) m/z: 356.2 $[M+NH_4]^+$.

2,2-dimethyl-5-pentadecyl-4H-benzo[d][1,3]dioxin-4-one (3a)

The product was obtained using procedure 2 starting from **2a** and it was purified by column chromatography using EtOAc/Hex 1:6 (v/v) as eluent. The product was obtained as colourless solid (0.31 g, 60%); R_f = 0.61 (EtOAc/Hex 1:2); ^{1}H NMR (200 MHz, $CDCl_3$): δ = 0.87 (3H, t, J = 6.5 Hz), 1.20-1.60 (26H, m), 1.69 (6H, s), 3.08 (2H,

t, *J* = 7,6 Hz), 6.79 (1H, d, *J* = 8.2 Hz), 6.92 (1H, d, *J* = 7.6 Hz), 7.38 ppm (1H, t, *J* = 7.9 Hz). ^{13}C NMR (50 MHz, $CDCl_3$): δ = 14.3, 22.8, 25.8, 29.5, 29.6, 29.8, 31.3, 32.1, 34.5, 105.1, 112.2, 115.2, 125.2, 135.2, 148.7, 157.2, 160.3ppm; MS (ESI): *m/z* 389.5 $[M+H]^+$.

2,2-dimethyl-5-decyl-4H-benzo[d][1,3]dioxin-4-one (3b)

The product was obtained using procedure 2 starting from **2b** and it was purified by column chromatography using EtOAc/Hex 1:5 as eluent. The product was obtained as a white solid (0.29 g, 65%); R_f = 0.60 (EtOAc/Hex 1:1); ^{1}H NMR (200 MHz, $CDCl_3$): δ = 0.87 (3H, t, *J* = 6.8 Hz), 1.25-1.66 (16H, m), 1.69 (6H, s), 3.08 (2H, t, *J* = 7.6 Hz), 6.78 (1H, d, *J* = 8.2 Hz), 6.92 (1H, d, *J* = 7.6 Hz), 7.38 ppm (1H, t, *J* = 7.9 Hz); ^{13}C NMR (50 MHz, $CDCl_3$): δ = 14.3, 22.8, 25.8, 28.7, 29.5, 29.6, 29.8, 31.3, 32.1, 33.4, 34.5, 105.1, 112.2, 115.2, 125.2, 135.2, 148.7, 157.2, 160.4 ppm; MS (ESI): *m/z* 319.3 $[M+H]^+$.

5-(4-heptylphenethyl)-2,2-dimethyl-4H-benzo[d][1,3]dioxin-4-one (3c)

The product was obtained using procedure 2 starting from **2c** and it was purified by column chromatography using EtOAc/Hex 1:12 as eluent. The product was obtained as dark yellow solid (0.55 g, 97%); R_f = 0.41 (EtOAc/Hex 1:5); ^{1}H NMR (200 MHz, $CDCl_3$): δ = 0.88 (3H, t, *J* = 6.5 Hz), 1.30 (8H, m), 1.60 (2H, m), 1.69 (6H, m), 2.56 (2H, t, *J* = 7.6), 2.86 (2H, t, *J* = 8.0), 3.38 (2H, t, *J* = 8.0), 6.79-6.90 (2H, m), 7.06-7.19 (4H, m), 7.34-7.42 ppm (1H, m); ^{13}C NMR (50 MHz, $CDCl_3$): δ = 14.2, 22.8, 25.8, 29.3, 29.4, 31.7, 31.9, 35.7, 36.8, 37.2, 105.1, 105.2, 112.3, 115.5, 125.5, 125.9, 127.2, 128.4, 128.6, 128.9, 135.2, 139.0, 140.6, 147.4, 157.2, 160.4 ppm; MS (ESI): *m/z* 381.3 $[M+H]^+$.

2,2-dimethyl-5-(4-(pentyloxy)phenethyl)-4H-benzo[d][1,3]dioxin-4-one (3d)

A suspension of the starting material **2d** (0.55 g, 1.5 mmol) and Pd/C (10%) (16 mg, 0.15 mmol) in methanol (30 mL) was stirred under 3 atm. H_2 pressure at 40 °C for 36 h in a PARR apparatus. The mixture was filtered through Celite and the filtrate was concentrated under reduced pressure. The residue was purified by column chromatography using EtOAc/Hex 1:14 (v/v) as eluent. The product was obtained as yellow oil (0.51 g, 93%); R_f = 0.38 (EtOAc/Hex 1:10); ^{1}H NMR (200 MHz, $CDCl_3$): δ = 0.88 (3H, t, *J* = 3.5 Hz), 1.38-1.44 (4H, m), 1.70 (6H, s), 1.73-1.79 (2H, m), 2.84 (2H, t, *J* = 8.1 Hz), 3.36 (2H, t, *J* = 7.9 Hz), 3.93 (2H, t, *J* = 6.8 Hz), 6.80-6.84 (m, 2H), 6.86 (1H, d, *J* = 7.7 Hz), 7.06 (1H, d, *J* = 8.5 Hz), 7.14-7.16 (m, 2H), 7.35-7.39 ppm (m, 1H); ^{13}C NMR (50 MHz, $CDCl_3$): δ = 14.1, 22.5, 25.7, 28.3, 29.1, 34.9, 36.7, 36.9, 68.0, 105.1, 112.2, 114.4, 115.4, 125.5, 129.3, 129.6, 133.7, 135.2, 147.2, 157.2 157.4, 160.0 ppm; MS (ESI): *m/z* 369.4 $[M+H]^+$.

5-(3-(2-methoxyphenoxy)propyl)-2,2-dimethyl-4H-benzo[d][1,3] dioxin-4-one (3e)

The product was obtained using procedure 2 starting from **2e** and it was purified by column chromatography using EtOAc/Hex 1:8 (v/v) as eluent. The product was obtained as yellow oil (0.46 g, 90%); R_f = 0.49 (EtOAc/Hex 1:2); ^{1}H NMR (200 MHz, $CDCl_3$): δ = 1.70 (3H, m), 2.13-2.24 (2H, m), 3.28 (2H, t, J = 7.6 Hz), 3.87 (3H, s), 4.09 (2H, t, J = 6.6 Hz), 6.82 (1H, d, J = 7.0 Hz), 6.90 (4H, m), 6.98 (1H, d, J = 7.6 Hz), 7.36-7.44 ppm (1H, t, J = 7.9 Hz); ^{13}C NMR (50 MHz, $CDCl_3$): δ = 26.4, 31.1, 31.5, 56.7, 69.1, 105.8, 112.7, 114.1, 116.2, 121.7, 126.1, 126.1, 135.9, 147.7, 149.3, 150.3, 158.0, 161.0 ppm; MS (ESI) m/z 360.3 $[M+H]^+$.

2-pentadecyl-6-hydroxybenzoic acid (anacardic acid, 4a)

The product was obtained using procedure 3 starting from **3a** and it was purified by crystallization from EtOAc/Hex 1:6 (v/v) at 4 °C. The product was obtained as a white solid (0.30 g, 85%); R_f = 0.31 (100% EtOAc); mp: 90-91 °C ; ^{1}H NMR (200 MHz, $CDCl_3$): δ = 0.88 (3H, t, J = 6.5 Hz), 1.20-1.50 (24H, m), 1.55-1.60 (2H, m), 2.97 (2H, t, J = 7.6 Hz), 6.77 (1H, d, J = 7.3 Hz), 6.87 (1H, d, J = 8.2 Hz), 7.36 ppm (1H, t, J = 7.9 Hz); ^{13}C NMR (50 MHz, $CDCl_3$): δ = 14.4, 22.9, 29.6, 29.7, 29.9, 30.1, 32.2, 32.3, 36.7, 110.6, 116.1, 123.0, 135.7, 148.1, 163.9, 176.4 ppm; HRMS: m/z $[M-H]^-$, calcd for $C_{22}H_{35}O_3$ 347.2586, found 347.2576.

2-decyl-6-hydroxybenzoic acid (4b)

The product was obtained using procedure 3 starting from **3b** and it was purified by column chromatography using EtOAc/Hex 1:6 (v/v) as eluent. The product was obtained as pale yellow solid (0.14 g, 51%); R_f = 0.53 (100% EtOAc); mp: 81-82 °C; ^{1}H NMR (200 MHz, $CDCl_3$): δ = 0.87 (3H, t, J = 6.5 Hz), 1.20-1.45 (14H, m), 1.50-1.60 (2H, m), 2.98 (2H, t, J = 7,6 Hz), 6.78 (1H, d, J = 7.6 Hz), 6.87 (1H, d, J = 7.6Hz), 7.36 ppm (1H, t, J = 7.9 Hz); ^{13}C NMR (50 MHz, $CDCl_3$): δ = 14.3, 22.8, 29.4, 29.5, 29.6, 29.8, 30.0, 32.1, 32.2, 36.6, 110.5, 116.0, 122.9, 135.6, 148.0, 163.8, 176.3 ppm; HRMS: m/z $[M-H]^-$ calcd for $C_{17}H_{25}O_3$ 277.1804, found 277.1807.

2-(4-heptylphenethyl)-6-hydroxybenzoic acid (4c)

The product was obtained using procedure 3 starting from **3c** and it was purified by column chromatography using EtOAc/Hex 1:2 (v/v) as eluent. The product was obtained as white powder (0.23 g, 67%); R_f = 0.4 (100% EtOAc); mp: 110-111 °C; ^{1}H NMR (200 MHz, $CDCl_3$): δ = 1.03 (3H, t, J = 5.5 Hz), 1.43-1.46 (8H, m), 1.71-1.78 (2H, m), 2.72 (2H, t, J = 7.6 Hz), 3.00-3.08 (2H, m), 3.40-3.48 (2H, m), 6.86 (1H, d, J = 7.5 Hz), 7.06 (1H, d, J = 7.5 Hz), 7.20 (4H, m), 7.39-7.56 ppm (1H, m); ^{13}C NMR (50 MHz, $CDCl_3$): δ = 14.2, 22.8, 29.3, 29.5, 31.7, 32.0, 35.7, 38.0, 38.7, 110.6, 116.4,

123.2, 127.0, 128.4, 128.5, 129.0, 135.8, 139.0, 140.8, 146.7, 163.8, 176.1 ppm; HRMS: *m/z* [M-H]$^-$ calcd for $C_{22}H_{27}O_3$ 339.1965, found 339.1969.

2-hydroxy-6-(4-(pentyloxy)phenethyl)benzoic acid (4d)

The product was obtained using procedure 3 starting from **3d** and it was purified by column chromatography using EtOAc/Hex 1:5 (v/v) as eluent. The product was obtained as yellow solid (0.17 g, 51%); R_f = 0.43 (100% EtOAc); mp: 98-99 °C; ^{1}H NMR (200 MHz, CD_3OD): δ = 0.94 (3H, t, J = 7.0 Hz), 1.38-1.45 (m, 4H), 1.72-1.75 (m, 2H), 2.70-2.85 (2H, m), 3.10-3.20 (2H, m), 3.92 (t, J = 6.5 Hz), 6.66-6.80 (m, 4H), 7.08 (2H, d, J = 8.5 Hz), 7.23-7.27 ppm (m, 1H); ^{13}C NMR (50 MHz, CD_3OD): δ = 13.4, 22.5, 28.4, 29.2, 37.7, 38.7, 68.0, 106.4, 114.3, 115.1, 122.2, 129.2, 133.2, 134.4, 144.9, 157.8, 161.7, 171.7 ppm; HRMS *m/z* [M-H]$^+$ calcd for $C_{20}H_{23}O_4$ 327.1601, found 327.1614.

2-hydroxy-6-(3-(2-methoxyphenoxy)propyl)benzoic acid (4e)

The product was obtained using procedure 3 starting from **3e** and it was purified by column chromatography using EtOAc/Hex 1:4 (v/v) as eluent. The product was obtained as white powder (0.22 g, 73%); R_f = 0.42 (EtOAc); mp: 147-148 °C; ^{1}H NMR (200 MHz, CD_3OD): δ = 2.03-2.11 (2H, m), 3.09 (2H, t, J = 7.6 Hz), 3.83 (3H, s), 3.98 (2H, t, J = 6.5 Hz), 6.75-6.79 (2H, m), 6.89-6.94 (4H, m), 7.12-7.29 ppm (1H, m); ^{13}C NMR (50 MHz, CD_3OD): δ = 32.4, 21.7, 56.6, 69.7, 106.4, 113.6, 115.1, 116.1, 122.2, 122.4, 123.2, 134.3, 145.6, 149.9, 151.0, 162.5, 174.1; HRMS *m/z* [M-H]$^+$ calcd for $C_{17}H_{17}O_5$ 301.1081, found 301.1074.

(Z)-2,2-dimethyl-5-(4-(pentyloxy)styryl)-4H-benzo[d][1,3]dioxin-4-one (5d)

The product was obtained using the procedure 2 starting from **2d** and purified by column chromatography using EtOAc/Hex 1:14 (v/v) as eluent. The product was obtained as yellow oil (0.44 g, 80%); R_f = 0.51 (EtOAc/Hex 1:2); ^{1}H NMR (200 MHz, $CDCl_3$): δ = 1.10-1.19 (3H, m), 1.54-1.67 (4H, m), 1.92-2.07 (8H, m), 4.09-4.18 (2H, m), 6.90-6.93 (2H, m), 7.01-7.10 (2H, m), 7.16-7.23 (3H, m), 7.23-7.25 (1H, m), 7.35-7.39 ppm (1H, m); ^{13}C NMR (50 MHz, $CDCl_3$): δ = 14.8, 23.2, 26.5, 28.9, 29.7, 68.6, 106.2, 112.8, 114.8, 115.1, 116.1, 116.6, 126.1, 128.3, 129.7, 131.1, 131.2, 134.4, 135.7, 143.0, 159.0, 161.0 ppm; MS (ESI): *m/z* 367.3 [M+H]$^+$.

(Z)-2-hydroxy-6-(4-(pentyloxy)styryl)benzoic acid (6d)

The product was obtained using procedure 3 starting from **5d** and it was purified by column chromatography using EtOAc/Hex 1:5 (v/v) as eluent. The product was obtained as yellow solid (0.18 g, 55%); R_f = 0.67 (100% EtOAc); mp: 94-95 °C; ^{1}H NMR (400 MHz, $CDCl_3$): δ = 0.91 (3H, t, J = 7.0 Hz), 1.33-1.42 (4H, m), 1.71-1.78(2H,

m), 3.89 (2H, t, J = 6.4), 6.58 (1H, d, J = 12.1), 6.68 (2H, d, J = 8.4), 6.77 (1H, d, J = 8.3), 6.83 (1H, d, J = 12.1), 6.93 (1H, d, J =8.2), 7.00 (2H, d, J = 8.4), 7.27-7.32 ppm (1H, m); ^{13}C NMR (50 MHz, $CDCl_3$): δ = 14.1, 22.6, 28.3, 29.0, 68.0, 110.3, 114.2, 114.6, 116.9, 122.9, 128.7, 129.0, 129.3, 130.6, 135.8, 142.6, 158.4, 163.6, 175.5 ppm; HRMS: m/z $[M-H]^+$ calcd for $C_{20}H_{21}O_4$ 325.1445, found 325.1443.

Benzyl 2,4-bis(benzyloxy)-6-(((trifluoromethyl)sulfonyl)oxy) benzoate (10)

Triflic anhydride (35 mmol, 5.9 mL) was added dropwise to a solution of benzyl 2,4-bis(benzyloxy)-6-hydroxybenzoate (30 mmol, 13 g) and pyridine (0.11 mol, 8.1 mL) in dry dichloromethane (30 mL) at 0 °C. The resulting mixture was stirred for 1.5 hours at 0 °C. The excess of triflic anhydride was quenched by dropwise addition of water (5 mL). The mixture was slowly poured into a saturated solution of $NaHCO_3$ (50 mL), the two layers were separated in a separation funnel, and the organic layer was collected. The water layer was washed with dichloromethane (2 x 50 mL). The combined organic layers were washed with water (1 x 100 mL), brine (1 x 100 mL), and dried over Na_2SO_4 and concentrated under reduced pressure. The crude product was purified by column chromatography using EtOAc/Hex 1:10 (v/v) as eluent to yield the product as a white solid (9.6 g, 56%); R_f = 0.46 (EtOAc/Hex 1:4); ^{1}H NMR (400 MHz, $CDCl_3$): δ = 5.04 (s, 2H), 5.05 (s, 2H) 5.33 (s, 2H), 6.54 (s, 1H), 6.59 (s, 1H), 7.34 ppm (m, 15H); ^{13}C NMR (50 MHz, $CDCl_3$): δ = 67.9, 71.1, 71.3, 100.7, 100.8, 110.9, 127.5, 127.8, 128.5, 128.7, 128.8, 128.9, 129.1, 135.5, 135.7, 148.3, 158.8, 161.6, 163.3 ppm; MS (ESI): m/z 590.2 $[M+NH_4]^+$.

Benzyl 2,4-bis(benzyloxy)-6-(pentadec-1-yn-1-yl)benzoate (11a)

The product was obtained using procedure 1 starting from **10** (1.2 g, 2.0 mmol) and 1-pentadecyne (0.46 mg, 2.2 mmol) using either oil bath heating or microwave irradiation. It was purified by column chromatography using EtOAc/Hex 1:25 (v/v) as eluent. The product was obtained as colorless oil in 83% yield (1.1 g) for oil bath heating and 88% (1.1 g) for microwave irradiation; R_f = 0.53 (EtOAc/Hex 1:7 v/v); ^{1}H NMR (400 MHz, $CDCl_3$): δ = 0.88 (3H, t, J = 6.3 Hz,), 1.20-1.60 (22H, m), 2.28 (2H, t, J = 6.6 Hz,), 5.00 (1H, s), 5.02 (1H, s), 5.33 (1H, s), 6.50 (1H, d, J = 2.4 Hz), 6.63 (1H, d, J = 2.4 Hz), 7.24-7.39 ppm (15H, m); ^{13}C NMR (50 MHz, $CDCl_3$): δ = 14.2, 19.5, 22.7, 28.6, 29.0, 29.2, 29.4, 29.6, 29.7, 31.9, 66.9, 70.2, 70.5, 77.8, 94.6, 101.1, 109.6, 119.8, 124.1, 127.1, 127.6, 127.9, 128.0, 128.2, 128.4, 128.5, 128.7, 136.0, 136.2, 136.3, 156.8, 160.2, 166.9 ppm; MS (ESI): m/z 631.4 $[M+H]^+$.

Benzyl 2,4-bis(benzyloxy)-6-(dec-1-yn-1-yl)benzoate (11b)

The product was obtained using procedure 1 starting from **10** (1.2 g, 2.0 mmol) and 1-decyne (0.30 g, 2.2 mmol) using microwave irradiation. It was purified by column

chromatography using EtOAc/Hex 1:20 (v/v) as eluent. The product was obtained as brown oil (0.89 g, 79%); R_f = 0.66 (EtOAc/Hex 1:4); ^{1}H NMR (400 MHz, $CDCl_3$): δ = 0.88 (t, J = 6.6, 3H), 1.27-1.55 (m, 12H), 2.28 (t, J = 6.9, 2H), 4.99 (s, 2H), 5.02 (s, 2H), 5.33 (s, 2H), 6.50 (1H, d, J = 4.3 Hz), 6.62 (1H, d, J = 4.3 Hz), 7.27-7.40 ppm (m, 15H); ^{13}C NMR (50 MHz, $CDCl_3$): δ = 14.1, 19.4, 22.6, 28.5, 28.9, 29.1, 29.2, 31.8, 66.9, 70.2, 70.5, 94.6, 101.1, 109.6, 119.8, 124.1, 127.0, 127.5, 127.8, 127.9, 128.2, 128.3, 128.5, 128.6, 135.9, 136.2, 136.3, 156.8, 160.2, 166.9 ppm; MS (ESI): m/z 561.4 $[M+H]^+$.

2,4-Dihydroxy-6-pentadecylbenzoic acid (12a)

The product was obtained using procedure 2 starting from **10a** and purified by column chromatography using EtOAc/Hex 1:3 (v/v) as eluent. The product was obtained as a white solid (0.49 g, 89.5%); R_f = 0.19 (100% EtOAc); mp: 124-125 °C; ^{1}H NMR (400 MHz, CD_3OD): δ = 0.88 (3H ,t, J = 6.8 Hz), 1.22-1.31 (24H, m), 1.51-1.56 (2H, m), 2.86 (2H, t, J = 7.7 Hz), 6.14 (1H, d, J = 2.2 Hz), 6.18 ppm (1H, d, J = 2.2 Hz); ^{13}C NMR (50 MHz, CD_3OD): δ = 13.1, 22.4, 29.1, 29.2, 29.4, 29.6, 31.7, 31.8, 36.2, 100.3, 103.5, 110.4, 148.7, 162.2, 165.5, 173.4 ppm; MS (ESI): m/z 363.4; $[M-H]^-$; HRMS: m/z $[M-H]^-$ calcd for $C_{22}H_{35}O_4$ 363.2540, found 363.2542.

2-decyl-4,6-dihydroxybenzoic acid (12b)

The product was obtained using procedure 2 starting from **10b** and it was purified by column chromatography using EtOAc/Hex 1:3 (v/v) as eluent. The product was obtained as a pale orange solid (0.34 g, 76.5%); R_f=0.48 (100% EtOAc); mp: 107-108 °C; ^{1}H NMR (400 MHz, CD_3OD): δ = 0.90 (3H, t, J = 6.8 Hz), 1.29-1.33 (m, 14H), 1.54-1.57 (2H, m), 2.86-2.90 (2H t, J = 7.9 Hz), 6.14 (1H d, J = 2.6 Hz), 6.19 ppm (1H d, J = 2.6 Hz); ^{13}C NMR (50 MHz, CD_3OD): δ = 14.4, 23.7, 30.5, 30.7, 30.8, 30.9, 33.1, 33.2, 37.6, 101.7, 111.4, 111.7, 150.2, 163.5, 166.8, 173.5 ppm; HRMS: m/z $[M-H]^-$ calcd for $C_{17}H_{25}O_4$ 293.1758, found 293.1761.

5-(benzyloxy)-2,2-dimethyl-4H-benzo[d][1,3]dioxin-4-one (14)

The starting material **13** (2.2 g, 11 mmol) was dissolved in DMF (20 mL), and cooled to 0 °C. K_2CO_3 (3.1 g, 22 mmol) was added and benzylbromide (1.5 mL, 12 mmol) was added dropwise, and the mixture was stirred for 1h at 0 °C and then overnight at room temperature. The reaction mixture was extracted with EtOAc (3 x 20 mL), and the combined organic layers were washed with brine (1 x 40 mL), dried with $MgSO_4$, and filtered. The solvent was evaporated to give the pure compound as a yellow solid (2.6 g, 84%); R_f = 0.23 (EtOAc/Hex 1:5); ^{1}H NMR (200 MHz, $CDCl_3$): δ = 1.71 (6H, s), 5.25 (2H, s), 6.53 (1H, d, J = 8.2 Hz), 6.63 (1H, d, J = 8.5 Hz), 7.26-7.43 (5H, m), 7.53-7.57 ppm (1H, m); ^{13}C NMR (50 MHz, $CDCl_3$): δ = 25.8, 70.8, 104.2,

105.1, 105.4, 107.3, 109.6, 126.8, 127.9, 128.7, 136.4, 158.0, 158.2, 160.5 ppm; MS (ESI): *m/z* 285.2 $[M+H]^+$.

2-(benzyloxy)-6-hydroxybenzoic acid (15)

The product was obtained using procedure 3 starting from **14** and it was purified by column chromatography using EtOAc/Hex 1:2 (v/v) as eluent. The product was obtained as white solid (0.12 g, 49%); R_f = 0.39 (100% EtOAc); mp: 122-123 °C; ^{1}H NMR (200 MHz, CD_3OD): δ = 5.27 (2H, s), 6.59 (1H, d, J = 8.2), 6.67 (1H, d, J = 8.2), 7.35 (5H, m), 7.48-7.53 ppm (1H, m). ^{13}C NMR (50 MHz, CD_3OD): δ = 73.0, 105.2, 112.0, 112.2, 121.1, 129.8, 130.1, 136.4, 137.8, 160.5, 164.5, 171.5 ppm; HRMS: *m/z* $[M-H]^-$ calcd for $C_{14}H_{11}O_4$ 243.0662, found 243.0666.

2,2-dimethyl-5-(tetradecyloxy)-4H-benzo[d][1,3]dioxin-4-one (16)

5-hydroxy-2,2-dimethyl-4H-benzo[d][1,3]dioxin-4-one (**13**) (0.99 g, 5.1 mmol) and 1-tetradecanol (1.6 g, 7.5 mmol) were dissolved in dry THF (15 mL), and the reaction mixture was cooled down to 0 °C. PPh_3 (2.0 g, 7.5 mmol) and DIAD (1.5 mL, 7.5 mmol) were added, and the mixture was first stirred for 1 h at 0 °C and then overnight at room temperature. The reaction mixture was concentrated under reduced pressure, and the compound was purified by column chromatography using EtOAc/Hex 1:12 as eluent. The product was obtained as white solid (0.54 g, 27%); R_f = 0.33 (EtOAc/Hex 1:10); ^{1}H NMR (200 MHz, $CDCl_3$): δ = 0.84 (3H, m), 1.09-1.33 (22H, m), 1.51 (2H, m), 1.70 (6H, s), 4.03 (2H, t, J = 6.8 Hz), 6.50 (1H, d, J = 7.4 Hz), 6.57 (1H, d, J = 8.5 Hz), 7.32-7.39 ppm (1H, m); ^{13}C NMR (50 MHz, $CDCl_3$): δ = 14.09, 22.8, 25.7, 25.9, 26.8, 27.5, 29.1, 29.5, 29.6, 29.7, 32.2, 69.5, 103.6, 105.2, 106.5, 109., 136.3, 157.9, 158.0, 161.2 ppm; MS (ESI): *m/z* 391.3 $[M+H]^+$.

2-hydroxy-6-(tetradecyloxy)benzoic acid (17)

The product was obtained using procedure 3 starting from **16** and it was purified by column chromatography using EtOAc/ Hex 1:5 (v/v) as eluent. The product was obtained as pale pink solid (0.23 g, 66%); R_f = 0.63 (100% EtOAc); mp: 93-94 °C; ^{1}H NMR (200 MHz, $CDCl_3$): δ = 0.87 (3H, t, J = 6.8 Hz), 1.21-1.26 (22H, m), 1.86-1.90 (2H, m), 4.21 (2H, t, J = 6.2), 6.46 (1H, d, J = 8.2), 6.69 (1H, d, J = 8.5), 7.33-7.41 ppm (1H, m). ^{13}C NMR (50 MHz, $CDCl_3$): δ = 14.2, 22.8, 25.9, 26.0, 26.7, 27.5, 28.9, 29.2 29.5, 29.6, 29.7, 32.1, 70.9, 101.8, 102.3, 112.2, 134.2, 135.6, 158.2, 171.0 ppm; HRMS: *m/z* $[M-H]^-$ calcd for $C_{21}H_{33}O_4$ 349.2384, found 349.2383.

Methyl 2-hydroxy-6-pentadecylbenzoate (18)

The starting material **4a** (0.17 g, 0.5 mmol) was dissolved in 5 mL methanol. Concentrated H_2SO_4 (0.5 mL) was slowly added and the solution was stirred for 4h

at reflux. The mixture was then cooled down to room temperature, diluted with 20 mL dichloromethane and extracted with NaOH 1M (3 x 20 mL). The organic layer was washed with brine (1 x 15 mL), dried over Na_2SO_4 and filtered. The solvent was evaporated to give the pure product as a pale yellow solid (0.12 g, 65%); R_f = 0.73 (EtOAc/Hex 1:6); mp: 77-78 °C; ^{1}H NMR (200 MHz, CD_3OD): δ = 0.85-0.88 (3H, m), 1.26-1.53 (26H, m), 2.88 (2H, t, J = 7.6), 3.96 (3H, s), 6.72 (1H, d, J = 6.8), 6.82 (1H, d, J = 7.8), 7.25-7.29 ppm (1H, m); ^{13}C NMR (50 MHz, CD_3OD): δ = 14.3, 22.8, 25.1, 25.7, 29.5, 29.7, 29.8, 30.0, 32.1, 32.3, 34.1, 36.8, 52.2, 112.0, 115.7, 122.6, 134.3, 146.3, 162.7, 172.1 ppm; HRMS: *m/z* $[M-H]^-$ calcd for $C_{23}H_{37}O_3$ 361.2746, found 361.2748.

Cell culture and histone extraction

All cell culture reagents were purchased from Invitrogen. The human cancer cell line HEP G2 (liver) was cultured in Dulbecco's modified Eagle Medium (DMEM) containing 10% heat-inactivated fetal serum bovine (FBS), 50 IU/mL penicillin, and 50 mg/mL streptomycin at 37 °C in a humidified atmosphere containing 5% CO_2. For the experiments, cells were seeded in T-175 flasks, allowed to grow until about 70% confluency and FBS-starved for 16 hours. Cells were then treated at sub-toxic (see supplementary data) concentration of inhibitor for 24 hours. The histone extraction was performed as previously described in literature with minor modifications.[139] Protein concentrations of samples were determined using the Bradford Assay using BSA as a standard for calibration.

Immunoblot protocol

Approximately 5 µg of extracted histones were loaded on a 12.5% polyacrylamide gel, resolved by SDS-PAGE electrophoresis and electroblotted to PVDF membranes. The membranes were incubated with rabbit anti-acetyl-Histone H4 antibody (Millipore, 06-598) followed by a swine anti-rabbit HRP conjugated antibody (DakoCytomation, P0217). Bands were visualized using AEC detection kit (Sigma). Bands were scanned using a BioRad GS-710 densitometer and quantified using ImageJ quantification software. Equal amount of loading were determined by Coomassie blue staining. The experiments were performed in triplicate.

Histone acetyltransferase assay

An indirect ELISA was used to test the inhibition of the HAT PCAF activity. A solution 0.1% of bovine serum albumin (BSA) in 100 mM HEPES 7.4 was used as buffer unless differently specified. C96 Maxisorp 96-well plate (Nunc) was coated overnight at 4 °C with 50 µL per well of a solution 19 µg/mL streptavidin in 0.2 M Na_2CO_3 pH 9.4. After washing with buffer, the wells were blocked with 200 µL of a

solution 3% BSA in buffer for 1 h at room temperature (RT). The plate was washed with buffer, and then coated with 50 µL per well of a solution 300 nM biotinylated histone H4 peptide (Millipore, 12-372) for 1h at RT. After washing, 40 µL reaction buffer (0.1% BSA + 0.8% Triton X-100 in 100 mM HEPES pH 7.4) was added to the wells, followed by 20 µL recombinant PCAF 240 nM in reaction buffer, and 10 µL of the selected inhibitor solution at different concentration in reaction buffer. After 15 min incubation, 10 µL solution 40 µM AcCoA in reaction buffer was added to the well, except for the negative control. The enzymatic reaction was allowed to proceed for 15 min before washing. Each well was then incubated for 1h with 50 µL rabbit anti-acetyl-Lys antibody (Millipore, AB3879) dilution 1:1800. After washing, wells were incubated with 50 µL swine anti-rabbit HRP-conjugated dilution 1:1000 (DakoCytomation, P0217). The plate was washed with buffer and incubated with 100 µL per well of chromogen solution (0.1 mg/ml 3,3',5,5'-tetramethyl benzidine + 0.003% H_2O_2 in 0.1 M Acetate buffer pH 5.5). The reaction was terminated by addition of 100 µL H_2SO_4 1.0 M and the optical extinction read at 450 nm. The positive controls were the values of wells with no inhibitor, which were set as 100%. The negative controls were the values of wells with no AcCoA and were set as 0%. Stock solutions of inhibitors were prepared in dimethyl sulfoxide (DMSO) and diluted in reaction buffer. The final concentration of DMSO was tested not to have any effect on the assay. Each compound was tested in triplicate on one plate.

Molecular docking

The Crystal structure of PCAF chain B was downloaded from Protein Data Bank (code 1CM0). All molecules were drawn using Chemaxon MarvinSketch (www.chemaxon.com) and prepared (structure recognition and protonation) using SPORES (www.tcd.uni-konstanz.de/research/spores.php). Molecular docking simulations were performed using PLANTS v1.6.[140,141] The docking site center was determined by considering all residues within 5 Å from the co-crystallized CoA. One active site water molecule (pdb ID6) was kept for the docking. Fifteen poses were generated for each compound. The docking results were analyzed using MOE 2008.10 (www.chemcomp.com) and Molegro Virtual Docker (www.molegro.com). Pictures were generated using PyMOL (www.pymol.org).

CHAPTER 5

6-ALKYLSALICYLATES ARE SELECTIVE TIP60 INHIBITORS AND BIND COMPETITIVE TO ACETYL-COA

Ghizzoni M,* Wu J,* Gao T, Haisma HJ, Dekker FJ, Zheng YG;

Submitted for publication 2011

* *These authors contributed equally to this work.*

Abstract

Histone acetyltransferases are important enzymes that regulate various cellular functions, such as epigenetic control of DNA transcription. Development of HAT inhibitors with high selectivity and potency will provide powerful mechanistic tools for the elucidation of the biological functions of HATs and may also have pharmacological value for potential new therapies. In this work, analogs of the known HAT inhibitor anacardic acid were synthesized and evaluated for inhibition of HAT activity. Biochemical assays revealed novel anacardic acid analogs that inhibit the human recombinant enzyme Tip60 selectively compared to PCAF and p300. Enzyme kinetics studies demonstrated that inhibition of Tip60 by one such novel anacardic acid derive, ***20****, was essentially competitive with Ac-CoA and noncompetitive with the histone substrate. In addition, these HAT inhibitors effectively inhibited acetyltransferase activity of cellular nuclear extracts on the histone H3 and H4 at micromolar concentrations.*

INTRODUCTION

The plant natural product anacardic acid (AA, 6-pentadecylsalicylic acid) is isolated from cashew nut shell liquid and is used in traditional medicine.[142] It exerts beneficial biological effects such as antitumor activity and antioxidant activity.[143,144] AA was also shown to inhibit the activity of oxidative enzymes, such as tyrosinase, cyclooxygenase, and lipoxygenase.[145-147] Interestingly, AA and its derivatives were reported to modulate the enzymatic activity of histone acetyltransferases (HATs) such as p300 and p300/CBP-associated factor (PCAF) and affect HAT-dependent gene transcription.[78,130,148,149]

HATs are grouped into distinct families based on their sequence and structural homology.[95] The best studied families are the GNAT (GCN5-related N-acetyltransferase) family that includes PCAF and GCN5, the p300/CBP family that includes p300, and the MYST family that includes Tip60 (TAT-interacting protein 60) and MOF (Maleless On the First). Acetylation of histones and other proteins by HATs regulates chromatin restructuring, protein stability, enzyme activity, protein-protein interaction, metabolism, etc.[150-154] On the chromatin template, generally, histone acetylation is connected to activation of gene transcription, whereas acetylation of transcription factors can either activate or inactive gene transcription.[128] Combinations of acetylation and other posttranslational modifications regulate gene transcription in response to extra- and intracellular stimuli. Moreover, accumulating evidence reveals that HAT activities are deregulated in many diseases, which highlights the pharmacologic importance of HATs as potential drug targets.[97,155] Acetylations of the nuclear factor κB (NF-κB) transcription factor as well as the histones play a crucial role in activation of this pathway.[156] Recent years have seen great efforts for designing and screening chemical HAT modulators.[93,157,158] The known HAT inhibitor AA has been shown to inhibit NF-κB mediated gene transcription, presumably by inhibition of the HAT p300.[79] Furthermore, it has been shown that AA inhibits Tip60, which is one key member of the MYST family. AA blocks the Tip60-dependent activation of the ataxia telangiectasia mutated (ATM) protein kinase and the DNA-dependent protein kinase, catalytic subunit (DNA–PKcs) by DNA damage and sensitizes human tumor cells to the cytotoxic effects of ionizing radiation.[159] This indicates that HAT inhibition by small molecules provides a potential novel therapeutic approach for cancer and inflammatory diseases.

The molecular mechanism by which AA and its analogs inhibit HAT activity remains, however, poorly understood. It has been suggested that the salicylate

functionality of anacardic acid binds to the same pocket as the Ac-CoA pyrophosphate, which suggest competitive binding in respect to Ac-CoA.[148] In contrast, some studies suggested noncompetitive inhibition for AA against Ac-CoA in p300 and PCAF assays, which implicates a different inhibitory mechanism for p300 and PCAF.[78,160]

Herein, we describe the design and synthesis of a series of AA analogs and the evaluation of their regulatory activity on the human recombinant HATs p300, PCAF, and Tip60 as well as cellular HAT activity. We aim to develop potent and selective inhibitors for recombinant HATs that also inhibit cellular HATs. Furthermore, we aim to gain a better understanding of the HAT inhibitory mechanism of AA analogs.

RESULTS AND DISCUSSION

Synthesis

A focused compound collection based on AA was synthesized using a versatile route in which Sonogashira couplings are the key steps. The Sonogashira couplings were performed under microwave irradiation, which provided fast conversion with moderate to high yields. Arylbromides were alkylated using alkylhalides to give the products **2a-2d** in high yields (> 90%) (Scheme 1). Alkylation of **1c** provided the N-alkylated product **2e** as the main product in 55% yield. The O-alkylated product was isolated in minor amounts. The N-alkylated product **2e** showed a characteristic amide carbonyl signal in the IR spectrum, whereas this signal was absent in the corresponding O-alkylated product. Subsequently, the arylbromides were coupled to trimethylsilylacetylene by a Sonogashira coupling to yield the corresponding trimethylsilylalkynes in yields between 36 and 76%. The trimethylsilyl protective group was cleaved to give the corresponding alkynes **3a-3e.**

Alkynes **3a-3e** were coupled to triflate **4** using Sonogashira couplings to provide compounds **5a-5e** in yields between 49 and 82% (Scheme 2). Hydrogenation of the alkynes using Pd/C under H_2 atmosphere and hydrolysis of the acetonide using KOH in THF provided compounds **6a-6c** and **6f**. Hydrogenation of **5c** using higher catalyst loading resulted in partial or complete reduction of the acetyl group to give either the ethyl (**6e**) or hydroxyethyl (**6d**) functionality. Furthermore, hydrogenation of alkyne **5e** resulted in reduction of the pentylpyridin-2(1H)-one functionality (**5e**) to give a pentylpiperidin-2-one functionality (**6g**).

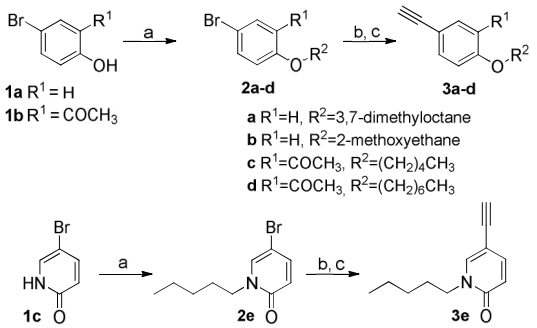

Scheme 5.1: *synthesis of acetylene building blocks for Sonogashira coupling. a) R-halide, K_2CO_3, DMF, b) TMS-acetylene, $PdCl_2(PPh_3)_2$, Et_2NH, CuI, PPh_3, CH_3CN, c) TBAF, THF.*

Compounds **9**, **12** and **15** (Scheme 2) present variations to the 6-alkyl substitution pattern of AA. These compounds were synthesized by Sonogashira couplings of alkynes on building blocks **7**, **10** and **13**. Products **8**, **11** and **14** were obtained in yields around 60%. These alkynes were hydrogenated using Pd/C under H_2 atmosphere. The methyl ester and methoxy functionality in **8** were simultaneously deprotected using BBr_3 and the methyl ester in **11** was hydrolyzed using KOH in THF. Hydrogenation of **14** provided the final product **15** in one step.

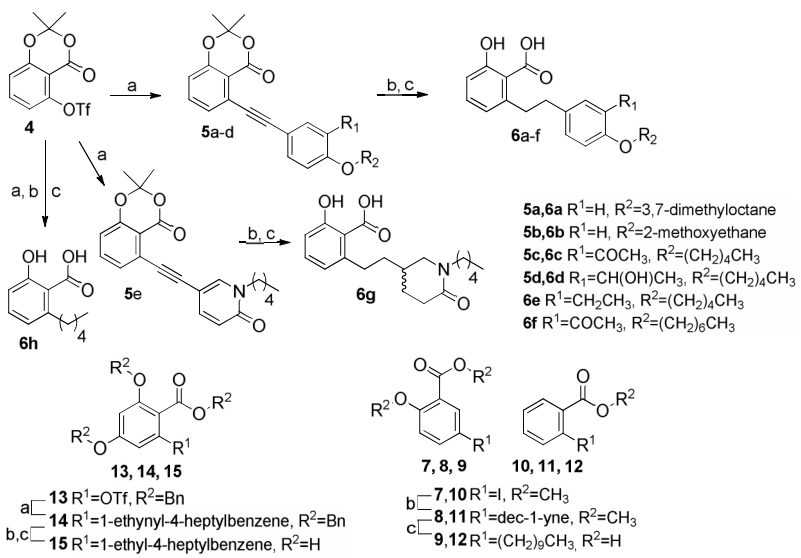

Scheme 5.2: *Sonogashira coupling and subsequent hydrogenation and deprotection to give anacardic acid derivatives* ***6a-6h****. a) $PdCl_2(PPh_3)_2$, Et_2NH, CuI, PPh_3, CH_3CN, b) H_2, Pd/C, MeOH, c) KOH, THF.*

Inhibitory potency of the AA analogs on three major HAT proteins

The potencies of AA and its analogs to modulate the acetyltransferase activities of recombinant HATs were evaluated using human recombinant Tip60, PCAF and p300, which represent the three major HAT families in mammalian cells. Standard radioisotope-labeled histone acetyltransferase assays were carried out with ^{14}C-labeled Ac-CoA as the acetyl donor. Histone N-terminal peptides were used as the acetyl acceptor of the HAT reaction: H4-20 for p300 and Tip60 catalysis, and H3-20 for PCAF catalysis. The compounds shown in Scheme 1, 2 and in table 5.1 were screened for inhibition of HAT activity. The compounds in table 5.1 were published previously [148]. The activities of the three HATs in the presence of 200 µM of each compound are collectively shown in figure 5.1. Clearly, the effect of the AA analogs on the enzymatic activity of the three HAT enzymes varies significantly from one another, which offers the opportunity to derive structure-activity relationship (SAR).

Table 5.1: *previously published anacardic acid* ***(16)*** *derivatives that were applied in this study.*[148]

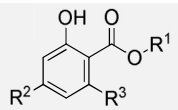	*R¹*	*R²*	*R³*
16	H	H	-$(CH_2)_{14}CH_3$
17	H	H	-$(CH_2)_9CH_3$
18	H	OH	-$(CH_2)_{14}CH_3$
19	H	OH	-$(CH_2)_9CH_3$
20	H	H	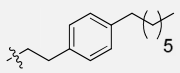
21	H	H	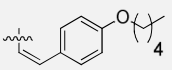
22	CH_3	H	-$(CH_2)_{14}CH_3$
23	H	H	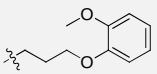
24	H	H	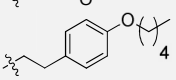
25	H	H	-$O(CH_2)_{13}CH_3$
26	H	H	-OCH_2Ph

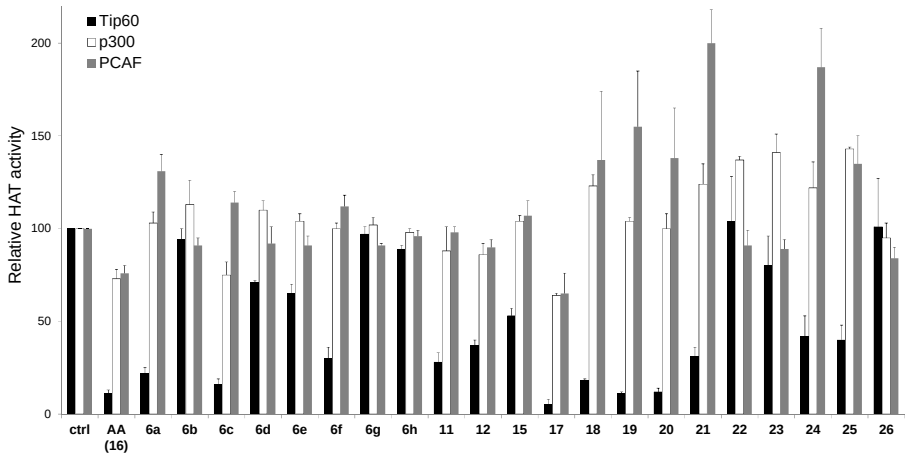

Figure 5.1: *the effect of AA (**16**) and its analogs on the HAT activity of the enzymes Tip60, p300, and PCAF. The inhibitors were applied at a concentration of 200 μM. For the Tip60 assay, the reaction mixture contained 100 nM Tip60, 10 μM Ac-CoA, 100 μM H4-20. For the p300 assay, the reaction mixture contained 5 nM p300, 10 μM Ac-CoA, and 100 μM H4-20. For the PCAF assay, the reaction mixture contained 5 nM PCAF, 10 μM Ac-CoA, and 100 μM H3-20.*

The overall observation is that the AA analogs show stronger inhibitory potency for Tip60 compared to p300 and PCAF, suggesting that the studied AA analogs have a general tendency for specific inhibition for the MYST HATs. In particular, compounds **6c, 16**, **17**, **18**, **19**, **6a**, and **20** inhibited more than 76% of the Tip60 activity at 200 μM, whereas their inhibitory effect on the activity of p300 and PCAF was little or very modest (≤35%). All these compounds have the conserved 6-substituted salicylate functionality, which highlights that this motif is critical for Tip60 inhibition. In contrast to AA that inhibits the Tip60 activity almost completely, compound **22**, in which the carboxylate is replaced for a methyl ester, completely lost its inhibitory potency. Moreover, all the compounds with more than 70% inhibitory activity at 200 μM have an extended hydrophobic substituent in 6-position. In contrast, compounds with hydrophilic substituents, e.g. **6b** and **6d**, very weakly inhibit Tip60 at 200 μM. This indicates that hydrophobic substitution in the salicylate 6-position is indispensable for Tip60 inhibition. Compounds **16**, **17** and **6h** show that aliphatic side chains with 10 to 15 carbon atoms (**16**, **17**) in the salicylate 6-position provide good inhibition potency in contrast to aliphatic chains with 5 carbon atoms (**6h**). These data indicate that side chains that correspond to the length of a linear aliphatic chain with 10 to 15 carbon atoms provide good inhibitory potency. Also, it seems plausible that the first atom of the side chain adjacent to the salicylic ring needs to be a hydrophobic carbon, as replacement of this carbon by a

hydrophilic oxygen greatly diminished inhibitory activity of the compounds. This was exemplified in **25** that contains an alpha-oxygen and shows only modest inhibitory activity.

Of interest, some of the AA analogs showed activation of the acetyltransferase activity of p300 and PCAF in contrast with the observed inhibitory effect on Tip60. For example, **21** and **24** enhance the PCAF activity significantly. Our observation is not unique: the activation of HAT activity by several AA analogs was also observed previously.[78,161,162] The exact mechanism by which certain AA analogs activate HAT activity is not clear, however it is not likely that this behavior is caused by competitive binding to the Ac-CoA binding pocket.[89] Therefore, binding to an alternative binding pocket can be presumed. Future investigation of the binding pocket that presumably causes activation is required for rational design of optimized HAT activators.

Among the effective Tip60 inhibitors, there are three salicylates with a phenethyl substitution in the 6-position, **6a, 6c and 20**. These inhibitors have calculated logD values at pH 7.4 of respectively 4.53, 3.07 and 4.19, which are lower than the calculated value 5.21 for AA (calculated using MarvinSketch v5.4). The high logD value for AA is generally considered to be a disadvantage for its bioactivity and therefore the inhibitors with the 6-phenethyl salicylate type can considered to be improved leads for development of Tip60 inhibitors. Inhibitor **20** inhibited the Tip60 activity by 88% at 200 µM and had no observable inhibitory effect on p300 and PCAF, in contrast to AA that shows about 20% inhibition of these enzymes at 200 µM. We therefore selected this inhibitor for further evaluation in order to understand the potency and selectivity of this AA analog for HAT inhibition. We determined the IC_{50} value for inhibition of the HAT activity of Tip60 and MOF for **20** and compared that with AA. MOF is another MYST family HAT that is relevant in eukaryotic gene transcription. The IC_{50} was determined as the concentration of the inhibitor at which half of the enzyme activity was inhibited. The results are shown in table 5.2. Under these experimental conditions, IC_{50} of AA and **20** are 64 µM and 74 µM for Tip60, and 43 µM and 47 µM for MOF. In contrast, IC_{50} of both AA and **20** are higher than 200 µM for p300 and PCAF (the exact IC_{50} values cannot be determined due to compound insolubility at high concentrations). These data indicate that AA and the other tested AA analogs tend to be specific inhibitors for the MYST family HATs. This is exemplified by **20**, which inhibited about 90% of Tip60 activity but had no appreciable inhibitory impact on p300 and PCAF (figure 5.1). The comparable inhibitory potency for the MYST family HATs Tip60 and MOF can be explained by the 67% sequence similarity in their catalytic region (Blast sequence alignment).[163]

Table 5.2: *IC_{50} data of **AA** and **20** for the inhibition of HATs.*

	*IC_{50} of **AA***	*IC_{50} of **20***
Tip60	64 ± 15 µM	74 ± 20 µM
PCAF	> 200 µM (60% retained)	> 200 µM (97% retained)
p300	> 200 µM (60% retained)	> 200 µM (70% retained)
MOF	43 ± 2 µM	47 ± 14 µM

For the Tip60 assay, the reaction contained 10 nM Tip60, 1 µM Ac-CoA, 100 µM H4-20 and the reaction time was 7 min; For the PCAF assay, the reaction contained 1 nM PCAF, 1 µM Ac-CoA, 100 µM H3-20 and the reaction time was 3.5 min; For the p300 assay, the reaction contained 5 nM p300, 1 µM Ac-CoA, 100 µM H4-20 and the reaction time was 5 min; For the MOF assay, the reaction contained 1 nM MOF, 1 µM Ac-CoA, 100 µM H4-20 and the reaction time was 5 min.

Kinetic pattern of Tip60 inhibition by compound 20

We carried out steady-state kinetic characterization of **20** for inhibition of Tip60 with respect to Ac-CoA and the H4 peptide to understand the mechanism by which the AA analogs inhibit the HAT activity of Tip60. The inhibition pattern was analyzed by measuring initial velocities of Tip60 at different concentrations of one substrate, a fixed concentration of the second substrate, and several selected concentrations of **20** (i.e. 0, 80, 120 µM). The Michaelis-Menten plots and the Lineweaver-Burk double reciprocal plots are shown in figure 5.2. In the primary double reciprocal plot of *E*/*V* versus 1/[Ac-CoA] a series of straight lines intersect at a point very close to the ordinate. The Michaelis-Menten data were fit to the nonlinear noncompetitive inhibition equation and yielded K_{is} of 54 µM and K_{ii} of 572 µM.[73] Because K_{is} is 10-fold smaller than K_{ii}, it is concluded that the inhibition of Tip60 by **20** is essentially competitive with respect to Ac-CoA, binding to the same enzyme form. The measurable K_{ii} may be an indication that **20** has additional weak binding site(s) in Tip60. On the other hand, the intersecting point in the double reciprocal plot of *E*/*V* versus 1/[H4-20] is clearly positioned to the left of the ordinate. The kinetic data fitting yielded K_{is} of > 660 µM and K_{ii} of 78 µM. Therefore, **20** is noncompetitive against the peptide substrate, preferentially binding to the enzyme form which is different from that the peptide binds to. The inhibitory pattern of **20** also offers insight into the kinetic mechanism of Tip60 catalysis. It suggests a likely ordered substrate binding pathway: Ac-CoA binds to Tip60 first and the peptide binds at a point downstream of Ac-CoA binding.

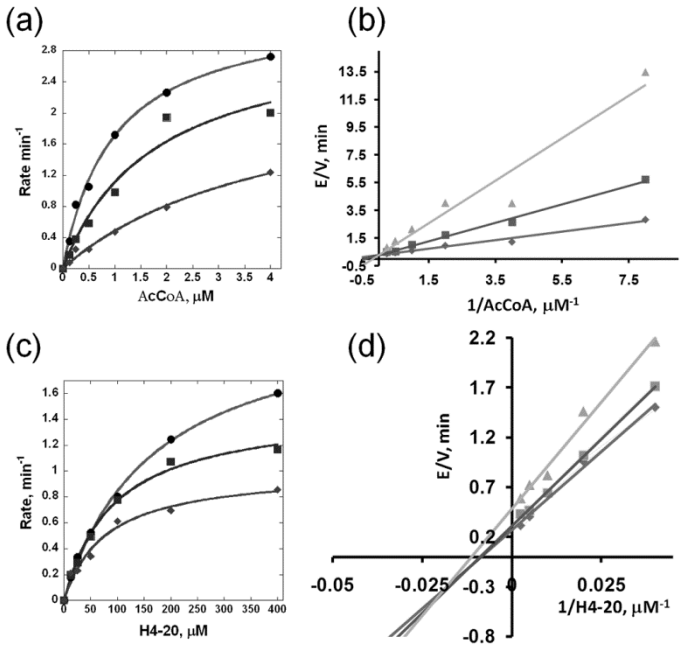

Figure 5.2: *steady-state kinetic characterization of Tip60 inhibition by* ***20****. (a) and (b) Michaelis-Menten and Lineweaver–Burk plots showing relation of Tip60 activity versus Ac-CoA concentration at three selected concentrations of* ***20*** *(0 µM, 80 µM, 120 µM). The reaction contained 50 nM Tip60 and 100 µM H4-20. (c) and (d) Michaelis-Menten and Lineweaver–Burk plots showing function of Tip60 activity versus H4-20 concentration at three selected concentrations of* ***20*** *(0 µM, 80 µM, 120 µM). The reaction contained 25 nM Tip60 and 2 µM Ac-CoA.*

Docking study

To elucidate the structural basis of Tip60 inhibition by the AA analogs, we performed a docking study of **20** with the crystal structure of Tip60 HAT domain (PDB ID 2OU2). As showed in figure 5.3, the 50 structural poses of the ligand were found to be located at four different regions in the Tip60 structure. In particular, half of the generated poses are located in the Ac-CoA binding pocket of Tip60 (i.e. region I). A further zoom-in examination reveals that in this site **20** and the adenine group of Ac-CoA interacts with several common amino acid residues of the Tip60, such as Ser364, Lys331, and Arg326. It is also interesting that the hydrophobic tail in molecule **20** shows a similar orientation as the long chain of Ac-CoA. These docking results suggest that **20** targets the active site of Tip60, which coincides well with the aforementioned steady-state kinetic analysis showing that inhibition by **20** is

predominantly competitive in respect to Ac-CoA. The docking model provides a structural basis for future optimization to obtain more potent and selective AA analog inhibitors.

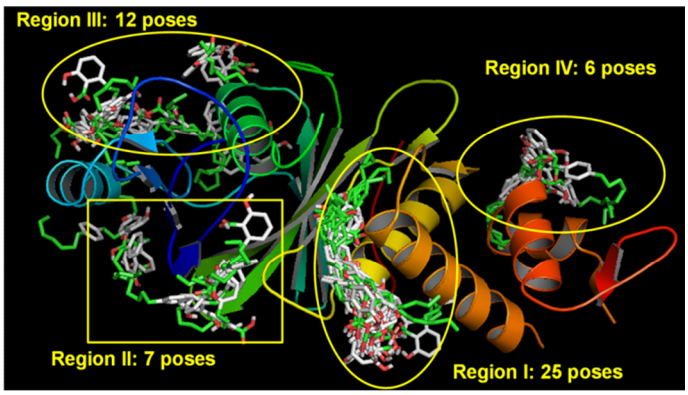

***Figure 5.3**: docking of **20** in the crystal structure (2OU2) of Tip60 HAT domain.*

Inhibition of cellular HAT activity

The inhibition of HAT activity in nuclear extracts from HeLa cells or tissue samples from different brains regions from rats was studied using an ELISA assay. In this assay either the biotinylated histone H3 (aa 1-21) or histone H4 (aa 2-24) peptides were linked to a 96-well plate via streptavidin. The histone peptides were subjected to acetylation by using nuclear extracts as enzyme source and histone acetylation was detected using an anti-acetyl Lysine antibody. Most of the studied 6-alkylsalicylates show concentration dependent inhibition of histone H4 acetylation (figure 5.4). Compounds with a polar chain in the salicylate 6-position have a strongly reduced HAT inhibitory potency (**6b, 6g, 6h, 23, 26**). Also methylation of the salicylate carboxylate (**22**) is detrimental for the HAT inhibitory activity. An aliphatic substituent in the salicylate 6-position is beneficial for inhibition of HAT activity (**16**, **17**, **18**, **19**). Interestingly, compound **21** that has been described previously to be a more potent inhibitor of histone acetylation than AA in HEP G2 cells also showed high inhibitory activity on HeLa nuclear extracts.[148]

It is of note that, the inhibition profile of the AA analogs on nuclear extract acetyltransferase activity correlates well with the assay on recombinant Tip60. For instance, the compound that inhibited the cellular HAT activity more than 50% at 200 µM, e.g. **6a**, **6c**, **6f**, **11**, **12**, **16**, **17**, **18**, **19**, **20**, **21**, **24**, and **25**, also inhibited the Tip60 HAT activity. On the other hand, most of the compounds that showed poor inhibition of HeLa nuclear extract activity, **6b**, **6g**, **6h**, **22**, **23**, and **26**, were also very

poor inhibitors in for the recombinant enzyme. The compounds **6d**, **6e** and **15** are exceptions because they seem to be more potent on HeLa nuclear extracts than for the recombinant Tip60. This is an indication for the presence of multiple HATs in nuclear extracts.

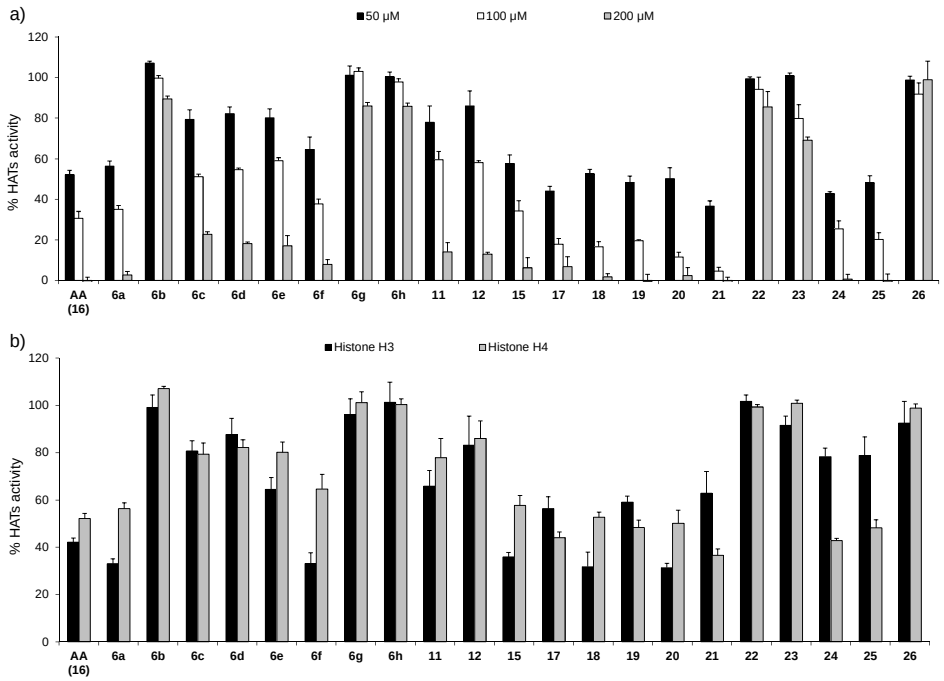

Figure 5.4: *inhibition of HAT activity of HeLa nuclear extract measured with ELISA assay. Averages and standard deviations of triplicates are reported relative to the positive control in which no inhibitor was present and the negative control where no enzyme was present. a) Concentration dependent inhibition of HAT activity by AA analogs. The ELISA plate was coated with histone H4; b) Inhibition of HAT activity by AA analogs (50 µM). The ELISA plate was coated with either histone H3 or histone H4.*

The inhibitory potency of the compound collection on histone H3 acetylation by HeLa nuclear extracts was investigated at 50 µM concentrations and compared to histone H4 acetylation (figure 5.4b). Interestingly, a change in inhibitory potency was observed between histone H3 and histone H4. For example **16** and **17** show almost equal potency for both histones, whereas for example, **6a, 6f**, **15, 18** and **20,** are more potent for histone H3 compared to histone H4. The opposite is true for compounds like **21**, **24** and **25**. Given the complexity of HAT enzyme composition, distribution, and catalytic turnover rates of each HAT complex in the nucleus, it would be very difficult to interpret the differential impact of the AA analogs on H3

acetylation and H4 acetylation. However, the data shown here indicate that selective inhibitors towards histone H3 or H4 acetylation could be developed.

The HAT activity of nuclear extracts of brain tissue samples from rats showed no significant difference between HAT activity in brain tissue in different brain regions ($n = 3$, $p > 0.05$) (figure 5.5). Studies on two different animals showed no significant deviations between the animals ($n = 2$, $p > 0.05$). The inhibitors **16** and **20** both inhibited the HAT activity of the nuclear extracts of different regions significantly ($p < 0.05$). Compound **20** showed slightly impaired inhibition compared to **16**, which is statistically significant for the hippocampus ($p < 0.05$).

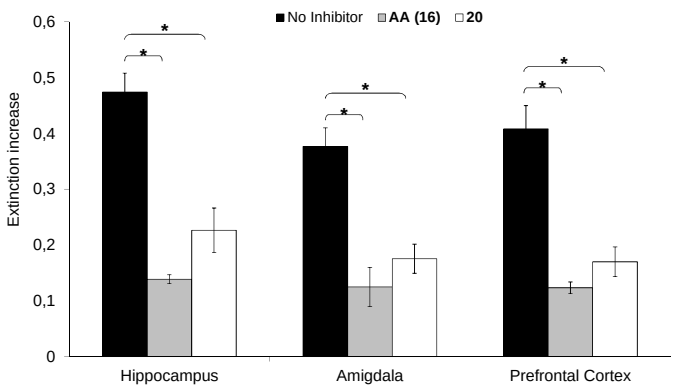

Figure 5.5: *acetyltransferase activity of nuclear extract from tissue samples from different brain regions in mice. The acetyltransferase activity was determined using an ELISA assay with histone H3 as acetyl acceptor. The inhibitors AA and* ***20*** *were applied in a concentration of 30 µM. Experiments were performed in triplicate for two different animals. The averages and standard deviations for the two animals are shown and blank values were subtracted.* * *$p < 0.05$.*

CONCLUSION

AA analogs with various 2-phenylethane substituents in the salicylate 6-position were synthesized and tested for modulating enzymatic activities of three major types of mammalian HAT proteins. The recombinant enzyme inhibition assays demonstrated that inhibitors **18**, **19**, **20** and **21** are selective for Tip60 in comparison with PCAF and p300. Compounds that inhibit Tip60 show in most cases also inhibition of HAT activity in HeLa nuclear extracts, which suggests that MYST type HATs play an important role in the HAT activity of the studied extracts. Inhibitor **20** was subjected to further investigation because its logD value is lower than AA, whereas it inhibitory potency on recombinant Tip60 as well as HeLa nuclear extracts

is maintained. Enzyme kinetics showed that inhibition of Tip60 by **20** is competitive to Ac-CoA and non-competitive to histone H4, which supports the hypothesis that AA derivatives bind to the Ac-CoA binding pocket. Inhibitor **20** showed also equal potency to AA in nuclear extracts of tissue samples from different brain regions of rats, which indicates that **20** may be applied successfully *in vivo*.

EXPERIMENTAL SECTION

Synthesis

General

Chemicals were purchased from commerical suppliers and used without further purification. If required, solvents were dried before use according to known procedures. Pd-catalysed cross-couplings were carried-out under a nitrogen atmosphere. Analytical thin-layer chromatography (TLC) was performed on aluminum sheets of Silica Gel 60 F254. Spots on TLC were detected by ultraviolet light or $KMnO_4$ solution. Column chromatography was performed with MP Ecochrom Silica Gel 32–63, 60 Å. Reactions under microwave irradiation reactions were carried out in a Biotage Initiator™ Microwave Synthesizer. ^1H and ^{13}C NMR spectra were recorded on a Varian Gemini-200. ^{13}C spectra were recorded using the attached proton test (APT) pulse sequence. Chemical shift values are reported as part per million (δ) relative to residual solvent peaks ($CDCl_3$, ^1H δ = 7.26, ^{13}C δ = 77.16, CD_3OD, ^1H δ = 3.31, ^{13}C δ = 49.00, CD_3CN ^1H δ = 1.94, ^{13}C δ = 118.26 DMSO ^1H δ = 2.50, ^{13}C δ = 39.52). The coupling constants (*J*) are reported in Hertz (Hz). Electrospray ionization mass spectra (ESI-MS) were recorded on an Applied Biosystems/SCIEX API3000-triple quadrupole mass spectrometer. Infrared (IR) spectra were recorder on a Thermo Nicolet 380 Smart Orbit ATR FTIR apparatus. Melting points were determined on an Electrothermal digital melting point apparatus and are uncorrected. High-resolution mass spectra (HR-MS) were recorded using a flow injection method on a LTQ-Orbitrap XL mass spectrometer (Thermo Electron, Bremen, Germany) with a resolution of 60,000 at m/z 400. Protonated testosterone (lock mass m/z = 289.2162) was used for internal recalibration in real time.

General procedure 1

K_2CO_3 (18 mmol, 2.5 g) was suspended in 15 mL of DMF. The phenol (6.0 mmol) and the alkyl halide (6.6 mmol) were added subsequentially and the suspension was stirred overnight at 60 °C. The reaction mixture was diluted with 50 mL demiwater

and the resulting reaction mixture was extracted with with EtOAc (3 x 30 mL). The combined organic layers were, washed with brine (1 x 50 mL), dried over Na_2SO_4 and filtered. The solvent was evaporated under reduced pressure to give the product in high purity.

General procedure 2

Freshly distilled diethylamine (23 mmol, 2.3 mL) and trimethylsilylacetylene (5.5 mmol, 0.78 mL) were subsequently added to a solution of the aryl halide (5.0 mmol), CuI (0.25 mmol, 48 mg), PPh_3 (1 mmol, 0.26 g) and $PdCl_2(PPh_3)_2$ (0.25 mmol, 0,17 g) in degassed anhydrous acetonitrile (2.0 mL). The mixture was stirred under microwave irradiation for 30 min at 120 °C . The mixture was diluted with EtOAc (30 mL), extracted with water (3 x 30 mL), and brine (1 x 30 mL). The resulting solution was dried over Na_2SO_4 and filtered. The solvent was evaporated under reduced pressure and the residue was purified by column chromatography.

General procedure 3

The starting material (3.0 mmol) was dissolved in THF (10 mL) and solution was cooled down to 0 °C. A solution 1 M of tetra-*n*-butylammonium fluoride (TBAF) in THF (3.3 mmol, 3.3 mL) was added slowly and the reaction mixture was stirred for 30 min at 0 °C. The solution was diluted with satured solution of NH_4Cl (15 mL) and extracted with diethyl ether (3 x 30 mL). The combined organic layers were dried over Na_2SO_4 and filtered.The solvent was evaporated under reduced pressure to give the product in high purity.

General procedure 4

Freshly distilled diethylamine (5.0 mmol, 0.52 mL) and the alkyne (2.7 mmol) were subsequently added to a solution of aryl triflate **4** or **13** or jodide **7** or **10** (2.5 mmol), CuI (0.25 mmol, 48 mg), and $PdCl_2(PPh_3)_2$ (0.13 mmol, 88 mg) in degassed anhydrous acetonitrile (1.5 mL). The mixture was stirred under microwave irradiation for 30 min at 100 °C. The mixture was diluted with EtOAc (20 mL), extracted with water (3 x 20 mL), and brine (1 x 20 mL). The resulting solution was dried over Na_2SO_4 and filtered. The solvent was evaporated under reduced pressure and the residue was purified by column chromatography.

General procedure 5

A suspension of the starting material (1.5 mmol) and Pd/C (10%) (0.15 mmol, 10 mol%) in methanol (30 mL) was shaken overnight at 40 °C, with 3 atm. H_2-pressure in a Parr apparatus. The mixture was filtered through Celite, and the filtrate was concentrated under reduced pressure.

General procedure 6

The starting material (1.0 mmol) was dissolved in THF (2.0 mL). KOH 5 N (10 mmol, 2.0 mL) was added and the mixture was stirred overnight at 55 °C. The reaction mixture was diluted with EtOAc (10 mL) and acidified with 1 N HCl (20 mL). The mixture was extracted with EtOAc (3 x 30 mL). The organic phases were collected, washed with brine (1 x 50 mL), dried over Na_2SO_4 and filtered. The solvent was evaporated and the product was purified by column chromatography or crystallization

1-bromo-4-((3,7-dimethyloctyl)oxy)benzene (2a)

The product was obtained using procedure 1 starting from 4-bromophenol (6.0 mmol, 1.0 g) and 1-bromo-3,7-dimethyloctane (6.6 mmol, 1.4 mL). The product was obtained as colorless oil (1.7 g, 93%). R_f = 0.88 (EtOAc/Hex 1:2). ^{1}H NMR (200 MHz, $CDCl_3$): δ = 0.87 (6H, d, J = 6.5 Hz), 0.93 (3H, d, J = 6.5 Hz), 1.13-1.35 (6H, m), 1.52-1.58 (2H, m), 1.60-1.65 (1H, m), 1.80-1.85 (1H, m), 3.92-3.97 (2H, m), 6.77 (2H, d, J = 8.8 Hz), 7.36 (2H, d, J = 8.8 Hz). ^{13}C NMR (50 MHz, $CDCl_3$): δ = 19.6, 22.6, 22.7, 24.6, 28.0, 29.8, 36.1, 37.3, 39.2, 66.6, 112.5, 116.3, 132.2, 158.2. MS (ESI): m/z 330.3 and 332.2 (ratio 1:1) $[M+NH_4]^+$.

1-bromo-4-(2-methoxyethoxy)benzene (2b)

The product was obtained using procedure 1 starting from 4-bromophenol (6.0 mmol, 1.0 g) and 1-bromo-2-methoxyethane (6.6 mmol, 0.54 mL). The product was obtained as colorless liquid (1.3 g, 96%). R_f = 0.48 (EtOAc/Hex 1:2). ^{1}H NMR (200 MHz, $CDCl_3$): δ = 3.44 (3H, s), 3.74 (2H, t, J = 8.0 Hz), 4.08 (2H, t, J = 8.0 Hz), 6.80 (2H, d, J = 6.5 Hz), 7.36 (2H, d, J = 6.5 Hz). ^{13}C NMR (50 MHz, $CDCl_3$): δ = 59.2, 67.5, 70.9, 112.4, 116.4, 132.2, 157.8. MS (ESI): m/z 248.1 $[M+NH_4]^+$.

1-(5-bromo-2-(pentyloxy)phenyl)ethanone (2c)

The product was obtained using procedure 1 starting from 1-(5-bromo-2-hydroxyphenyl)ethanone (6.0 mmol, 1.3 g) and 1-bromopentane (6.6 mmol, 1.0 mL) The product was obtained as a pale yellow solid (1.6 g, 98%). R_f= 0.49 (EtOAc/Hex 1:2). ^{1}H NMR (400 MHz, $CDCl_3$) δ 0.94 (3H, t, J = 7.2 Hz), 1.38-1.48 (4H, m), 1.81-1.87 (2H, m), 2.61 (3H, s), 4.03 (2H, t, J = 6.5 Hz), 6.83 (1H, d, J = 8.8 Hz), 7.51 (1H, dd, J = 2.6, 8.8 Hz), 7.83 (1H, d, J = 2.6 Hz). ^{13}C NMR (100 MHz, $CDCl_3$) δ 14.1, 22.5, 28.4, 28.9, 32.1, 69.0, 112.5, 114.4, 128.4, 134.5, 137.2, 158.7, 199.0. MS (ESI): (m/z) 285.2 and 287.2 (ratio 1:1) $[M+H]^+$.

1-(5-bromo-2-(heptyloxy)phenyl)ethanone (2d)

The product was obtained using procedure 1 starting from 1-(5-bromo-2-hydroxyphenyl)ethanone (6.0 mmol, 1.3 g) and 1-bromo-heptane (6.6 mmol, 1.0 mL). The product was obtained as pale yellow solid (1.7 g, 92%). R_f = 0.71 (EtOAc/Hex 1:2). ^{1}H NMR (200 MHz, $CDCl_3$): δ = 0.89 (3H, t, J = 6.5 Hz), 1.30-1.49 (8H, m), 1.80-1.87 (2H, m), 2.60 (3H, s), 4.02 (2H, t, J = 6.5 Hz), 6.82 (1H, d, J = 8.5 Hz), 7.49 (1H, dd, J = 2.6, 6.2 Hz), 7.82 (1H, d, J = 2.6 Hz). ^{13}C NMR (50 MHz, $CDCl_3$): δ = 14.2, 22.7, 26.2, 29.1, 29.2, 31.8, 32.0, 69.1,112.9, 114.3, 129.7, 133.1, 136.1, 157.6, 198.4. MS (ESI): m/z 313.0 and 315.0 (ratio 1:1) $[M+H]^+$.

5-bromo-1-pentylpyridin-2(1H)-one (2e)

The product was obtained using procedure 1 starting from 5-bromo-2-hydroxypyridine (6.0 mmol, 1.0 g) and 1-bromo-pentane (6.6 mmol, 0.82 mL). The product was obtained as pale yellow solid (0.81 g, 55%). R_f = 0.33 (EtOAc/Hex 1:2). ^{1}H NMR (200 MHz, $CDCl_3$): δ = 0.87 (3H, t, J = 6.8 Hz), 1.26-1.33 (4H, m), 1.66-1.74 (2H, m), 3.85 (2H, t, J = 7.5 Hz), 6.45 (1H, d, J = 9.7 Hz), 7.28-7.37 (2H, m). ^{13}C NMR (50 MHz, $CDCl_3$): δ = 13.9, 22.3, 28.6, 28.9, 50.1, 97.7, 122.2, 137.4, 142.2, 160.9. MS (ESI): m/z 244.2 and 246.2 (ration 1:1) $[M+H]^+$. IR (neat): ν_{max} = 823, 1152, 1436, 1525, 1581, 1651. The O-alkylated product 5-bromo-2-(pentyloxy)pyridine lacks the amide carbonyl signal at 1651.

((4-((3,7-dimethyloctyl)oxy)phenyl)ethynyl)trimethylsilane

The product was obtained using procedure 2 starting from 1-bromo-4-((3,7-dimethyloctyl)oxy)benzene (5.0 mmol, 1.6 g). After work-up, the reaction product was dissolved in EtOAc/Hex 1:1 (v/v) and filtered over Celite. The solvent was evaporated to get the crude product that was used for the next step with further purification.

((4-(2-methoxyethoxy)phenyl)ethynyl)trimethylsilane

The product was obtained using procedure 2 starting from 1-bromo-4-(2-methoxyethoxy)benzene (5.0 mmol, 1.2 g). It was purified by column chromatography using EtOAc/Hex 1:8 (v/v) as eluent. The product was obtained as orange oil (0.50 g, 40%). R_f = 0.45 (EtOAc/Hex 1:2). ^{1}H NMR (200 MHz, $CDCl_3$): δ = 0.08 (9H, s), 3.29 (3H, s), 3.58 (2H, d, J = 8.0 Hz), 3.92 (2H, d, J = 8.0 Hz), 6.63-6.71 (2H, m), 7.19-7.23 (2H, m). ^{13}C NMR (50 MHz, $CDCl_3$): δ = 0.1, 59.2, 67.2, 70.9, 92.5, 105.1, 113.1, 114.4, 116.4, 132.2, 133.4, 157.9. MS (ESI): m/z 249.2 $[M+H]^+$.

1-(2-(pentyloxy)-5-((trimethylsilyl)ethynyl)phenyl)ethanone

The product was obtained using procedure 2 starting from 1-(5-bromo-2-(pentyloxy)phenyl)ethanone (5.0 mmol, 1.4 g). The product was purified by column

chromatography using EtOAc/Hex 1:10 (v/v) as eluent. The product was obtained as yellow solid (1.1 g, 76%). R_f= 0.62 (EtOAc/Hex 1:2). ^{1}H NMR (400 MHz, $CDCl_3$) δ 0.22 (9H, s), 0.93 (3H, t, *J* = 7 Hz), 1.34-1.50 (4H, m), 1.81-1.88 (2H, m), 2.60 (3H, s), 4.05 (2H, t, *J* = 6.7 Hz), 6.85 (1H, d, *J* = 8.8 Hz), 7.50 (1H, dd, *J* = 2.3, 8.8 Hz), 7.84 (1H, d, *J* = 2.3 Hz). ^{13}C NMR (100 MHz, $CDCl_3$) δ 0.0, 14.0, 22.4, 28.3, 28.8, 31.9, 68.8, 93.3, 104.0, 112.2, 115.4, 128.1, 134.3, 136.8, 158.3, 198.9. MS (ESI): (*m/z*) 303.2 $[M+H]^+$.

1-(2-(heptyloxy)-5-((trimethylsilyl)ethynyl)phenyl)ethanone

The product was obtained using procedure 2 starting from 1-(5-bromo-2-(heptyloxy)phenyl)ethanone (5.0 mmol, 1.6 g). Purification was performed by column chromatography using 100% hexane as eluent. The product was obtained as yellow solid (0.60 g, 36%). R_f = 0.59 (EtOAc/Hex 1:2). ^{1}H NMR (200 MHz, $CDCl_3$): δ = 0.21-0.24 (9H, s), 0.89 (3H, t, *J* = 6.5 Hz) 1.30-1.43 (8H, m), 1.80-1.84 (2H, m), 2.60 (3H, s), 4.05 (2H, t, *J* = 6.5 Hz), 6.85 (1H, d, *J* = 8.5 Hz), 7.50 (1H, dd, *J* = 2.3, 6.2 Hz), 7.84 (1H, d, *J* = 2.4 Hz). ^{13}C NMR (50 MHz, $CDCl_3$): δ = 0.1, 14.2, 22.7, 26.2, 29.1, 29.2, 31.8, 32.1, 68.9, 93.5, 104.2, 112.4, 115.5, 128.2, 134.5, 136.9, 158.5, 199.0. MS (ESI): *m/z* 331.3 $[M+H]^+$.

1-pentyl-5-((trimethylsilyl)ethynyl)pyridin-2(1H)-one

The product was obtained using procedure 2 starting from 5-bromo-1-pentylpyridin-2(1H)-one (5.0 mmol, 1.2 g). The product was purified by column chromatography using EtOAc/Hex 1:6 (v/v) as eluent. The product was obtained as orange oil (0.61 g, 47%). R_f = 0.56 (EtOAc/Hex 1:2). ^{1}H NMR (200 MHz, $CDCl_3$): δ = 0.13-0.23 (9H, s), 0.89 (3H, t, *J* = 6.7 Hz), 1.28-1.35 (4H, m), 1.65-1.76 (2H, m), 3.87 (2H, t, *J* = 7.4 Hz), 6.47 (1H, d, *J* = 9.4 Hz), 7.30 (1H, dd, *J* = 2.4, 7.0 Hz), 7.48 (1H, d, *J* = 2.4 Hz). ^{13}C NMR (50 MHz, $CDCl_3$): δ = 0.1, 14.0, 22.4, 28.8, 29.1, 50.3, 94.9, 100.7, 102.4, 120.8, 135.2, 141.7, 161.1. MS (ESI): *m/z* 262.3 $[M+H]^+$.

1-((3,7-dimethyloctyl)oxy)-4-ethynylbenzene (3a)

The product was obtained using procedure 3 starting from ((4-((3,7-dimethyloctyl)oxy)phenyl)ethynyl)trimethylsilane (3.0 mmol, 1.0 g). The product was purified by column chromatography using Hexane as eluent. It was obtained as yellow solid (0.74 g, 95%). R_f= 0.59 (EtOAc/Hex 1:8). ^{1}H NMR (200 MHz, $CDCl_3$): *δ* = 0.87 (6H, d, *J* = 6.7 Hz), 0.94 (3H, d, *J* = 6.4 Hz), 1.14-1.36 (6H, m), 1.51-1.62 (2H, m), 1.65-1.68 (1H, m), 1.80-1.85 (1H, m), 3.00 (1H, s), 3.96-4.01 (2H, m), 6.83 (2H, d, *J* = 8.8 Hz), 7.42 (2H, d, *J* = 8.8 Hz). ^{13}C NMR (50 MHz, $CDCl_3$): *δ* = 19.6, 22.6, 22.7, 24.6, 28.0, 29.8, 36.1, 37.3, 39.2, 66.4, 75.6, 83.8, 113.9, 114.5, 133.5, 159.5. MS (ESI): *m/z* 259.4 $[M+H]^+$.

1-ethynyl-4-(2-methoxyethoxy)benzene (3b)

The product was obtained using procedure 3 starting from ((4-(2-methoxyethoxy)phenyl)ethynyl)trimethylsilane (3.0 mmol, 0.74 g). The product was obtained as orange oil (0.49 g, 93%). R_f = 0.34 (EtOAc/Hex 1:2). ^{1}H NMR (200 MHz, $CDCl_3$): δ = 2.91 (1H, s), 3.36 (3H, s), 3.67 (2H, t, J = 8.0 Hz), 4.03 (2H, d, J = 8.0 Hz), 6.79 (2H, d, J = 6.6 Hz), 7.33 (2H, d, J = 6.6 Hz); ^{13}C NMR (50 MHz, $CDCl_3$): δ = 59.2, 67.3, 70.9, 75.8, 83.6, 114.4, 115.2, 133.5, 159.1. MS (ESI): m/z 177.2 $[M+H]^+$.

1-(5-ethynyl-2-(pentyloxy)phenyl)ethanone (3c)

The product was obtained using procedure 3 starting from 1-(2-(pentyloxy)-5-((trimethylsilyl)ethynyl)phenyl)ethanone (3.0 mmol, 0.91 g). The crude product was purified using column chromatography with EtOAc/Hex 1:30 (v/v) as eluent to yield the product as a white solid (0.55 g, 79%). R_f= 0.60 (EtOAc/Hex 1:2 (v/v). ^{1}H NMR (400 Mhz, $CDCl_3$) δ 0.94 (3H, t, J = 7.2 Hz), 1.38-1.47 (4H, m), 1.84-1.87 (2H, m), 2.61 (3H, s), 3.00 (1H, s), 4.06 (2H, t, J = 6.5 Hz), 6.88 (1H, d, J = 8.8 Hz), 7.54 (1H, dd, 2.3, 8.8 Hz), 7.86 (1H, d, J = 2.3 Hz). ^{13}C NMR (100 MHz, $CDCl_3$) δ 13.9, 22.3, 28.3, 28.8, 31.9, 68.8, 77.3, 82.6, 112.4, 114.2, 128.3, 134.4, 137.0, 158.6, 198.9. MS (ESI): (m/z) 231.1 $[M+H]^+$.

1-(5-ethynyl-2-(heptyloxy)phenyl)ethanone (3d)

The product was obtained using procedure 3 starting from 1-(2-(heptyloxy)-5-((trimethylsilyl)ethynyl)phenyl)ethanone (3.0 mmol, 0.99 g). The product was obtained as yellow solid (0.73 g, 94%). R_f = 0.56 (EtOAc/Hex 1:2). ^{1}H NMR (200 MHz, $CDCl_3$): δ = 0.88 (3H, t, J = 6.8 Hz), 1.29-1.49 (8H, m), 1.76-1.87 (2H, m), 2.60, (3H, s), 2.98 (1H, s), 4.04 (2H, t, J = 6.5 Hz), 6.87 (1H, d, J = 8.8 Hz), 7.52 (1H, dd, J = 6.4, 2.2 Hz), 7.84 (1H, d, J = 2.4 Hz). ^{13}C NMR (50 MHz, $CDCl_3$): δ = 14.0, 22.5, 26.1, 28.9, 29.1, 31.7, 31.9, 59.1, 68.8, 82.6, 112.4, 114.2, 128.2, 134.3, 137.0, 158.6, 198.8. MS (ESI): m/z 259.5 $[M+H]^+$.

5-ethynyl-1-pentylpyridin-2(1H)-one 3e)

The product was obtained using procedure 3 starting from 1-pentyl-5-((trimethylsilyl)ethynyl)pyridin-2(1H)-one (3 mmol, 0.78 g). The product was obtained as dark orange solid (0.55 g, 97%). R_f = 0.49 (EtOAc/Hex 1:2). ^{1}H NMR (200 MHz, $CDCl_3$): δ = 0.83 (3H, t, J = 6.8 Hz), 1.22-129 (4H, m), 1.66 (2H, m), 2.95 (1H, s), 3.83 (2H, t, J = 7.5 Hz), 6.42 (1H, d, J = 9.3 Hz), 7.25 (1H, dd, J = 9.0, 2.3 Hz), 7.44 (1H, d, J = 2.4 Hz). ^{13}C NMR (50 MHz, $CDCl_3$): δ = 13.6, 19.7, 22.2, 24.1, 50.1, 59.0, 79.8, 89.9, 101.0, 120.8, 141.4, 141.8, 161.2. MS (ESI): m/z 190.1 $[M+H]^+$.

5-((4-((3,7-dimethyloctyl)oxy)phenyl)ethynyl)-2,2-dimethyl-4H-benzo[d][1,3]dioxin-4-one (5a)

The product was obtained using procedure 4 starting from 1-((3,7-dimethyloctyl)oxy)-4-ethynylbenzene (2.7 mmol, 0.70 g) and triflate **4** (2.5 mmol, 0.82 g). The product was purified by column chromatography using EtOAc/Hex 1:16 (v/v) as eluent. The product was obtained as brown oil (0.73 g, 67%). R_f = 0.4 (EtOAc/Hex 1:4). ^{1}H NMR (200 MHz, $CDCl_3$): δ = 0.80 (6H, d, J = 6.8 Hz), 0.87 (3H, d, J = 6.2 Hz), 1.07-1.28 (6H, m), 1.43-1.64 (2H, m), 1.66 (6H, m), 1.68-1.74 (2H, m), 3.90-3.97 (2H, m), 6.78-6.84 (3H, m), 7.19-7.24 (1H, m), 7.34-7.42 (1H, m), 7.47-7.52 (2H, m). ^{13}C NMR (50 MHz, $CDCl_3$): δ = 19.6, 22.6, 22.7, 25.7, 27.9, 29.8, 36.1, 37.3, 39.2, 66.4, 86.6, 96.8, 105.0 (why this peak ?), 105.6, 114.5, 114.8, 116.6, 113.7, 125.9, 128.1, 133.6, 134.8, 156.6, 159.0, 159.7. MS (ESI): m/z 435.3 $[M+H]^+$.

5-((4-(2-methoxyethoxy)phenyl)ethynyl)-2,2-dimethyl-4H-benzo[d][1,3]dioxin-4-one (5b)

The product was obtained using procedure 4 starting from 1-ethynyl-4-(2-methoxyethoxy)benzene (2.7 mmol, 0.48 g) and triflate **4** (2.5 mmol, 0.82 g). The product was purified by column chromatography using EtOAc/Hex 1:4 (v/v) as eluent. The product was obtained as yellow gum (0.65 g, 74%). R_f = 0.27 (EtOAc/Hex 1:2). ^{1}H NMR (200 MHz, $CDCl_3$): δ = 1.66 (6H, s), 3.39 (3H, s), 3.67-3.72 (2H, m), 4.05-4.10 (2H, m), 6.80- 6.87 (4H, m), 7.19-7.24 (1H, m), 7.35-7.39 (1H, m), 7.48-7.53 (1H, m). ^{13}C NMR (50 MHz, $CDCl_3$): δ = 25.9, 59.4, 67.4, 71.0, 86.9, 93.5, 96.8, 105.7, 114.8, 114.9, 115.5, 116.8, 125.9, 128.3, 133.8, 134.2, 135.0, 156.8, 158.9, 159,5. MS (ESI): m/z 370.2 $[M+NH_4]^+$.

5-((3-acetyl-4-(pentyloxy)phenyl)ethynyl)-2,2-dimethyl-4H-benzo[d][1,3]dioxin-4-one (5c)

The product was obtained using procedure 4 starting from 1-(5-ethynyl-2-(pentyloxy)phenyl)ethanone (2.7 mmol, 0.62 g) and triflate **4** (2.5 mmol, 0.82 g).. The crude product was purified using column chromatography with EtOAc/Hex 1:7 (v/v) as eluent to yield the compound as a pale yellow solid (0.54 g, 49%). R_f = 0.42 EtOAc/Hex 1:2 (v/v). ^{1}H NMR (400 MHz, $CDCl_3$) δ 0.93 (3H, t, J = 7.2 Hz), 1.36-1.49 (4H, m), 1.72 (6H, s), 1.82-1.87 (2H, m), 2.62 (3H, s), 4.08 (2H, t, J = 6.5 Hz), 6.89-6.94 (2H, m), 7.28 (1H, dd, J = 1.0, 8.0 Hz), 7.46 (1H, t, J = 8.1 Hz), 7.72 (1H, dd, J = 2.4, 8.5 Hz), 7.96 (1H, d, J = 2.1 Hz). ^{13}C NMR (100 MHz, $CDCl_3$) δ 14.0, 22.4, 25.7, 28.3, 28.8, 31.9, 68.9, 87.1, 95.5, 105.6, 112.5, 113.8, 115.2, 117.0, 125.4, 128.3, 128.4, 134.1, 134.9, 137.2, 156.6, 158.7,159.0, 198.9. MS (ESI): (m/z) 407.2 $[M+H]^+$.

5-((3-acetyl-4-(heptyloxy)phenyl)ethynyl)-2,2-dimethyl-4H-benzo[d][1,3]dioxin-4-one (5d)

The product was obtained using procedure 4 starting from 1-(5-ethynyl-2-(heptyloxy)phenyl)ethanone (2.7 mmol, 0.70 g) and triflate **4** (2.5 mmol, 0.82 g).. Purification was performed by column chromatography using EtOAc/Hex 1:7 (v/v) as eluent. The product was obtained as yellow oil (0.84 g, 83%). R_f = 0.39 (EtOAc/Hex 1:2). ^{1}H NMR (200 MHz, $CDCl_3$): δ = 0.89 (3H, t, J = 6.4 Hz), 1.31-1.65 (8H, m), 1.73-1.75 (6H, m), 1.82-1.93 (2H, m), 2.62 (3H, s), 4.08 (2H, t, J = 6.5 Hz), 6.88-7.05 (2H, m), 7.26-7.30 (1H, m), 7.42-7.50 (1H, m), 7.73 (1H, dd, J = 2.2, 6.5 Hz), 7.96 (1H, d, J = 2.35 Hz). ^{13}C NMR (50 MHz, $CDCl_3$): δ = 14.0, 22.6, 25.6, 26.1, 29.0, 29.1, 31.7, 31.9, 68.8, 87.1, 95.5, 105.6, 106.8, 112.5, 115.2, 116.9, 122.4, 125.5, 128.3, 128.4, 134.1, 134.9, 137.2, 156.6, 158.7, 159.0, 198.9. MS (ESI): m/z 452.3 $[M+NH_4]^+$.

5-((2,2-dimethyl-4-oxo-4H-benzo[d][1,3]dioxin-5-yl)ethynyl)-1-pentylpyridin-2(1H)-one (5e)

The product was obtained using procedure 4 starting from 5-ethynyl-2-(pentyloxy)pyridine (2.7 mmol, 0.51 g) and triflate **4** (2.5 mmol, 0.82 g). The product was purified by column chromatography using EtOAc/Hex 1:4 (v/v) as eluent. The product was obtained as yellow solid (0.68 g, 69%). R_f = 0.31 (EtOAc/Hex 1:1). ^{1}H NMR (200 MHz, $CDCl_3$): δ = 0.84 (3H, t, J = 6.5 Hz), 1.18-1.31 (6H, m), 3.87 (2H, t, J = 7.5 Hz), 6.50 (1H, d, J = 9.4 Hz), 6.85 (1H, d, J = 7.0 Hz), 7.18-7.19 (1H, m), 7.36-7.45 (2H, m), 7.63 (1H, d, J = 2.4 Hz). ^{13}C NMR (50 MHz, $CDCl_3$): δ = 13.9, 22.3, 25.7, 28.7, 29.0, 50.3, 88.4, 92.1, 102.4, 105.8, 113.5, 117.1, 120.6, 125.0, 127.7, 135.2, 141.4, 142.1, 156.7, 159.1, 161.3. MS (ESI): m/z 366.2 $[M+H]^+$.

2,2-dimethyl-5-(pent-1-yn-1-yl)-4H-benzo[d][1,3]dioxin-4-one (5f)

The product was obtained using procedure 4 starting from 1-pentyne (2.7 mmol, 0.23 mL) and triflate **4** (2.5 mmol, 0.82 g). The product was purified by column chromatography using with EtOAc/Hex 1:9 (v/v) as eluent. The compound was obtained as yellow solid (0.48 g, 82%). R_f = 0.44 EtOAc/Hex 1:2 (v/v). ^{1}H NMR (400 MHz, $CDCl_3$) δ 1.08 (3H, t, J = 7.3), 1.65-1.70 (8H, m), 2.48 (2H, t, J = 7.0 Hz), 6.85 (1H, dd, 0.9, 7.3 Hz), 7.18 (1H, dd, J = 0.88, 6.7 Hz), 7.39 (1H, t, J = 7.9 Hz). ^{13}C NMR (100 MHz, $CDCl_3$) δ 13.6, 22.0, 25.7, 78.9, 98.4, 105.5, 114.1, 116.4, 126.3, 128.9, 134.7, 156.5, 159.0. MS (ESI): (m/z) 245.1 $[M+H]^+$.

5-(4-((3,7-dimethyloctyl)oxy)phenethyl)-2,2-dimethyl-4H-benzo[d][1,3]dioxin-4-one

The product was obtained using procedure 5 starting from 5-((4-((3,7-dimethyloctyl)oxy)phenyl)ethynyl)-2,2-dimethyl-4H-benzo[d][1,3]dioxin-4-one (1.5

mmol, 0.65 g). The product was purified by column chromatography using EtOAc/Hex 1:18 (v/v) as eluent. The product was obtained as brown solid (0.62 g, 94%). R_f = 0.57 (EtOAc/Hex 1:4). ^{1}H NMR (200 MHz, $CDCl_3$): δ = 0.87 (6H, d, J = 6.8 Hz), 0.94 (3H, d, J = 6.5 Hz), 1.10-1.37 (6H, m), 1.47-1.64 (2H, m), 1.69 (6H, s), 1.73-1.77 (2H, m), 2.80-2.88 (2H, m), 3.32-3.40 (2H, m), 3.96 (2H, t, J = 6.0 Hz), 6.79-6.88 (4H, m), 7.12-7.26 (2H, m), 7.37 (1H, t, J = 7.9 Hz). ^{13}C NMR (50 MHz, $CDCl_3$): δ = 19.7, 22.6, 22.7, 24.6, 25.6, 28.0, 29.9, 36.3, 36.6, 36.9, 37.3, 39.2, 66.3, 105.0, 112.1, 114.3, 115.4, 125.4, 129.5, 133.6, 135.1, 147.2, 157.1, 157.4, 160.3. MS (ESI): m/z 439.2 $[M+H]^+$.

5-(4-(2-methoxyethoxy)phenethyl)-2,2-dimethyl-4H-benzo[d][1,3]dioxin-4-one

The product was obtained using procedure 5 starting from 5-((4-(2-methoxyethoxy)phenyl)ethynyl)-2,2-dimethyl-4H-benzo[d][1,3]dioxin-4-one (1.5 mmol, 0.53 g). The product was purified by column chromatography using EtOAc/Hex 1:5 (v/v) as eluent. The product was obtained as white solid (0.49 g, 92%). R_f = 0.61 (EtOAc/Hex 1:1). ^{1}H NMR (200 MHz, $CDCl_3$): δ = 1.69 (6H, m), 2.79-2.87 (2H, m), 3.31-3.35 (2H, m), 3.45 (3H, s), 3.71-3.74 (2H, m), 4.08-4.11 (2H, m), 6.79-6.85 (4H, m), 7.12-7.16 (2H, m), 7.36 (1H, t, J = 7.9 Hz). ^{13}C NMR (50 MHz, $CDCl_3$): δ = 25.6, 36.6, 36.9, 59.2, 67.2, 71.1, 105.0, 112.1, 114.4, 115.4, 125.5, 129.2, 134.1, 135.1, 147.1, 157.1, 160.3, 173.4. MS (ESI): m/z 374.2 $[M+H]^+$.

5-(3-acetyl-4-(pentyloxy)phenethyl)-2,2-dimethyl-4H-benzo[d][1,3]dioxin-4-one

The product was obtained using procedure 5 starting from 5-((3-acetyl-4-(pentyloxy)phenyl)ethynyl)-2,2-dimethyl-4H-benzo[d][1,3]dioxin-4-one (1.5 mmol, 0.61 g). The product was purified by column chromatography using EtOAc/Hex 1:10 (v/v) as eluent. The product was obtained as a white solid (0.25 g, 40%). R_f = 0.52 (EtOAc/Hex 1:2). ^{1}H NMR (400 MHz, $CDCl_3$): δ 0.94 (3H, t, J = 7.2 Hz), 1.39-1.47 (4H, m), 1.70 (6H, s), 1,82-1,84 (2H, m), 2.62 (3H, s), 2,83-2.87(2H, m), 3,31-3.35 (2H, m), 4,03 (2H, t, J = 6.5 Hz), 6.81-6.88 (3H, m), 7.36 (2H, m), 7,57 (1H, d, J = 2.4 Hz). ^{13}C NMR (100 MHz, $CDCl_3$) δ 14.0, 22.4, 25.6, 28.9, 32.1, 36.3, 36.8, 68.6, 105.1, 112.0, 112.4, 115.6, 125.4, 127.8, 130.2, 133.6, 134.0, 135.3, 146.8, 157.0, 157.2, 160.3, 200.1. MS (ESI): (m/z) 411.2 $[M+H]^+$.

5-(3-(1-hydroxyethyl)-4-(pentyloxy)phenethyl)-2,2-dimethyl-4H-benzo[d][1,3]dioxin-4-one

The product was obtained using procedure 5 starting from 5-((3-acetyl-4-(pentyloxy)phenyl)ethynyl)-2,2-dimethyl-4H-benzo[d][1,3]dioxin-4-one (1.5 mmol, 0.61 g) using 20 % (w/w) Pd/C 10% mol (which percentage ?). The product was obtained as yellow solid (0.53 g, 86%): R_f = 0.52 (EtOAc/Hex 1:2); ^{1}H NMR (MHz,

$CDCl_3$): δ 0.93 (3H, t, *J* = 7.2 Hz), 1.36-1.47 (4H, m), 1.50 (3H, d, *J* = 6.5 Hz), 1.60 (3H, s), 1.80 (3H, s), 1,77-1,84 (2H, m), 2.84 (2H, t, *J* = 7.9 Hz), 3,33-3.37 (2H, m), 3.98 (2H, t, *J* = 6.4 Hz), 5.03 (1H, q, *J* = 6.5 Hz), 6.76-6.87 (3H, m), 7.10 (1H, dd, *J* = 2.4, 10.6 Hz), 7,15 (1H, d, *J* = 2.34 Hz), 7.37 (1H, t, *J* = 7.9 Hz) ppm. ^{13}C NMR (100 MHz, $CDCl_3$) δ 14.0, 22.4, 22.9, 25.6, 25.7, 28.4, 29.0, 36.7, 36.9, 67.2, 68.0, 105.1, 111.2, 112.1, 115.4, 125.5, 126.6, 128.1, 133.0, 133.8, 135.1, 147.1, 154.4, 157.2 ppm. MS (ESI): (*m/z*) 430.3 $[M+NH_4]^+$.

5-(3-ethyl-4-(pentyloxy)phenethyl)-2,2-dimethyl-4H-benzo[d][1,3]dioxin-4-one

The product was obtained using procedure 2 starting from 5-((3-acetyl-4-(pentyloxy)phenyl)ethynyl)-2,2-dimethyl-4H-benzo[d][1,3]dioxin-4-one (1.5 mmol, 0.61 g) using 40 % (w/w) Pd/C 10% mol (which percentage ?). The product was obtained as yellow solid (0.40 g, 98%): R_f = 0.78 (EtOAc/Hex 1:2); ^{1}H NMR (400MHz, $CDCl_3$): δ 0.94 (3H, t, *J* = 7.2 Hz), 1.18 (3H, t *J* = 7.5Hz), 1,36-1,48 (4H, m), 1.70 (6H, s), 1.77-1.81 (2H, m), 2.61 (2H, q, *J* = 7,5 Hz), 2,82 (2H, t, *J* = 7,9 Hz), 3.36 (2H, t, 7.9 Hz), 3.93 (2H, t, *J* = 6.4 Hz), 6.73 (1H, d, 8.8 Hz), 6.81 (1H, d, *J* = 8.2 Hz), 6.87 (1H, d, *J* = 7.6 Hz), 7.00-7.02 (2H, m), 7.38 (1H, t, 7.9 Hz) ppm. ^{13}C NMR (100 MHz, $CDCl_3$) δ 14.0, 14.3, 22.4, 23.4, 25.6, 28.4, 29.1, 36.8, 37.0, 67.9, 105.0, 111.0, 112.1, 115.3, 125.5, 126.6, 129.4, 132.5, 133.3, 135.1, 147.4, 155.1, 157.1, 160.3 ppm. MS (ESI): (*m/z*) 397.2 $[M+H]^+$.

5-((3-acetyl-4-(heptyloxy)phenyl)ethyl)-2,2-dimethyl-4H-benzo[d][1,3]dioxin-4-one

The product was obtained using procedure 5 starting from 5-((3-acetyl-4-(heptyloxy)phenyl)ethynyl)-2,2-dimethyl-4H-benzo[d][1,3]dioxin-4-one (1.5 mmol, 0.61 g). Purification was performed by column chromatography using EtOAc/Hex 1:8 (v/v) as eluent. The product was obtained as yellow oil (0.52 g, 84%); R_f = 0.51 (EtOAc/Hex 1:2); ^{1}H NMR (200 MHz, $CDCl_3$): *δ* = 0.81 (3H, t, *J* = 6.4 Hz), 1.22-1.40 (8H, m), 1.60 (6H, s), 1.71-1.78 (2H, m), 2.53 (3H, s), 2.72-2.80 (2H, m), 3.21-3.29 (2H, m), 3.93, (2H, t, *J* = 5.1 Hz), 6.70-6.80 (3H, m), 7.25-7.32 (2H, m), 7.48 (1H, d, *J* = 2.4 Hz); ^{13}C NMR (50 MHz, $CDCl_3$): *δ* = 14.1, 22.6, 25.6, 26.2, 29.0, 29.3, 31.8, 32.1, 36.3, 36.8, 68.6, 105.1, 112.0, 112.4, 115.6, 125.4, 127.8, 130.2, 133.6, 134.1, 135.3, 146.8, 157.0, 157.2, 160.3, 200.0 ppm; MS (ESI): *m/z* 456.3 $[M+NH_4]^+$.

5-(2-(2,2-dimethyl-4-oxo-4H-benzo[d][1,3]dioxin-5-yl)ethyl)-1-pentylpiperidin-2-one

The product was obtained using procedure 5 starting from 2-dimethyl-5-((6-(pentyloxy)pyridin-3-yl)ethynyl)-4H-benzo[d][1,3]dioxin-4-one (1.5 mmol, 0.55 g). The product was purified by column chromatography using EtOAc/Hex 1:1 (v/v) as

eluent. The product was obtained as orange oil (0.44 g, 80%); R_f = 0.30 (EtOAc/Hex 3:1); ^{1}H NMR (200 MHz, $CDCl_3$): δ = 0.87 (3H, t, J = 6.7 Hz), 1.11-1.36 (6H, m), 1.43-1.59 (5H, m), 1.68 (6H, s), 1.88-1.95 (2H, m), 2.30-2.49 (2H, m), 3.02-3.08 (2H, m), 3.31-3.37 (2H, m), 6.79-6.91 (2H, m), 7.40 (1H, t, J = 7.9 Hz). ^{13}C NMR (50 MHz, $CDCl_3$): δ = 14.0, 22.5, 25.6, 26.7, 27.3, 29.1, 31.5, 32.0, 34.1, 34.9, 47.3, 53.0, 105.1, 111.8, 115.6, 125.0, 135.4, 147.3, 157.2, 160.3, 169.5 ppm; MS (ESI): m/z 374.4 $[M+H]^+$.

2,2-dimethyl-5-pentyl-4H-benzo[d][1,3]dioxin-4-one

The product was obtained using procedure 5 starting from 2-dimethyl-5-(pent-1-yn-1-yl)-4H-benzo[d][1,3]dioxin-4-one (1.5 mmol, 0.37g). The product was obtained as pale yellow solid (0.31 g, 85%): R_f = 0.54 (EtOAc/Hex 1:2); ^{1}H NMR (400 MHz, $CDCl_3$): δ 0.88 (3H, t, J = 7.2 Hz), 1.30-1.38 (4H, m), 1.56-1.70 (8H, m), 3.08 (2H, t, J = 7.8 Hz), 6.78 (1H, dd, J = 1.2, 8.2 Hz), 6.91 (1H, dd, J = 1.0, 8.5 Hz), 7.38 (1H, t, J = 7.9 Hz) ppm. ^{13}C NMR (100 MHz, $CDCl_3$) δ 14.0, 22.5, 25.6, 30.8, 31.8, 34.3, 104.9, 112.1, 115.0, 125.1, 135.0, 148.5, 157.1, 160.2 ppm. MS (ESI): (m/z) 249.3 [M+H]

2-(4-((3,7-dimethyloctyl)oxy)phenethyl)-6-hydroxybenzoic acid (6a)

The product was obtained using procedure 6 starting from 5-(4-((3,7-dimethyloctyl)oxy)phenethyl)-2,2-dimethyl-4H-benzo[d][1,3]dioxin-4-one (1 mmol, 0.44 g). The product was purified by column chromatography using EtOAc/Hex 1:6 (v/v) as eluent. The product was obtained as yellow solid (0.0.37 g, 93%); R_f = 0.38 (EtOAc/Hex 1:1); ^{1}H NMR (200 MHz, $CDCl_3$): δ = 0.83 (6H, d, J = 6.8 Hz), 0.94 (3H, d, J = 6.5 Hz), 1.07-1.25 (6H, m), 1.43-1.46 (2H, m), 1.50-1.56 (2H, m), 2.11-2.82 (2H, m), 3.15-3.23 (2H, m), 3.89 (2H, t, J = 6.0 Hz), 6.64 (1H, d, J = 7.6 Hz), 6.73-7.00 (3H, m), 7.04-7.19 (2H, m), 7.28 (1H, t, J = 8.1 Hz), ^{13}C NMR (50 MHz, $(CD_3)_2SO$): δ = 19.6, 22.6, 22.7, 24.7, 28.0, 29.9, 36.3, 37.3, 37.4, 38.8, 39.2, 66.4, 110.5, 114.5, 116.2, 123.0, 129.3, 133.6, 135.6, 146.4, 157.4, 163.7, 175.7 ppm; HRMS: m/z $[M-H]^-$, calcd for $C_{25}H_{33}O_4$ 397.2379, found 397.2381.

2-hydroxy-6-(4-(2-methoxyethoxy)phenethyl)benzoic acid (6b)

The product was obtained using procedure 6 starting from 5-(4-(2-methoxyethoxy)phenethyl)-2,2-dimethyl-4H-benzo[d][1,3]dioxin-4-one (1 mmol, 0.36 g). The product was purified by column chromatography using EtOAc/Hex 1:4 (v/v) as eluent. The product was obtained as white solid (0.18 g, 58%); R_f = 0.49 (100 %EtOAc); ^{1}H NMR (200 MHz, CD_3CN): δ = 2.74-2.81 (2H, m), 3.11-3.19 (2H, m), 3.36 (3H, s), 3.65-3.70 (2H, m), 4.03-4.08 (2H, m), 6.73-6.85 (4H, m), 7.09-7.14 (2H, m), 7.28-7.35 (1H, m); ^{13}C NMR (50 MHz, CD_3CN): δ = 42.3, 43.6, 63.3, 72.4, 76.1, 117.6,

119.6, 120.6, 127.7, 134.7, 139.5, 139.7, 150.7, 162.4, 167.7, 177.8 ppm; HRMS: *m/z* [M-H]$^-$, calcd for $C_{18}H_{19}O_5$ 315.1238, found 315.1239.

2-(3-acetyl-4-(pentyloxy)phenethyl)-6-hydroxybenzoic acid (6c)

The product was obtained using procedure 6 starting from 5-(3-acetyl-4-(pentyloxy)phenethyl)-2,2-dimethyl-4H-benzo[d][1,3]dioxin-4-one (1.0 mmol, 0.41 g). The product was obtained a pale green solid (0.26 g, 71%); mp:106 ˚C; R_f = 0.46 (EtOAc 100%); ^{1}H NMR (400MHz, CD_3CN): δ 0.95 (3H, t, *J* = 7.2 Hz), 1.41-1.50 (4H, m), 1.82-1.87 (2H, m), 2.59 (3H, s), 2.84 (2H, t, *J* = 8.2 Hz), 3.18 (2H, t, *J* = 8,2 Hz), 4.09 (2H, t, *J* = 6.64 Hz), 6.78 (1H, d, *J* = 7.3 Hz), 6.83 (1H, dd, *J* = 1.2, 8.2 Hz), 7.01 (1H, d, *J* = 8.5 Hz), 7.32-7.36 (2H, m), 7.49 (1H, d, *J* = 2.3 Hz) ppm. ^{13}C NMR (50 MHz, CD_3OD) δ 14.4, 23.5, 29.6, 30.1, 32.2, 38.4, 39.4, 69.8, 113.8, 114.9, 116.3, 123.3, 128.8, 130.8, 134.5, 135.2, 135.3, 145.6, 158.5, 162.9, 174.2, 202.3 ppm. HRMS: *m/z* [M-H]$^-$, calcd for $C_{22}H_{25}O_5$ 369.1708, found 369.1711.

2-hydroxy-6-(3-(1-hydroxyethyl)-4-(pentyloxy)phenethyl)benzoic acid (6d)

The product was obtained using procedure 6 starting from 5-(3-(1-hydroxyethyl)-4-(pentyloxy)phenethyl)-2,2-dimethyl-4H-benzo[d][1,3]dioxin-4-one (1.0 mmol, 0.41 g). The compound was obtained as white solid (0.14 g, 38%); mp: 113 ˚C; R_f = 0.46 (EtOAc 100%); ^{1}H NMR (400MHz, CD_3OD): δ 0.94 (3H, t, *J* = 6.9 Hz), 1.36-1.46 (7H, m), 1.75-1.78 (2H, m), 2.79 (2H, t, *J* = 7.9 Hz), 3.07-3.17 (2H, m), 3.93 (2H, d, *J* = 3.5 Hz), 5.16 (1H, q, *J* = 6.2 Hz), 6.68 (1H, d, *J* = 7.3 Hz), 6.75-6.78 (2H, m), 6.98 (1H, d, *J* = 7.3 Hz), 7.21-7.27 (2H, m) ppm. ^{13}C NMR (50 MHz, CD_3OD) δ 13.0, 22.1, 23.1, 28.2, 28.8, 37.5, 38.1, 64.0, 67.7, 110.8, 114.0, 114.6, 121.9, 125.1, 127.2, 132.9, 133.8, 134.0, 144.5, 153.5, 161.0, 172.9 ppm. HRMS: *m/z* [M-H]$^-$, calcd for $C_{22}H_{27}O_5$ 371.1864, found 371.1867.

2-(3-ethyl-4-(pentyloxy)phenethyl)-6-hydroxybenzoic acid (6e)

The product was obtained using procedure 6 starting from 5-(3-ethyl-4-(pentyloxy)phenethyl)-2,2-dimethyl-4H-benzo[d][1,3]dioxin-4-one (1.0 mmol, 0.39 g). The compound was obtained as white solid (0.11 g, 32%); mp: 96 ˚C; R_f = 0.65 (EtOAc 100%); ^{1}H NMR (400MHz, CD_3OD): δ 0.95 (3H, t, *J* = 7.2 Hz), 1.16 (3H, t, *J* = 7.5 Hz), 1.38-1.51 (4H, m), 1.76-1.81 (2H, m), 2.59 (2H, q, *J* = 7.4 Hz), 2.78 (2H, t, *J* = 7.8 Hz), 3.16-3.20 (2H, m), 3.95 (2H, t, *J* = 6.3 Hz), 6.76-6.83 (3H, m), 6.98-7.00 (2H, m), 7.33 (1H, t, *J* = 7.9 Hz) ppm. ^{13}C NMR (50 MHz, CD_3OD) δ 13.4, 14.0, 22.2, 23.1, 28.1, 28.9, 37.2, 38.4, 67.9, 111.3, 112.3, 115.3, 122.3, 126.5, 126.6, 129.2, 129.3, 132.2, 133.8, 134.1, 145.6, 155.1, 162.6, 172.7 ppm. HRMS: *m/z* [M-H]$^-$, calcd for $C_{22}H_{27}O_4$ 355.19148, found 355.19125.

2-(3-acetyl-4-(heptyloxy)phenethyl)-6-hydroxybenzoic acid (6f)

The product was obtained using procedure 6 starting from 5-(3-acetyl-4-(heptyloxy)phenethyl)-2,2-dimethyl-4H-benzo[d][1,3]dioxin-4-one (1.0 mmol, 0.41 g). Purification was performed by column chromatography using EtOAc/Hex 1:5 (v/v) as eluent. The product was obtained as pale yellow solid (0.21 g, 58%); R_f = 0.47 (100% EtOAc); ^{1}H NMR (200 MHz, $CDCl_3$): δ = 0.82 (3H, t, J = 6.6 Hz), 1.23-1.30 (8H, m), 1.72-1.76 (2H, m), 2.61 (3H, s), 2.78-2.82 (2H, m), 3.13-3.17 (2H, m), 3.95 (2H, t, J = 6.5 Hz), 6.65 (1H, d, J = 6.5 Hz), 6.75-6.84 (2H, m), 7.15-7.30 (2H, m), 7.62 (1H, d, J = 2.4 Hz); ^{13}C NMR (50 MHz, $CDCl_3$): δ = 14.1, 22.6, 26.2, 29.0, 29.2, 31.7, 32.1, 37.3, 38.8, 68.7, 110.9, 112.3, 116.2, 122.7, 127.6, 130.3, 133.8, 134.1, 135.1, 145.8, 157.3, 163.6, 174.6, 201.5 ppm; HRMS: m/z $[M-H]^-$, calcd for $C_{24}H_{29}O_5$ 397.2021, found 397.2018.

2-(2-(1-butyl-6-oxopiperidin-3-yl)ethyl)-6-hydroxybenzoic acid (6g)

The product was obtained using procedure 6 starting from 2,2-dimethyl-5-(2-(6-(pentyloxy)-2,3,4,5-tetrahydropyridin-3-yl)ethyl)-4H-benzo[d][1,3]dioxin-4-one (1 mmol, 0.37 g). The product was purified by column chromatography using DCM/MeOH 9:1 (v/v) as eluent. The product was obtained as white solid (0.24 g, 73%); R_f = 0.60 (DCM/MeOH 2:1); ^{1}H NMR (200 MHz, $(CD_3)_2SO$): δ = 0.87 (3H, t, J = 6.9 Hz), 1.16-1.59 (9H, m), 1.78-1.84 (2H, m), 2.17-2.24 (2H, m), 2.63-2.69 (2H, m), 2.87-2.98 (2H, m), 3.13-3.30 (2H, m), 6.70-6.75 (2H, m), 7.14-7.22 (1H, m); ^{13}C NMR (50 MHz, $(CD_3)_2SO$): δ = 14.4, 22.3, 26.6, 27.2, 29.0, 31.5, 33.6, 35.1, 46.5, 52.7, 114.1, 120.5, 120.1, 131.1, 141.6, 156.4, 168.5, 170.7 ppm; HRMS: m/z $[M-H]^-$, calcd for $C_{19}H_{26}O_4N_1$ 332.1867, found 332.1869.

2-hydroxy-6-pentylbenzoic acid (6H)

The product was obtained using procedure 6 starting from 2,2-dimethyl-5-pentyl-4H-benzo[d][1,3]dioxin-4-one (1.0 mmol, 0.25 g). The product was obtained as white solid (0.19 g, 90%); mp:84 ˚C; R_f = 0.57 (EtOAc 100%); ^{1}H NMR (400MHz, $CDCl_3$): δ 0.89 (3H, t, J = 7.0 Hz), 1.30-1.36 (4H, m), 1.55-1.59 (2H, m), 2.87 (2H, t, J = 7.8 Hz), 6.69-6.73 (2H, m), 7.22 (1H, t, J = 7.9 Hz). NMR (50 MHz, $CDCl_3$) δ 13.0, 22.1, 31.5, 31.7, 35.2, 105.0, 114.2, 121.4, 132.4, 145.4, 160.7, 173.2 ppm. HRMS: m/z $[M-H]^-$, calcd for $C_{12}H_{15}O_3$ 207.1027, found 207.1028

Methyl 5-(dec-1-ynyl)-2-methoxybenzoate (8)

The product was obtained using procedure 4 starting from dec-1-yne (2.7 mmol, 0.48 mL) and methyl 5-iodo-2-methoxybenzoate (2.5 mmol, 0.73 g). The product was purified by column chromatography using EtOAc/Hex 1:8 (v/v) as eluent. The product was obtained as orange solid (0.53 g, 68%); R_f = 0.40 (EtOAc/Hex 1:3); ^{1}H

NMR (200 MHz, $CDCl_3$): δ = 0.85-0.91 (3H, m), 1.25-1.31 (8H, m), 1.39-1.44 (2H, m), 1.51-1.56 (2H, m), 2.37 (2H, t, J = 6.9 Hz), 3.87 (3H, s), 3.89 (3H, s), 6.88 (1H, d, J = 8.7 Hz), 7.47 (1H, dd, J = 8.6, 2.2 Hz), 7.83 (1H, d, J = 2.2 Hz); ^{13}C NMR (50 MHz, $CDCl_3$): δ = 14.1, 19.3, 22.6, 28.7, 28.9, 29.1, 29.2, 31.8, 52.0, 56.1, 79.2, 89.8, 111.9, 116.1, 120.0, 134.9, 136.4, 158.3, 165.9 ppm; MS (ESI): m/z 303.2 $[M+H]^+$.

Methyl 5-decyl-2-methoxybenzoate

The product was obtained using procedure 5 starting from methyl 5-(dec-1-yn-1-yl)-2-methoxybenzoate (1.5 mmol, 0.47 g). The product was obtained as dark yellow oil (0.45 g, 95%); R_f = 0.45 (EtOAc/Hex 1:3); ^{1}H NMR (200 MHz, $CDCl_3$): δ =0.76 (3H, t, J = 6.5 Hz), 1.26 (14H, m), 1.58-1.64 (2H, m), 2.55 (2H, t, J = 7.4 Hz), 3.87 (3H, s), 3.88 (3H, s), 6.88 (1H, d, J = 8.5 Hz), 7.26 (1H, dd, J = 8.5, 2.4 Hz), 7.60 (1H, d, J = 2.3 Hz) ; ^{13}C NMR (50 MHz, $CDCl_3$): δ = 14.1, 22.7, 29.2, 29.3, 29.5, 29.6, 29.7, 31.5, 31.9, 34.8, 51.9, 56.1, 112.0, 119.6, 131.3, 133.3, 134.6, 157.2, 166.9 ppm; MS (ESI): m/z 307.2 $[M+H]^+$

5-decyl-2-hydroxybenzoic acid (9)

Methyl 5-decyl-2-methoxybenzoate (1 mmol, 0.32 g) was dissolved in dry CH_2Cl_2 (20 mL) and the solution was cooled to -78 °C. A solution 1 M of boron tribromide (BBr_3) in CH_2Cl_2 (5.0 mmol, 5.0 mL) was slowly added and the reaction mixture was stirred for 5 h at room temperature. The reaction mixture was quenched with few drops of water and extract with a saturated Na_2CO_3 solution (30 mL). The water layer was acidified with HCl 1 N and extracted with EtOAc (3 x 50 mL). The organic layers were collected, washed with brine (1 x 50 mL), dried over Na_2SO_4 and filtered. The solvent was evaporated and the product was purified by column chromatography using EtOAc/Hex 1:3 (v/v) as eluent. The product was obtained as pink solid (0.20 g, 73%); R_f = 0.32 (100 % EtOAc); ^{1}H NMR (200 MHz, $CDCl_3$): δ = 0.88 (3H, t, J = 6.5 Hz), 1.26 (14H, m), 1.55-1.62 (2H, m), 2.56 (2H, t, J = 7.4 Hz), 6.93 (1H, d, J = 8.5 Hz), 7.34 (1H, dd, J = 8.5, 2.3 Hz), 7.71 (1H, d, J = 2.1 Hz); ^{13}C NMR (50 MHz, $CDCl_3$): δ = 14.1, 22.7, 29.1, 29.3, 29.4, 29.6, 31.4, 31.9, 34.8, 45.8, 110.8, 117.5, 129.9, 134.0, 137.3, 160.3, 174.4 ppm; HRMS: m/z $[M-H]^-$, calcd for $C_{17}H_{25}O_3$ 277.1809, found 277.1811.

Methyl 2-(pentadec-1-ynyl)benzoate (11)

The product was obtained using procedure 4 starting from pentadec-1-yne (1.1 mmol, 0.27 mL) and methyl 2-iodobenzoate (0.95 mmol, 0.25 g). The reaction mixture was subjected to microwave irradiation at 100 °C (85 W) for 45 minutes. The mixture was extracted with diethyl ether (3 x 50mL) and the solvents were evaporated under reduced pressure. The reaction mixture was separated by column chromatography

on silica using diethyl ether/pentane 1:4 (v/v) as solvent. The product was obtained as brown oil (0.20 g, 62%): R_f = 0,67 (diethyl ether/pentane 1:10); ^{1}H NMR (400 MHz, $CDCl_3$) δ 0.88 (3H, t, *J* = 6.9 Hz), 1.21-1.65 (22H, m), 2.47 (2H, t, *J* = 7.1 Hz), 3.91 (3H, s), 7.30 (1H, td, *J* = 1.3, 7.7 Hz), 7.41 (1H, td, *J* = 1.4, 7.6 Hz), 7.50 (1H, dd, *J* = 1.1, 7.8 Hz), 7.88 (1H, dd, *J* = 7.9, 1.1); ^{13}C NMR (50 MHz, $CDCl_3$) δ 14.1, 19.8, 22.7, 28.7, 29.0, 29.2, 29.4, 29.6, 29.6, 29.7, 31.9, 52.1, 105.0, 114.1, 127.1, 130.1, 131.5, 134.2, 144.8.

Methyl 2-pentadecylbenzoate

The product was obtained using procedure 5 starting from methyl 2-(pentadec-1-yn-1-yl)benzoate (0.51 g, 1.5 mmol). The product was obtained as colorless oil (0.40 g, 78 %): R_f = 0.87 (diethyl ether/ pentane 1:4); ^{1}H NMR (400 MHz, $CDCl_3$) δ 0.88 (3H, t, *J* = 6.9), 1.15-1.70 (26H, m), 2.85-2.99 (2H, m), 3.89 (3H, s), 7.14-7.29 (2H, m), 7.31-7.50 (1H, m), 7.84 (1H, dd, *J* = 1.2, 7.7); ^{13}C NMR (50 MHz, $CDCl_3$) δ 14.1, 22.7, 29.4, 29.5, 29.7, 29.8, 31.8, 31.9, 34.5, 51.9, 125.6, 130.5, 130.9, 131.8, 144.7.

2-pentadecylbenzoic acid (12)

Methyl 2-pentadecylbenzoate (0.40 mmol, 0.15 g) and LiOH (2.2 mmol, 0.050 g,) were dissolved in THF/Methanol/H_2O 3:1:1 (5 mL) and refluxed overnight in a round bottom flask equipped with a condenser. The solvents were evaporated under reduced pressure. Water (50 mL) was added and the mixture was acidified to pH 2 with aqueous HCl 2 M. The mixture was extracted with diethyl ether (3 x 50 mL) and the combined organic layers were dried over $MgSO_4$. The solvent was evaporated under reduced pressure to give the product as pale yellow solid (0.13 g, 91%): R_f: 0.49 (diethyl ether/pentane 1:4); ^{1}H NMR (400 MHz, $CDCl_3$) δ 0.89 (3H, t, *J* = 6.9 Hz), 1.07-1.70 (26H, m), 2.99-3.10 (2H, m), 7.23-7.33 (2H, m), 7.47 (1H, td, *J* = 1.4, 7.8 Hz), 8.06 (1H, dd, *J* = 1.2, 8.4 Hz); ^{13}C NMR (101 MHz, $CDCl_3$) δ 14.1, 22.7, 29.4, 29.5, 29.6, 29.7, 31.8, 31.9, 34.6, 125.8, 128.1, 131.2, 131.6, 132.8, 146.0, 173.6.

Benzyl 2,4-bis(benzyloxy)-6-((4-heptylphenyl)ethynyl)benzoate (14)

The product was obtained using procedure 4 starting from 1-ethynyl-4-heptylbenzene (2.7 mmol, 0.59 g) and **13** (0.95 mmol, 0.25 g). The product was purified by column chromatography using EtOAc/Hex 1:9 (v/v) as eluent. The product was obtained as brown oil (0.97 g, 62%); R_f = 0.43 (EtOAc/Hex 1:3); ^{1}H NMR (200 MHz, $CDCl_3$): *δ* = 0.81 (3H, t, *J* = 6.4 Hz), 1.21-1.23 (8H, m), 1.49-1.53 (2H, m), 2.53 (2H, t, *J* = 7.4 Hz), 4.96 (2H, s), 4.99 (2H, s), 5.29 (2H, s), 6.48 (1H, d, *J* = 2.4 Hz), 6.7 (1H, d, *J* = 2.4 Hz), 7.02-7.31 (19H, m); ^{13}C NMR (50 MHz, $CDCl_3$): *δ* = 14.2, 22.2, 22.8, 29.2, 31.4, 31.9, 36.1, 67.2, 70.4, 70.7, 86.2, 93.4, 101.9, 109.6, 119.8,

120.0, 123.8, 127.2, 127.7, 128.0, 128.1, 128.3, 128.4, 128.5, 128.6, 128.8, 131.8, 136.0, 136.3, 136.4, 144.0, 157.2, 160.5, 166.8 ppm; MS (ESI): *m/z* 623.3 $[M+H]^+$.

2-(4-heptylphenethyl)-4,6-dihydroxybenzoic acid (15)

The product was obtained using procedure 5 starting from benzyl 2,4-bis(benzyloxy)-6-((4-heptylphenyl)ethynyl) benzoate (1.5 mmol, 0.94 g). The product was purified by column chromatography using EtOAc/Hex 1:5 (v/v) as eluent. The product was obtained as white solid (0.40 g, 74%); R_f = 0.60 (100 % EtOAc); ^{1}H NMR (200 MHz, $CDCl_3$): δ = 0.85 (3H, t, J = 6.4 Hz), 1.25-1.31 (8H, m), 1.58-1.62 (2H, m), 2.58 (2H, t, J = 7.4 Hz), 2.83-2.91 (2H, m), 3.18-3.27 (2H, m), 6.25-6.34 (1H, m), 7.09-7.40 (4H, m), 7.40 (1H, s); ^{13}C NMR (50 MHz, $CDCl_3$): δ = 14.2, 22.8, 29.3, 29.5, 31.7, 32.0, 35.7, 60.8, 70.1, 100.2, 104.5, 112.0, 127.7, 128.4, 128.5, 128.8, 136.1, 139.1, 140.6, 161.5, 163.9, 172.0. HRMS: *m/z* $[M-H]^-$, calcd for $C_{22}H_{27}O_4$ 355.1915, found 355.1918.

Protein expression

His-tagged PCAF HAT domain (493-658) was expressed with the pET28a vector. His-tagged full length Tip60 was expressed with the pET21a(+) vector. Recombinant p300 HAT domain was a gift from Dr. Philip Cole. Human MOF (125-458) was expressed with the pET19 vector. All the protein expression was carried out with *E. coli* BL21(DE3). The His-tagged proteins were purified on Ni-NTA beads. Protein concentrations were determined using the Bradford assay. Proteins were flash frozen in a storage buffer containing 25 mM HEPES pH=7.0, 500 mM NaCl, 10 mM DTT, 1 mM EDTA and 10% Glycerol, and stored at -80°C.

Biochemical inhibition assays

Radioisotope-labeled acetyltransferase assays were carried out at 30 °C in a reaction volume of 30 µL. The reaction buffer contained 50 mM HEPES at pH 8.0, 0.1 mM EDTA, 50 µg/mL BSA, 1 mM dithiothreitol, 0.1% Triton-X100, and 2% DMSO. ^{14}C-labeled Ac-CoA (Perkin Elmer) was used as the acetyl donor. The peptide containing the N-terminal 20-amino acid sequence of histone H4 (i.e. H4-20) was used as substrate for p300 and Tip60, and the peptide containing the N-terminal 20-amino acid sequence of histone H3 (i.e. H3-20) was employed as substrate for PCAF. For IC_{50} determination, a range of at least seven inhibitor concentrations varied at least 20-fold around the IC_{50} were tested. The reaction was initiated with the HAT enzyme after the other components (Ac-CoA, peptide substrate, and the inhibitor) were equilibrated at 30 °C for 5 min. Rate measurements were based on initial conditions (generally less than 15% consumption of the limiting substrate). After the reaction, the mixture was loaded onto a Waterman P81 filter paper and then washed with 50 mM sodium bicarbonate (pH 9.0) for three times. The paper was air dried

and the amount of radioactivity incorporated into the peptide substrate was quantified by liquid scintillation counting. In all the cases, background acetylation (in the absence of enzyme) was subtracted from the total signals. The IC_{50} was determined as the concentration of an inhibitor at which half of the enzyme activity was inhibited. All the assays were performed at least twice, and duplicates generally agreed within 20%.

Acetyltransferase assays with nuclear extracts

Nuclear extracts were prepared from HeLa cells or tissue samples for distinct brain regions using procedures described by Dignam *et al.*[164] The HAT activity in the nuclear extracts was determined using an ELISA assay in which either a biotinylated histone H3 peptide (aa 1 to 21, Anaspec – 61702) or a histone H4 peptide (aa 2-24, Millipore, 12-372) was immobilized using steptavidin-biotin linkage. The ELISA was performed as described previously [148]. The buffer for the enzymatic reaction contained 0.01% Triton X-100, 0.1 mM EDTA, 50 µg/mL BSA, 1mM DTT and 50 mM HEPES pH 7.4. The nuclear extracts were standardized based on the protein concentration. The final protein concentration of the HeLa nuclear extract in the enzyme reaction was 2.5 µg/mL. For nuclear extracts of brain tissue samples the concentration was 40 µg/mL. The reaction time for the enzymatic reaction was 15 min. The brain tissue samples were obtained from Prof. Dr. B. Roozendaal, Neurosciences, UMCG, Groningen, The Netherlands. The samples were obtained from animal experiments that were approved by the animal experiment committee (Dier Experimenten Commissie, DEC) from this institute according to national regulations described in the 'law for animal experiments'.

Modeling

The PDB file of Tip60 structure (2OU2) was modified with Maestro 9.0.211 software to add hydrogens and delete the water and Ac-CoA molecules. The 3-dimensional structure of **20** was also constructed with Maestro 9.0.211. AutoDock Version 4.2 was then employed to generate PDBQT files for both the ligand and the macromolecule for docking. AutoGrid was used to generate a grid box covering the whole protein unit for docking processing. The Genetic Algorithm with 2500,000 maximum numbers of evaluations and 50 generations for picking individuals was selected as the docking parameters. Structural analysis with PyMOL was performed following the docking process

ACKNOWLEDGEMENTS

The group of Prof. Dr. Y. G. Zheng performed biochemical inhibition assays and docking studies. Y. G. Zheng would like to acknowledge the partial financial support from AHA grant 09BGIA2220207 and NIH grant R01GM086717. We acknowledge Prof. Dr. B. Roozendaal, Neurosciences, University Medical Centre Groningen, The Netherlands for providing samples from rat brain tissue. We acknowledge A. Boltjes for his contribution to the synthesis of the anacardic acid analogs.

CHAPTER 6

SUMMARY AND GENERAL DISCUSSION

The use of small molecule modulators of epigenetic modifications, in order to regulate the expression of certain genes during disease manifestations, represents a new potential therapeutic approach. Furthermore, it provides a new powerful investigation tool for pharmacological studies.

Several inhibitors of enzymes involved in epigenetic modifications have been identified and have played an important role in elucidating epigenetic regulatory mechanisms. Several DNA methylation inhibitors and HDAC inhibitors are under investigation in clinical trials. Some of them are already available for clinical use in the United States. On the contrary, the development of HAT inhibitors has proved more challenging. Despite significant efforts, HAT inhibitors have still limited efficacy, selectivity or low cell-permeability. The design of new and improved HAT inhibitors is necessary because of the potential applications of this class of compounds in the field of inflammation and cancer. Recent studies clearly demonstrate that inappropriate or excessive inflammatory responses are often accompanied by hyperacetylation of histones and non-histone proteins involved in the transcription of pro-inflammatory genes. Similarly, increasing evidences suggest that dysfunctions of acetylation processes are often associated with development of numerous cancer types.

The work described in this thesis focuses on the synthesis and biological evaluation of novel HAT inhibitors. The major challenge is to find potent and selective HAT inhibitors that show biological activity in cells. We report the design of potent isothiazolone-based inhibitors of the HAT PCAF, which are also cytotoxic for different cancer cell lines. We develop an anacardic acid (AA) derivative that is a potent inhibitor of histone acetylation in cells. Furthermore, we identify a 6-alkylsalicylate derivative that is a selective inhibitor of the recombinant HAT Tip60 in comparison with the HATs PCAF and p300. In conclusion, we provide new chemical tools for pharmacological studies to validate HATs inhibitors as potential new drugs for treatment of cancer and inflammation.

ISOTHIAZOLONES AS HAT INHIBITORS

The first part of this thesis describes the design of new HAT inhibitors based on the isothiazolone scaffold. In **chapter 2** we described the synthesis of a small collection of isothiazolone derivatives, which were screened *in vitro* for the inhibition of the recombinant HAT PCAF in order to resolve the structure-activity relationship (SAR). In this study we identified compound **2.2e** (figure 6.1) as the most potent inhibitor, which suggests that a methyl ester at two carbon atoms distance from the

isothiazolone ring provides additional interactions with PCAF. Interestingly, we also observed that a chloride in the 5-position of N-aliphatic substituted isothiazolones was essential for their inhibitory properties. In contrast, there were no pronounced differences in PCAF inhibitory potency between N-aromatic substituted 5-chloroisothiazolones and isothiazolones. The small differences between the IC_{50} values of different 5-chloroiosthiazolones indicate that the reactivity of these compounds towards the thiolates in the enzyme active site plays a predominant role in enzyme inhibition. In addition, we found that compound **2.4e** (figure 6.1) also inhibited PCAF, which identifies 5-chloroisothiazolone-1-oxide as a novel class of HAT inhibitors.

Figure 6.1: *novel isothiazolone-based HAT inhibitors described in this thesis.*

In **chapter 3** we investigated the reaction of isothiazolones derivatives with thiols and thiolates to better understand the chemical reactivity of these compounds. We showed that 5-chloroisothiazolones reacted quickly with thiolates providing multiple products. In contrast, the reaction of 5-chloroisothiazolone-1-oxides with thiolates occurred through addition in the 5-position and elimination of the chloride to give the correspondent 5-alkylthioisothiazolone-1-oxides. This supports the hypothesis that the inhibition of HATs by isothiazolone derivatives is due to their reactivity towards thiolates. The elucidation of chemical reactivity confirms that isothiazolones might find applications in ABPP because they react with thiolates.

In addition, we explored synthetic modifications of the isothiazolone ring in order to modulate its reactivity and we tested the effects of these modifications on the *in vitro* inhibition of the recombinant HAT PCAF. The isothiazolone reactivity could be modulated by introduction of electron- donating or electron-withdrawing groups in the 4-position. We showed that the introduction of a methyl group in the 4-position of the isothiazolone ring caused a significant drop in inhibitory potency. On the other hand, introduction of a chlorine atom in the 4-position did not affect the inhibitory properties of 5-chloroisothiazolones, whereas it caused a drop in inhibitory potency of 5-chloroisothiazolone-1-oxides. The relationship between thiolate reactivity and HAT inhibition cannot easily be derived, because changes in inhibitory potency might originate both from their binding properties to the enzyme active site as well as from their reactivity. Nevertheless, this study demonstrates

that the inhibitory potency of 5-chloroisothiazolones cannot easily be improved by introduction of substituent in the 4-position.

In **chapter 2** and **3** we explored the growth inhibition of several cancer cell lines upon treatment with isothiazolones to explore the toxicity of these compounds. These studies showed that N-aliphatic substituted 5-chloroisothiazolones inhibited proliferation of the cancer cell lines HEP G2, A2780 and HEK 293 at micromolar concentrations. Little or no growth inhibition was observed with other classes of isothiazolone derivatives. In general, the differences in PCAF inhibitory potency were not reflected in the inhibition of cell proliferation. This might be due to differences in cell membrane permeability between the compounds, even though other mechanisms might be involved. Nevertheless, the cytotoxic effects exerted by N-aliphatic substituted 5-chloroisothiazolones suggest possible anticancer properties for these compounds.

ANACARDIC ACID DERIVATIVES AS HAT INHIBITORS

The second part of this thesis describes the development of novel HAT inhibitors using the natural product AA as starting point. In **chapter 4** we proposed a binding model for AA in the HAT PCAF active site in which the salicylate is bound in the pyrophosphate binding pocket and the alkyl chain is located in the CoA substrate binding cleft. This binding model can be used as starting point for the design of new molecules in order to optimize the inhibitory potency. We design several AA derivatives and synthesized them using a novel, convenient and versatile synthetic route. We investigated the *in vitro* inhibitory potency of these derivatives towards the recombinant HAT PCAF to elucidate the SAR. In general, the synthesized compounds showed poor inhibition of PCAF, with potencies comparable to or lower than AA. An important consideration is that AA has poor drug-like properties, such as a log P value higher than 5. Our new inhibitors represent an improvement from this point of view. Compound **4.6d** (figure 6.2) was the only compound that proved to be more potent than AA in the enzyme inhibition studies. Moreover, this derivative showed also a two-fold improved potency for inhibition of histone H4 acetylation in cell-based studies. Therefore, compound **4.6d** represents a novel pharmacological probe to study inhibition of histone acetylation in cells. It is interesting to point out that **4.6d** was the only compound with a *cis* double bond in the substituent on salicylate 6-position. This conformational restriction could explain the increase in inhibitory potency. However, more compounds with a *cis* double bond have to be evaluated to confirm this possible correlation.

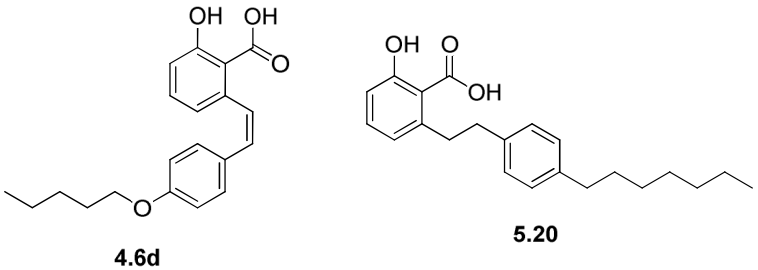

Figure 6.2: *novel anacardic acid-based HAT inhibitors described in this thesis.*

In **chapter 5** we addressed the issue of specificity of AA derivatives among different classes of HATs. We synthesized several compounds with various 2-phenylethane substituents in the salicylate 6-position in order to enhance binding by providing specific interactions with the enzymes. All the salicylate derivatives were screened for the inhibition of the recombinant HATs Tip60, PCAF and p300, which represent the three major HAT families in mammalian cells. In general, the synthesized compounds showed stronger inhibitory potency for Tip60 compared to p300 and PCAF. Compound **5.20** (figure 6.2) showed the highest selectivity for Tip60. Moreover its calculated logP value is significantly lower than that of AA, which represents an advantage for the bioactivity. Altogether, **5.20** is a novel HAT inhibitor with improved isoenzyme selectivity and drug-like properties. This compound could be used in cell-based study to explore Tip60 biological functions and implications in pathologies.

Compounds that inhibited the recombinant HAT Tip60 also inhibited HAT activity of nuclear extract from HeLa cells, with comparable potency. This suggests that Tip60 or closely related HATs are a major source of HAT activity in these cells. Interestingly, some inhibitors showed a difference in inhibitory potency between histone H3 and histone H4. These data indicate that selective inhibitors towards histone H3 or H4 acetylation could be developed. These kinds of compounds would represent new investigation tools for pharmacological studies.

We analyzed the HAT inhibitory mechanism of AA derivatives using enzyme kinetics. These studies showed that inhibition of Tip60 by **5.20** is competitive to Ac-CoA and non-competitive to histone H4. This supports our hypothesis that AA derivatives bind to the Ac-CoA binding pocket.

FUTURE PERSPECTIVES

Future work should be oriented towards the design of improved HAT inhibitors and the evaluation of their biological properties in pharmacological studies.

Several isothiazolone-based PCAF inhibitors described in thesis exerted cytotoxic effects towards different cancer cell lines. Further investigations are necessary to study the biological mechanisms underlying the cell growth inhibition showed by these compounds. For example, western blots analysis of histone acetylation levels in cell lines that are treated with N-aliphatic substituted 5-chloroisothiazolones are required to proof a connection between the PCAF HAT inhibition and the biological activity. These studies are needed to validate HATs inhibitors as drug candidates for cancer therapy.

We showed that compounds **2.2e** and **2.4** react quickly with thiolates. Functional groups that react covalently with thiolates have been extensively used for ABPP of enzymes with a cysteine in the active site. 5-chloroisothiazolones and 5-chloroisothiazolone-1-oxides might find applications in this field. HATs contain a cysteine in the active site and therefore the reactivity of isothiazolones could be employed for development of probes to detect the activity of HATs in cell-lysates. However, chemical probes that are applied in ABPP need a certain level of specificity. The evaluation of the SAR presented in this thesis is a first step towards the development of specific isothiazolone-based HAT inhibitors. An appropriate design and additional structure modifications are necessary before applying these compounds in ABPP.

Docking and enzyme kinetics studies suggest that AA derivatives bind to HATs in the Ac-CoA binding pocket. Nevertheless, the binding configuration remains to be solved. This could be done by resolution of the crystal structure of HATs in complex with AA or its derivatives. Detailed knowledge of the binding configuration will provide a good basis for structure-based design of novel inhibitors with improved affinity and selectivity. In our studies, the screening for inhibitory activity indicates that hydrophobic interactions are extremely important for the inhibition of HATs by 6-alkylsalicylates. Not only an extended and hydrophobic substituent in the salicylate 6-position is essential for HAT inhibition, but also the introduction of heteroatoms causes drop in potency. At the same time, the hydrophobicity and the amphiphilic nature of 6-alkylsalicylates are considered to be a disadvantage for the drug-like character. Consequently, it is particularly challenging to develop 6-

alkylsalicylates with high affinity for HATs, without compromising the drug properties compounds.

Despite their limited potency and selectivity, currently available HAT inhibitors have been extensively investigated as potential anticancer drugs. In contrast, the use of HAT inhibitors in studies on inflammation is still very limited. Inflammation is of particular interest because recent literature clearly indicates that HATs play crucial regulatory roles in the NF-κB signaling pathway. The novel HAT inhibitors described in this thesis could be applied in pharmacological studies to explore their potential as anti-inflammatory drugs. Recent experiments demonstrated that both AA and compound **2.2e** inhibited histone acetylation in human airway smooth muscle cells. Furthermore, both compounds inhibited the interleukin 8 release upon stimulation of cells with tumor necrosis factor α (unpublished data – Department of Molecular Pharmacology, University of Groningen). These data indicate that the effects of HAT inhibitors on the NF-κB-mediated expression of pro-inflammatory genes should be explored further. Ultimately, this would identify HAT inhibition as conceptually new approach for pharmacotherapy aimed at the suppression of inflammation.

APPENDIX

DUTCH SUMMARY
REFERENCES
ACKNOWLEDGMENTS
CV AND LIST OF PUBLICATIONS

Dutch summary (Nederlandse samenvatting)

De modulatie van epigenetische modificaties door kleine moleculen biedt mogelijkheden om de expressie van bepaalde ziekte gerelateerde genen te beïnvloeden. Dit soort kleine moleculen kunnen toegepast worden voor farmacologische studies aan specifieke ziektemodellen. Uiteindelijk zouden zulke kleine moleculen gebruikt kunnen worden in potentiële nieuwe geneesmiddelen.

Er zijn remmers geïdentificeerd voor verschillende enzymen die betrokken zijn bij epigenetische modificaties. Deze remmers hebben een belangrijke rol gespeeld bij het ontrafelen van epigenetische regulatie mechanismen. Verschillende DNA-methylatie-remmers en histone deacetylase (HDAC) remmers worden momenteel onderzocht in klinische studies. Sommigen van hen zijn reeds beschikbaar voor klinisch gebruik (Azacitidine, Vorinostat). De ontwikkeling van histone acetyltransferase (HAT) remmers bleek echter een grotere uitdaging. Ondanks aanzienlijke inspanningen hebben HAT-remmers nog steeds een beperkte werkzaamheid, een lage selectiviteit of een beperkte cel-permeabiliteit. Het ontwerp van nieuwe en verbeterde HAT-remmers biedt mogelijkheden voor onderzoek naar mogelijke therapeutische toepassingen van deze klasse van remmers op het gebied van ontstekingen en kanker. Recente studies tonen duidelijk aan dat ongepaste of buitensporige ontstekingsreacties vaak gepaard gaan met hyperacetylering van histonen en andere eiwitten die betrokken zijn bij de transcriptie van pro-inflammatoire genen. Er wordt ook steeds meer bewijs gevonden dat afwijkingen in acetyleringen vaak worden geassocieerd met de ontwikkeling van een groot aantal vormen van kanker.

Het werk beschreven in dit proefschrift richt zich op de synthese en biologische evaluatie van nieuwe HAT-remmers. De grote uitdaging is het vinden van krachtige en selectieve HAT-remmers die histon acetylering remmen in cellenlijnen. Wij rapporteren het ontwerp van krachtige isothiazolone gebaseerde remmers van het HAT PCAF, die cytotoxisch zijn voor verschillende kankercellijnen. Verder beschrijven we de ontwikkeling van een stoffen die afgeleid zijn van het natuurproduct ‘anacardic acid’ (AA) dat histonacetylering in cellen remt. Verder beschrijven we de identificatie van een nieuw 6-alkylsalicylaat derivaat als een selectieve remmer van de recombinante HAT, Tip60, ten opzichte van de HATs PCAF en p300.

Isothiazolon derivaten

Het eerste deel van dit proefschrift beschrijft het ontwerp van nieuwe HAT-remmers op basis van een isothiazolon kernstructuur. In hoofdstuk 2 beschrijven we de synthese van een kleine verzameling van isothiazolon derivaten, die *in vitro* gescreend zijn voor de remming van de recombinante HAT, PCAF waarmee de structuur-activiteit relatie (SAR) voor deze stofklasse zijn bestudeerd. In deze studie identificeerden we stof **2.2e** (figuur a.1) als de meest krachtige remmer, wat suggereert dat een methyl ester met een 'spacer' van twee koolstofatomen tussen de isothiazolone ring extra interacties met het enzym PCAF geeft. Verder hebben we vastgesteld dat een chloride atoom in de 5-positie van het isothiazolon met N-alifatische substituent essentieel is voor hun remmende eigenschappen. In tegenstelling daarmee, waren er geen uitgesproken verschillen in het PCAF remmende vermogen tussen de 5-chloroisothiazolonen en isothiazolonen met een N-aromatische substituent. De kleine verschillen tussen de IC_{50} waarden van verschillende 5-chloroiosthiazolones geven aan dat de reactiviteit van deze verbindingen naar het thiolaat in het actieve van het enzym een overheersende rol speelt in de remming van deze enzymen. Daarnaast hebben we gevonden dat stof 2.4e (figuur a.1) de HAT ook remt. Dit identificeert 5-chloroisothiazolone-1-oxides als een nieuwe klasse van HAT-remmers.

Figuur a.1: *isothiazolon derivaten.*

In hoofdstuk 3 hebben we de reactie van isothiazolon derivaten met thiolen en thiolaten beter onderzocht om meer inzicht te krijgen in de chemische reactiviteit van deze verbindingen. We laten zien dat 5-chloroisothiazolonen snel reageren met thiolaten en dat dit meerdere producten oplevert. In tegenstelling hiermee, levert de reactie van een 5-chloroisothiazolone-1-oxide met een thiolaat een gedefinieerd product op dat ontstaat door additie van het thiolaat op de 5-positie en eliminatie van het chloride. Dit resulteert in het 5-alkylthioisothiazolone-1-oxide. Dit ondersteunt de hypothese dat de remming van de HATs door isothiazolon derivaten het gevolg is van hun reactiviteit ten opzichte van thiolaten. De opheldering van de chemische reactiviteit bevestigt dat isothiazolonen toegepast kunnen worden in 'activity-based-protein-profiling (ABPP) omdat ze een covalente binding aangaan met thiolaten.

Daarnaast hebben we synthetische modificaties aangebracht in de isothiazolon ring en hebben we bestudeerd hoe dit de remming van de HAT PCAF beïnvloedt. De reactiviteit van het isothiazolon kan worden gemoduleerd door de invoering van elektron-zuigende of elektron-stuwende substituenten op de 4-positie. We hebben laten zien dat de invoering van een methylgroep in de 4-positie van de isothiazolon ring een aanzienlijke daling van de remmende potentie veroorzaakt. Aan de andere kant, heeft de invoering van een chlooratoom in de 4-positie geen invloed op de remmende eigenschappen van 5-chloroisothiazolonen, terwijl het wel een daling van het remmend vermogen van 5-chloroisothiazolone-1-oxiden veroorzaakt. De relatie tussen de thiolaat reactiviteit en HAT remming blijkt niet gemakkelijk te kunnen worden afgeleid. Dit kan verklaard worden doordat het remmend vermogen van deze stoffen zowel veroorzaakt wordt door hun bindende eigenschappen aan het actieve centrum van het enzym alsook door hun reactiviteit met de thiolaat in het actieve centrum van het enzym.

In de hoofdstukken 2 en 3 hebben we de groeiremming van verschillende cellijnen na behandeling met isothiazolonen bestudeerd om de toxiciteit van deze verbindingen vast te stellen. Deze studies tonen aan dat N-gesubstitueerde alifatische 5-chloroisothiazolonen de groei remmen van de kankercellijnen HEP G2, A2780 en HEK 293 bij micromolaire concentraties. Er wordt voor deze cellijnen weinig of geen groeiremming waargenomen bij de andere isothiazolon derivaten. De verschillen in de PCAF remming zijn niet gecorreleerd aan de remming van de celgroei. Dit kan te wijten zijn aan verschillen in de celmembraan permeabiliteit tussen de verbindingen of aan andere factoren. De waargenomen cytotoxische effect van de N-gesubstitueerde alifatische 5-chloroisothiazolonen geeft aan dat deze stoffen mogelijk toepassingen kunnen vinden bij het doden van tumorcellen.

Anacardic acid derivaten

Het tweede deel van dit proefschrift beschrijft de ontwikkeling van nieuwe HAT-remmers op basis van het natuurproduct 'anacardic acid' (AA). In hoofdstuk 4 presenteren we een bindingsmodel voor AA aan het active centrum van de HAT PCAF. Het salicylaat is gebonden aan de pyrofosfaat bindingsplaats en de alkylketen is gelegen in de CoA substraat bindingsplaats. Dit bindingsmodel kan worden gebruikt als uitgangspunt voor het ontwerp van nieuwe moleculen om het remmende vermogen te optimaliseren. Wij hebben een aantal AA-derivaten ontworpen en gesynthetiseerd. De synthese verliep via een nieuwe, handige en veelzijdige synthetische route. We hebben onderzoek gedaan naar het *in vitro* remmend vermogen van deze derivaten tegen de recombinante HAT PCAF. In het algemeen

vertoonden de gesynthetiseerde verbindingen een slechte remming van de HAT PCAF. De meeste stoffen waren even actief of minder actief dan AA. Het natuurproduct AA heeft slechte geneesmiddel-achtige eigenschappen, zoals een log P-waarde die hoger dan 5 is. Onze nieuwe remmers hebben een lagere log P waarde wat gunstig is voor de geneesmiddel-achtige eigenschappen. Stof **4.6d** (figuur a.2) was de enige verbinding die actiever was dan AA in de enzymremmingstudies. Bovendien, vertoonde dit derivaat ook een twee-voudig verbeterde potentie voor remming van histon H4 acetylering in cel-gebaseerde studies. Daarom kan stof **4.6d** als een nieuwe remmer gebruikt worden in farmacologische studies om de remming van histonacetylering in cellen te bestuderen. Het is een interessant punt dat stof **4.6d** de enige verbinding is met een cis dubbele binding in de substituent op salicylaat 6-positie. Deze conformationele restrictie zou de de verbeterde remming kunnen verklaren. Echter, er moeten meer verbindingen met een cis dubbele binding worden beoordeeld om deze mogelijke correlatie te bevestigen.

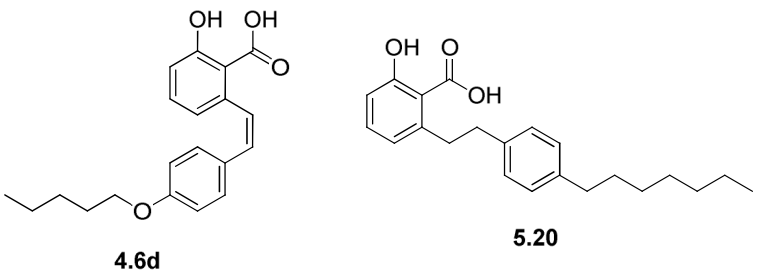

Figuur a.2: *anacardic acid derivaten.*

In hoofdstuk 5 hebben we de specificiteit bestudeerd van een verzameling van salicylaat derivaten voor de verschillende klassen HATs. We hebben nieuwe salicylaat derivaten gesynthetiseerd met verschillende 2-fenylethaan substituenten in de salicylaat 6-positie. Het doel was om de affiniteit van deze verbindingen voor het enzym te verbeteren door extra specifieke interacties. Alle salicylaat derivaten werden gescreend voor de remming van de recombinante HATs Tip60, PCAF en p300. Deze HATs zijn representatief voor de drie grote HAT families. In het algemeen vertonen de gesynthetiseerde verbindingen een sterker remmend effect op Tip60 in vergelijking met p300 en PCAF. Stof **5.20** (figuur a.2) laat de hoogste selectiviteit voor Tip60 zien. Bovendien is de berekende logP waarde aanzienlijk lager dan die van AA, wat, in het algemeen, een voordeel is voor de biologische activiteit. Al met al, is stof **5,20** een nieuwe HAT-remmer met een verbeterd iso-enzym selectiviteit en betere geneesmiddel-achtige eigenschappen. Deze verbinding

kunnen gebruikt worden in cel-gebaseerde studie naar de biologische functies van Tip60.

Verbindingen die de recombinante HAT Tip60 remmen die remmen in vergelijkbare concentraties ook de HAT-activiteit in nucleaire extracten van HeLa cellen. Dit suggereert dat Tip60 of nauw verwante HATs van belang zijn voor HAT-activiteit in deze cellen. Interessant is dat sommige remmers een verschil laten zien tussen het remmend vermogen voor histon H3 en H4. Deze gegevens suggereren dat selectieve remmers voor histon H3 of H4 acetylering kunnen worden ontwikkeld.

We hebben het mechanisme bestudeerd van de HAT-remming door de AA-derivaten met behulp van enzymkinetiek. Deze studies laten zien dat remming van Tip60 door stof **5,20** competitief is met Ac-CoA en niet-competitieve naar histon H4. Dit ondersteund onze hypothese dat AA derivaten binden aan de Ac-CoA-bindingsplaats.

Toekomstperspectieven

Toekomstige werkzaamheden zouden zich moeten richten op het ontwerp van verbeterde HAT-remmers en de evaluatie van hun biologische eigenschappen in farmacologische studies.

Er zijn verschillende isothiazolon-gebaseerde PCAF remmers in dit proefschrift beschreven die cytotoxisch zijn voor verschillende kankercellijnen. Verder onderzoek is nodig om de biologische mechanismen die ten grondslag liggen aan de celgroeiremming te bestuderen. Bijvoorbeeld, western blot analyse van histon acetylering niveaus in cellijnen die zijn behandeld met HAT remmers zijn nodig om het bewijs te leveren dat PCAF HAT inhibitie verband houdt met de groeiremming van kankercellijnen. Deze studies zijn nodig om HAT-remmers te valideren als kandidaat-geneesmiddelen voor de behandeling van kanker.

We hebben aangetoond dat de verbindingen **2.2e** en **2.4** snel covalent binden aan thiolaten. Functionele groepen die covalent reageren met thiolates worden vaak gebruikt voor activity-based-protein-profiling (ABPP) van enzymen met een cysteine in hun actieve centrum. 5-chloroisothiazolonen en 5-chloroisothiazolon-1-oxiden kunnen worden toegepast voor ABPP van HATs die een cysteine bevatten in hun actieve centrum. Echter, chemische detectiemoleculen die worden toegepast in ABPP moeten over een zekere mate van specificiteit beschikken. De evaluatie van de SAR voor remming van de HAT PCAF in dit proefschrift is een eerste stap in de ontwikkeling van specifieke isothiazolon-gebaseerde HAT-remmers en de toepassing daarvan in ABPP.

Docking studies en de enzymkinetiek suggereren dat AA derivaten een niet-covalente binding aangaan met HATs in de Ac-CoA bindingsplaats. Het is van belang dat de bindingsconfiguratie van deze stoffen in detail wordt opgehelderd. Dit zou gedaan kunnen worden door het maken van een kristalstructuur van HATs in complex met AA of derivaten daarvan. Gedetailleerde kennis van de bindingsconfiguratie is een goede basis voor 'structure-based design' van nieuwe remmers met een verbeterde affiniteit en selectiviteit. Onze studies met een verzameling van 30 6-alkylsalicylaten geeft aan dat hydrofobe interacties uiterst belangrijk zijn voor de remming van HATs door 6-alkylsalicylaten. Dit blijkt doordat een lange en hydrofobe substituent in de salicylaat 6-positie essentieel is voor HAT-remming en dat het invoeren van heteroatomen een daling veroorzaakt van hun activiteit. Tegelijkertijd, is de hydrofobiciteit en het amfifiele karakter van 6-alkylsalicylates een nadeel voor de geneesmiddel-achtig eigenschappen van deze stoffen. Hieruit blijkt dat het bijzonder uitdagend is 6-alkylsalicylates te ontwikkelen met een hoge affiniteit voor HATs, zonder afbreuk te doen aan de geneesmiddel-achtige eigenschappen van deze verbindingen.

Ondanks hun beperkte potentie en selectiviteit zijn de momenteel beschikbare HAT-remmers uitgebreid onderzocht als potentiële anti-kanker geneesmiddelen. In tegenstelling daarmee is het gebruik van de HAT-remmers in onderzoek naar onstekingen nog zeer beperkt. HAT remming is van bijzonder belang voor onstekingen. De recente literatuur geeft duidelijk aan dat de regulatie van de NF-κB signaal transductie route in belangrijke mate gestimuleerd wordt door de activiteit van HATs. De HAT-remmers beschreven in dit proefschrift kunnen worden toegepast in farmacologische studies om hun potentieel als anti-inflammatoire geneesmiddelen te onderzoeken. Recente experimenten hebben aangetoond dat zowel AA en stof **2.2e** de histon-acetylering remmen in humane gladde spiercellen uit de luchtwegen. Bovendien remmen beide verbindingen het vrijkomen van interleukine 8 na de stimulatie van cellen met tumor necrose factor α (ongepubliceerde gegevens - Afdeling Moleculaire Farmacologie, Universiteit van Groningen). Deze gegevens wijzen erop dat de effecten van de HAT-remmers op de NF-κB gemedieerde expressie van pro-inflammatoire genen verder moet worden onderzocht. Uiteindelijk zou dit HAT remming kunnen identificeren als conceptueel nieuwe benadering voor de farmacotherapie gericht op het onderdrukken van ontstekingen.

References

1. Van Speybroeck L. From epigenesis to epigenetics: the case of C. H. Waddington. Ann N Y Acad Sci 2002;981:61-81.
2. Wolffe AP, Matzke MA. Epigenetics: regulation through repression. Science 1999;286:481-6.
3. Esteller M. Cancer epigenomics: DNA methylomes and histone-modification maps. Nat Rev Genet 2007;8:286-98.
4. Peterson CL, Laniel M. Histone and histone modifications. Curr. Biol. 2004;14:R546-551.
5. Kouzarides T. Chromatin modifications and their function. Cell 2007;128:693-705.
6. Beckett D. Regulated assembly of transcription factors and control of transcription initiation. J Mol Biol 2001;314:335-52.
7. Roth SY, Denu JM, Allis CD. Histone Acetyltransferases. Annu. Rev. Biochem. 2001;70:81–120.
8. Baldwin AS,Jr. The NF-kappa B and I kappa B proteins: new discoveries and insights. Annu Rev Immunol 1996;14:649-83.
9. Chen LF, Mu Y, Greene WC. Acetylation of RelA at discrete sites regulates distinct nuclear functions of NF-kappaB. EMBO J 2002;21:6539-48.
10. Chen L, Fischle W, Verdin E, Greene WC. Duration of nuclear NF-kappaB action regulated by reversible acetylation. Science 2001;293:1653-7.
11. Huang B, Yang XD, Zhou MM, Ozato K, Chen LF. Brd4 coactivates transcriptional activation of NF-kappaB via specific binding to acetylated RelA. Mol Cell Biol 2009;29:1375-87.
12. Yang XD, Tajkhorshid E, Chen LF. Functional interplay between acetylation and methylation of the RelA subunit of NF-kappaB. Mol Cell Biol 2010;30:2170-80.
13. Yeung F, Hoberg JE, Ramsey CS, *et al.* Modulation of NF-kappaB-dependent transcription and cell survival by the SIRT1 deacetylase. EMBO J 2004;23:2369-80.
14. Kiernan R, Bres V, Ng RW, *et al.* Post-activation turn-off of NF-kappa B-dependent transcription is regulated by acetylation of p65. J Biol Chem 2003;278:2758-66.
15. Buerki C, Rothgiesser KM, Valovka T, *et al.* Functional relevance of novel p300-mediated lysine 314 and 315 acetylation of RelA/p65. Nucleic Acids Res 2008;36:1665-80.
16. Rothgiesser KM, Fey M, Hottiger MO. Acetylation of p65 at lysine 314 is important for late NF-kappaB-dependent gene expression. BMC Genomics 2010;11:22.
17. Furia B, Deng L, Wu K, *et al.* Enhancement of nuclear factor-kappa B acetylation by coactivator p300 and HIV-1 Tat proteins. J Biol Chem 2002;277:4973-80.
18. Deng WG, Wu KK. Regulation of inducible nitric oxide synthase expression by p300 and p50 acetylation. J Immunol 2003;171:6581-8.
19. Park J, Lee JH, La M, *et al.* Inhibition of NF-kappaB acetylation and its transcriptional activity by Daxx. J Mol Biol 2007;368:388-97.
20. Lee H, Herrmann A, Deng JH, *et al.* Persistently activated Stat3 maintains constitutive NF-kappaB activity in tumors. Cancer Cell 2009;15:283-93.
21. Faraco G, Pittelli M, Cavone L, *et al.* Histone deacetylase (HDAC) inhibitors reduce the glial inflammatory response in vitro and in vivo. Neurobiol Dis 2009;36:269-79.
22. Hassa PO, Haenni SS, Buerki C, *et al.* Acetylation of poly(ADP-ribose) polymerase-1 by p300/CREB-binding protein regulates coactivation of NF-kappaB-dependent transcription. J Biol Chem 2005;280:40450-64.

23. Kramer OH, Baus D, Knauer SK, *et al.* Acetylation of Stat1 modulates NF-kappaB activity. Genes Dev 2006;20:473-85.
24. Ito K, Yamamura S, Essilfie-Quaye S, *et al.* Histone deacetylase 2-mediated deacetylation of the glucocorticoid receptor enables NF-kappaB suppression. J Exp Med 2006;203:7-13.
25. Gerritsen ME, Williams AJ, Neish AS, Moore S, Shi Y, Collins T. CREB-binding protein/p300 are transcriptional coactivators of p65. Proc Natl Acad Sci U S A 1997;94:2927-32.
26. Sheppard KA, Rose DW, Haque ZK, *et al.* Transcriptional activation by NF-kappaB requires multiple coactivators. Mol Cell Biol 1999;19:6367-78.
27. Ashburner BP, Westerheide SD, Baldwin AS,Jr. The p65 (RelA) subunit of NF-kappaB interacts with the histone deacetylase (HDAC) corepressors HDAC1 and HDAC2 to negatively regulate gene expression. Mol Cell Biol 2001;21:7065-77.
28. Kawahara TL, Michishita E, Adler AS, *et al.* SIRT6 links histone H3 lysine 9 deacetylation to NF-kappaB-dependent gene expression and organismal life span. Cell 2009;136:62-74.
29. Ito K, Barnes PJ, Adcock IM. Glucocorticoid receptor recruitment of histone deacetylase 2 inhibits interleukin-1beta-induced histone H4 acetylation on lysines 8 and 12. Mol. Cell Biol. 2000;20:6891–6903.
30. Clarke DL, Sutcliffe A, Deacon K, Bradbury D, Corbett L, Knox AJ. PKCbetaII augments NF-kappaB-dependent transcription at the CCL11 promoter via p300/CBP-associated factor recruitment and histone H4 acetylation. J Immunol 2008;181:3503-14.
31. Nie M, Knox AJ, Pang L. beta2-Adrenoceptor agonists, like glucocorticoids, repress eotaxin gene transcription by selective inhibition of histone H4 acetylation. J Immunol 2005;175:478-86.
32. Vanden Berghe W, De Bosscher K, Boone E, Plaisance S, Haegeman G. The nuclear factor-kappaB engages CBP/p300 and histone acetyltransferase activity for transcriptional activation of the interleukin-6 gene promoter. J. Biol. Chem. 1999;274:32091–32098.
33. Clarke DL, Clifford RL, Jindarat S, *et al.* TNFalpha and IFNgamma synergistically enhance transcriptional activation of CXCL10 in human airway smooth muscle cells via STAT-1, NF-kappaB, and the transcriptional coactivator CREB-binding protein. J Biol Chem 2010;285:29101-10.
34. Edelstein LC, Pan A, Collins T. Chromatin modification and the endothelial-specific activation of the E-selectin gene. J Biol Chem 2005;280:11192-202.
35. Nie M, Pang L, Inoue H, Knox AJ. Transcriptional regulation of cyclooxygenase 2 by bradykinin and interleukin-1beta in human airway smooth muscle cells: involvement of different promoter elements, transcription factors, and histone h4 acetylation. Mol Cell Biol 2003;23:9233-44.
36. Schmeck B, Lorenz J, N'Guessan P D, *et al.* Histone acetylation and flagellin are essential for Legionella pneumophila-induced cytokine expression. J. Immunol. 2008;181:940–947.
37. Schmeck B, Beermann W, van Laak V, *et al.* Intracellular bacteria differentially regulated endothelial cytokine release by MAPK-dependent histone modification. J Immunol 2005;175:2843-50.
38. Tsaprouni LG, Ito K, Adcock IM, Punchard N. Suppression of lipopolysaccharide- and tumour necrosis factor-alpha-induced interleukin (IL)-8 expression by glucocorticoids involves changes in IL-8 promoter acetylation. Clin Exp Immunol 2007;150:151-7.

39. Gilmour PS, Rahman I, Donaldson K, MacNee W. Histone acetylation regulates epithelial IL-8 release mediated by oxidative stress from environmental particles. Am. J. Physiol. Lung Cell Mol. Physiol. 2003;284:533–540.
40. Su RC, Becker AB, Kozyrskyj AL, Hayglass KT. Altered epigenetic regulation and increasing severity of bronchial hyperresponsiveness in atopic asthmatic children. J Allergy Clin Immunol 2009;124:1116-8.
41. Ito K, Caramori G, Lim S, *et al.* Expression and activity of histone deacetylases in human asthmatic airways. Am. J. Respir. Crit. Care Med. 2002;166:392–326.
42. Cosio BG, Mann B, Ito K, *et al.* Histone acetylase and deacetylase activity in alveolar macrophages and blood mononocytes in asthma. Am. J. Respir. Crit. Care Med. 2004;170:141–147.
43. Ito K, Ito M, Elliott WM, *et al.* Decreased histone deacetylase activity in chronic obstructive pulmonary disease. N Engl J Med 2005;352:1967-76.
44. Adcock IM, Lee KY. Abnormal histone acetylase and deacetylase expression and function in lung inflammation. Inflamm Res 2006;55:311-21.
45. Rajendrasozhan S, Yao H, Rahman I. Current perspectives on role of chromatin modifications and deacetylases in lung inflammation in COPD. COPD 2009;6:291-7.
46. Mroz RM, Noparlik J, Chyczewska E, Braszko JJ, Holownia A. Molecular basis of chronic inflammation in lung diseases: new therapeutic approach. J Physiol Pharmacol 2007;58 Suppl 5:453-60.
47. Miao F, Gonzalo IG, Lanting L, Natarajan R. In vivo chromatin remodeling events leading to inflammatory gene transcription under diabetic conditions. J Biol Chem 2004;279:18091-7.
48. Chen S, Feng B, George B, Chakrabarti R, Chen M, Chakrabarti S. Transcriptional coactivator p300 regulates glucose-induced gene expression in endothelial cells. Am J Physiol Endocrinol Metab 2010;298:E127-37.
49. Liu B, Hong JS. Role of microglia in inflammation-mediated neurodegenerative diseases: mechanisms and strategies for therapeutic intervention. J Pharmacol Exp Ther 2003;304:1-7.
50. Zhu W, Zheng H, Shao X, Wang W, Yao Q, Li Z. Excitotoxicity of TNFalpha derived from KA activated microglia on hippocampal neurons in vitro and in vivo. J Neurochem 2010;114:386-96.
51. Qin H, Wilson CA, Lee SJ, Zhao X, Benveniste EN. LPS induces CD40 gene expression through the activation of NF-kappaB and STAT-1alpha in macrophages and microglia. Blood 2005;106:3114-22.
52. Ma X, Reynolds SL, Baker BJ, Li X, Benveniste EN, Qin H. IL-17 enhancement of the IL-6 signaling cascade in astrocytes. J Immunol 2010;184:4898-906.
53. Mattson MP, Camandola S. NF-kappaB in neuronal plasticity and neurodegenerative disorders. J Clin Invest 2001;107:247-54.
54. Wang SX, Hu LM, Gao XM, Guo H, Fan GW. Anti-inflammatory activity of salvianolic acid B in microglia contributes to its neuroprotective effect. Neurochem Res 2010;35:1029-37.
55. Hwang J, Zheng LT, Ock J, Lee MG, Suk K. Anti-inflammatory effects of m-chlorophenylpiperazine in brain glia cells. Int Immunopharmacol 2008;8:1686-94.
56. Debes JD, Sebo TJ, Lohse CM, Murphy LM, Haugen DA, Tindall DJ. P300 in Prostate Cancer Proliferation and Progression. Cancer Res 2003;63:7638-40.

57. Ishihama K, Yamakawa M, Semba S, *et al.* Expression of HDAC1 and CBP/p300 in human colorectal carcinomas. J Clin Pathol 2007;60:1205-10.
58. Bandyopadhyay D, Okan NA, Bales E, Nascimento L, Cole PA, Medrano EE. Down-regulation of p300/CBP histone acetyltransferase activates a senescence checkpoint in human melanocytes. Cancer Res 2002;62:6231-9.
59. Kitabayashi I, Aikawa Y, Yokoyama A, *et al.* Fusion of MOZ and p300 histone acetyltransferases in acute monocytic leukemia with a t(8;22)(p11;q13) chromosome translocation. Leukemia 2001;15:89-94.
60. Miyamoto N, Izumi H, Noguchi T, *et al.* Tip60 is regulated by circadian transcription factor clock and is involved in cisplatin resistance. J Biol Chem 2008;283:18218-26.
61. Hirano G, Izumi H, Kidani A, *et al.* Enhanced expression of PCAF endows apoptosis resistance in cisplatin-resistant cells. Mol Cancer Res 2010;8:864-72.
62. Iyer NG, Xian J, Chin SF, *et al.* p300 is required for orderly G1/S transition in human cancer cells. Oncogene 2007;26:21-9.
63. Ait-Si-Ali S, Polesskaya A, Filleur S, *et al.* CBP/p300 histone acetyl-transferase activity is important for the G1/S transition. Oncogene 2000;19:2430-7.
64. Mateo F, Vidal-Laliena M, Pujol MJ, Bachs O. Acetylation of cyclin A: a new cell cycle regulatory mechanism. Biochem Soc Trans 2010;38:83-6.
65. Paolinelli R, Mendoza-Maldonado R, Cereseto A, Giacca M. Acetylation by GCN5 regulates CDC6 phosphorylation in the S phase of the cell cycle. Nat Struct Mol Biol 2009;16:412-20.
66. Seligson DB, Horvath S, Shi T, *et al.* Global histone modification patterns predict risk of prostate cancer recurrence. Nature 2005;435:1262-6.
67. Bai X, Wu L, Liang T, *et al.* Overexpression of myocyte enhancer factor 2 and histone hyperacetylation in hepatocellular carcinoma. J Cancer Res Clin Oncol 2008;134:83-91.
68. Arif M, Vedamurthy BM, Choudhari R, *et al.* Nitric oxide-mediated histone hyperacetylation in oral cancer: target for a water-soluble HAT inhibitor, CTK7A. Chem Biol 2010;17:903-13.
69. Patel JH, Du Y, Ard PG, *et al.* The c-MYC oncoprotein is a substrate of the acetyltransferases hGCN5/PCAF and TIP60. Mol Cell Biol 2004;24:10826-34.
70. Fu M, Wang C, Wang J, *et al.* Androgen receptor acetylation governs trans activation and MEKK1-induced apoptosis without affecting in vitro sumoylation and trans-repression function. Mol Cell Biol 2002;22:3373-88.
71. Shiota M, Yokomizo A, Masubuchi D, *et al.* Tip60 promotes prostate cancer cell proliferation by translocation of androgen receptor into the nucleus. Prostate 2010;70:540-54.
72. Lau DO, Kundu TK, Soccio RE, *et al.* HATs off: selective synthetic inhibitors of Histone Acetyltransferase p300 and PCAF. Mol. Cell 2000;5:589–595.
73. Wu J, Xie N, Wu Z, Zhang Y, Zheng YG. Bisubstrate Inhibitors of the MYST HATs Esa1 and Tip60. Bioorg. Med. Chem. 2009;17:1381–1386.
74. Stimson L, Rowlands MG, Newbatt YM, *et al.* Isothiazolones as inhibitors of PCAF and p300 histone acetyltransferase activity. Mol. Cancer Ther. 2005;4:1521–1532.
75. Bowers EM, Yan G, Mukherjee C, *et al.* Virtual Ligand Screening of the p300/CBP Histone Acetyltransferase: Identification of a Selective Small Molecule Inhibitor. Chemistry & Biology 2010;17:471-82.

76. Mai A, Rotili A, Tarantino D, *et al.* Small-Molecule Inhibitors of Histone Acetyltransferase Activity: identification and biological properties. J. Med. Chem. 2006;49:6897-907.
77. Chimenti F, Bizzarri B, Maccioni E, *et al.* A novel histone acetyltransferase inhibitor modulating Gcn5 network: cyclopentylidene-[4-(4'-chlorophenyl)thiazol-2-yl)hydrazone. J Med Chem 2009;52:530-6.
78. Balasubramanyam K, Swaminathan V, Ranganathan A, Kundu TK. Small molecule modulators of histone acetyltransferase p300. J. Biol. Chem. 2003;278:19134–19140.
79. Sung B, Pandey MK, Ahn KS, *et al.* Anacardic acid (6-nonadecyl salicylic acid), an inhibitor of histone acetyltransferase, suppresses expression of nuclear factor-kappaB-regulated gene products involved in cell survival, proliferation, invasion, and inflammation through inhibition of the inhibitory subunit of nuclear factor-kappaBalpha kinase, leading to potentiation of apoptosis. Blood 2008;111:4880–4891.
80. Ravindra KC, Selvi BR, Arif M, *et al.* Inhibition of Lysine Acetyltransferase KAT3B/p300 Activity by a Naturally Occurring Hydroxynaphthoquinone, Plumbagin. J. Biol. Chem. 2009;284:24453–24464.
81. Sandur SK, Ichikawa H, Sethi G, Ahn KS, Aggarwal BB. Plumbagin (5-hydroxy-2-methyl-1,4-naphthoquinone) suppresses NF-kappaB activation and NF-kappaB-regulated gene products through modulation of p65 and IkappaBalpha kinase activation, leading to potentiation of apoptosis induced by cytokine and chemotherapeutic agents. J Biol Chem 2006;281:17023-33.
82. Balasubramanyam K, Varier RA, Altaf M, *et al.* Curcumin, a novel p300/CREB-binding protein-specific inhibitor of acetyltransferase, represses the acetylation of histone/nonhistone proteins and histone acetyltransferase-dependent chromatin transcription. J. Biol. Chem. 2004;279:51163–51171.
83. Lin YG, Kunnumakkara AB, Nair A, *et al.* Curcumin inhibits tumor growth and angiogenesis in ovarian carcinoma by targeting the nuclear factor-kappaB pathway. Clin Cancer Res 2007;13:3423-30.
84. Choi KC, Jung MG, Lee YH, *et al.* Epigallocatechin-3-gallate, a histone acetyltransferase inhibitor, inhibits EBV-induced B lymphocyte transformation via suppression of RelA acetylation. Cancer Res 2009;69:583-92.
85. Choi KC, Lee YH, Jung MG, *et al.* Gallic acid suppresses lipopolysaccharide-induced nuclear factor-kappaB signaling by preventing RelA acetylation in A549 lung cancer cells. Mol Cancer Res 2009;7:2011-21.
86. Adachi S, Shimizu M, Shirakami Y, *et al.* (-)-Epigallocatechin gallate downregulates EGF receptor via phosphorylation at Ser1046/1047 by p38 MAPK in colon cancer cells. Carcinogenesis 2009;30:1544-52.
87. Balasubramanyam K, Altaf M, Varier RA, *et al.* Polyisoprenylated benzophenone, garcinol, a natural histone acetyltransferase inhibitor, represses chromatin transcription and alters global gene expression. J. Biol. Chem. 2004;279:33716–33726.
88. Ahmad A, Wang Z, Ali R, *et al.* Apoptosis-inducing effect of garcinol is mediated by NF-kappaB signaling in breast cancer cells. J Cell Biochem 2010;109:1134-41.
89. Mantelingu K, Reddy BA, Swaminathan V, *et al.* Specific inhibition of p300-HAT alters global gene expression and represses HIV replication. Chem. Biol. 2007;14:645–657.
90. Berger SL. Histone Modifications in trascriptional regulation. Curr. Opin. Genet. Dev. 2002;12:142–148.

91. Strahl BD, Allis CD. The language of covalent histone modifications. Nature 2000;403:41-5.
92. Margueron R, Trojer P, Reinberg D. The key to development: interpreting the histone code? Curr. Opin. Genet. Dev. 2005;15:163-76.
93. Biel M, Wascholowsku V, Giannis A. Epigenetics-An epicenter of gene regulation: Histones and Histone-modifying enzymes. Angew. Chem. Int. Ed. 2005;44:3186–3216.
94. Yang X. The divers superfamily of lysine acetyltransferases and their roles in leukemia and other disease. Nucleic Acids Res. 2004;32:959–976.
95. Vetting MW, S de Carvalho LP, Yu M, *et al.* Structure and functions of the GNAT superfamily of acetyltransferases. Arch Biochem Biophys 2005;433:212-26.
96. Schiltz RL, Nakatani Y. Biochim. Biophys. ActA 2000;37:1470.
97. Heery DM, Fischer PM. Pharmacological targeting of lysine acetyltransferases in human disease: a progress report. Drug Discov. Today 2007;12:88.
98. Cheung P, Tanner KG, Cheung WL, Sassone-Corsi P, Denu JM, Allis CD. Synergistic coupling of histone H3 phosphorylation and acetylation in response to epidermal growth factor stimulation. Mol Cell 2000;5:905-15.
99. Howe L, Auston D, Grant P, *et al.* Histone H3 specific acetyltransferases are essential for cell cycle progression. Genes Dev 2001;15:3144-54.
100. Nagy Z, Tora L. Distinct GCN5/PCAF-containing complexes function as co-activators and are involved in transcription factor and global histone acetylation. Oncogene 2007;26:5341-57.
101. Schiltz RL, Nakatani Y. The PCAF acetylase complex as a potential tumor suppressor. Biochim Biophys Acta 2000;1470:M37-53.
102. Biel M, Kretsovali A, Karatzali E, Papamatheakis J, Giannis A. Design, Synthesis and biological Evaluation of a Smal-Molecule Inhibitor of the Histone Acetyltransferase Gcn5. Angew. Chem. Int. Ed. 2004;43:3974–3976.
103. Clerici F, Contini A, Gelmi ML, Pocar D. Isothiazoles. Part 14: new 3-aminosubstituted isothiazole dioxides and their mono- and dihalogeno derivates. Tetrahedron 2003;59:9399–9408.
104. Clements A, Rojas JR, Trievel RC, Wang L, Berger SL, Marmorstein R. Crystal structure of the histone acetyltransferase domain of the human PCAF transcriptional regulator bound to coenzyme A. EMBO J. 1999;18:3521–3532.
105. Hodawadekar SC, Marmorstein R. Chemistry of acetyl transfer by histone modifying enzymes: structure, mechanism and implications for effector design. Oncogene 2007;26:5528-40.
106. Trievel RC, Rojas JR, Sterner DE, *et al.* Crystal structure and mechanism of histone acetylation of the yeast GCN5 transcriptional coactivator. Proc Natl Acad Sci U S A 1999;96:8931-6.
107. Dekker FJ, Koch MA, Waldmann H. Protein structure similarity clustering (PSSC) and natural product structure as inspiration sources for drug development and chemical genomics. Curr. Opin. Chem. Biol. 2005;9:232–239.
108. Poux AN. Structure of the GCN5 histone acetyltransferase bound to a bisubstrate inhibitor. PNAS 2002;99:14065-70.
109. Lewis SN, Miller GA, Hausman M, Szamborski EC. Isopthiazoles IV: 4-Isothiazolin-3-one 1-Oxide and 1,1-Dioxides. J. Heterocycl. Chem. 1971;81:591.

110. Lewis SN, Miller GA, Szamborski EC, Hausman M. Isothiazoles III: 2-Carbamoyl-4-isothiazolin-3-ones. J. Heterocycl. Chem. 1971;81:587.
111. Nadel A, Palinkas J. New 2-Methylisothiazolones. J. Heterocyclic. Chem. 2000;37:1463-9.
112. Trievel RC, Li F, Marmorstein R. Application of a fluorescent Histone Acetyltransferase Assay to probe the substrate specificity of the Human p300/CBP-Associated Factor. Anal. Biochem. 2000;287:319-28.
113. Alvarez-Sánchez R, Basketter D, Pease C, Lepoittevin J. Studies of Chemical Selectivity of Hapten, Reactivity, and Skin Sensitization Potency. 3. Synthesis and Studies on the Reactivity toward Model Nucleophiles of the 13C-Labeled Skin Sensitizers, 5-Chloro-2methylisothiazolo-3-one (MCI) and 2-Methylisothiazol-3-one (MI). Chem. Res. Toxicol. 2003;16:627-36.
114. Root DE, Flaherty SP, Kelley BP, Stockwell BR. Biological mechanism profiling using an annotated compound library. Chem Biol 2003;10:881-92.
115. Basketter DA, Rodford R, Kimber I, Smith I, Wahlberg JE. Skin sensitization risk assessment: a comparative evaluation of 3 isothiazolinone biocides. Contact Dermatitis 1999;40:150-4.
116. Thomsen R, Christensen MH. MolDock: a new technique for high-accuracy molecular docking. J Med Chem 2006;49:3315-21.
117. Balamurugan R, Dekker FJ, Waldmann H. Design of compound libraries based on natural product scaffolds and protein structure similarity clustering (PSSC). Mol. BioSyst. 2005;1:36-45.
118. Barnes PJ, Adcock IM, Ito K. Histone acetylation and deacetylation: importance in inflammatory lung diseases. Eur. Respir. J. 2005;25:552–563.
119. Gorsuch S, Bavetsias V, Rowlands MG, *et al.* Synthesis of isothiazol-3-one derivatives as inhibitors of histone acetyltransferase (HATs). Bioorg. Med. Chem. 2009;17:467-74.
120. Dekker FJ, Ghizzoni M, van der Meer N, Wisastra R, Haisma HJ. Inhibition of PCAF histone acetyl tranferase and cell proliferation by isothiazolones. Bioorg. Med. Chem. 2009;17:460–466.
121. Yue EW, Wayland B, Douty B, *et al.* Isothiazolidinone heterocycles as inhibitors of protein tyrosine phosphatases: synthesis and structure-activity relationship of a peptide scaffold. Bioorg. Med. Chem. 2006;14:5833-49.
122. Combs AP, Glass B, Galya LG, Li M. Asymemetric Synthesis of the (S)-1,1-Dioxido-isothiazolidin-3-ones Phosphotyrosine Mimetic via Reduction of a Homochiral (R)-Oxido-isothiazolidin-3-one. Org. Lett. 2007;9:1279-82.
123. Lee HS, Kim DH. Synthesys and evaluation of disubstituted-3-mercaptopropanoic acids as inhibitors for carboxypeptidase A and implications with respect to enzyme inhibitor design. Bioorg. Med. Chem. 2003;11:4685–4691.
124. Collier PJ, Austin P, Gilbert P. Uptake and distribution of some isothiazolone biocides into *Escherichia Coli* ATCC 8739 and *Schizosaccharomyces pombe* NCYC 1354. Int. J. Pharm. 1990;66:201-6.
125. Trevillyan JM, Chiou XG, Ballaron SJ, *et al.* Inhibition of p56 ^{lck} Tyrosine Kinase by Isothiazolones. Arch. Biochem. Biophys. 1999;364:19–29.
126. Morley OJ, Kapur AJO, Charlton MH. Kinetic studies on the reactions of 3-isothiazolones with 2-methyl-2-propanethiol. Int J Chem Kinet 2007;39:254-360.

127. Goblyos A, de Vries H, Brussee J, IJzerman AP. Synthesis and biological evaluation of a new series of 2,3,5-substituted [1,2,4]-thiadiazoles as modulators of adenosine A_1 Receptors and their molecular mechanism of action. J. Med. Chem. 2005;48:1145-51.
128. Dekker FJ, Haisma HJ. Histone acetyl transferases as emerging drug targets. Drug Discov. Today 2009;14:942–948.
129. Ghizzoni M, Haisma HJ, Dekker FJ. Reactivity of isothiazolones and isothiazolone-1-oxides in the inhibition of the PCAF histone acetyltransferase. Eur. J. Med. Chem. 2009;44:4855–4861.
130. Souto JA, Conte M, Alvarez R, *et al.* Synthesis of benzamides related to anacardic acid and their histone acetyltransferase (HAT) inhibitory activities. ChemMedChem 2008;3:1435–1442.
131. Green IR, Tocoli FE, Lee SH, Nihei K, Kubo I. Molecular design of anti-MRSA agents based on the anacardic acid scaffold. Bioorg. Med. Chem. 2007;15:6236–6241.
132. Hird NW, Milner PH. Synthesis and ß-lactamase inhibition of anacardic acids and their analogues. Bioorg. Med. Chem. Lett. 1994;4:1423–1428.
133. Yamagiwa Y, Ohashi K, Sakamota Y, Hirakawa S, Kamikawa T, Kubo I. Syntheses of anacardic acids and ginkgoic acid. Tetrahedron 1987;43:3387–3394.
134. Uchiyama M, Ozawa H, Takuma K, *et al.* Regiocontrolled Intramolecular Cyclizations of Carboxylic Acids to Carbon-Carbon Triple Bonds Promoted by Acid or Base Catalyst. Org. Lett. 2006;8:5517–5520.
135. Fellermeier M, Zenk MH. Prenylation of olivetolate by a hemp transferase yields cannabigerolic acid, the precursor of tetrahydrocannabinol. FEBS Lett. 1998;427:283–285.
136. Dushin GR, Danishefsky SJ. Total syntheses of KS-501, KS-502, and their enantiomers. J. Am. Chem. Soc. 1992;114:655–659.
137. Kaeding WW. Oxidation of Aromatic Acids. IV. Decarboxylation of Salicylic Acids. J. Org. Chem. 1964;29:2556–2559.
138. Tranchimand S, Tron T, C. G, G. I. First Chemical Synthesis of Three Natural Depsides Involved in Flavonol Catabolism and Related to Quercetinase Catalysis. Synth. Commun. 2006;36:587–597.
139. Duan Q, Chen H, Costa M, Dai W. Phosphorylation of H3S10 blocks the access of H3K9 by specific antibodies and histone methyltransferase. Implication in regulating chromatin dynamics and epigenetic inheritance during mitosis. J. Biol. Chem. 2008;283:33585–33590.
140. Korb O, Stutzle T, Exner TE. Empirical scoring functions for advanced protein-ligand docking with PLANTS. J. Chem. Inf. Model 2009;49:84–96.
141. Korb O, Stützle T, Exner TE. An Ant Colony Optimization Approach to Flexible Protein-Ligand Docking. Swarm Intell. 2007;1:115–134.
142. Sullivan JT, Richards CS, Lloyd HA, Krishna G. Anacardic acid: molluscicide in cashew nut shell liquid. Planta Med 1982;44:175-7.
143. Rea AI, Schmidt JM, Setzer WN, Sibanda S, Taylor C, Gwebu ET. Cytotoxic activity of Ozoroa insignis from Zimbabwe. Fitoterapia 2003;74:732-5.
144. Trevisan MT, Pfundstein B, Haubner R, *et al.* Characterization of alkyl phenols in cashew (Anacardium occidentale) products and assay of their antioxidant capacity. Food Chem Toxicol 2006;44:188-97.
145. Kubo I, Kinst-Hori I, Yokokawa Y. Tyrosinase inhibitors from Anacardium occidentale fruits. J Nat Prod 1994;57:545-51.

146. Paramashivappa R, Phani Kumar P, Subba Rao PV, Srinivasa Rao A. Design, synthesis and biological evaluation of benzimidazole/benzothiazole and benzoxazole derivatives as cyclooxygenase inhibitors. Bioorg Med Chem Lett 2003;13:657-60.
147. Ha TJ, Kubo I. Lipoxygenase inhibitory activity of anacardic acids. J Agric Food Chem 2005;53:4350-4.
148. Ghizzoni M, Boltjes A, Graaf C, Haisma HJ, Dekker FJ. Improved inhibition of the histone acetyltransferase PCAF by an anacardic acid derivative. Bioorg Med Chem 2010;18:5826-34.
149. Eliseeva ED, Valkov V, Jung M, Jung MO. Characterization of novel inhibitors of histone acetyltransferases. Mol. Cancer Ther. 2007;6:2391.
150. Shogren-Knaak M, Ishii H, Sun JM, Pazin MJ, Davie JR, Peterson CL. Histone H4-K16 acetylation controls chromatin structure and protein interactions. Science 2006;311:844-7.
151. Faiola F, Liu X, Lo S, *et al.* Dual regulation of c-Myc by p300 via acetylation-dependent control of Myc protein turnover and coactivation of Myc-induced transcription. Mol Cell Biol 2005;25:10220-34.
152. Daujat S, Bauer UM, Shah V, Turner B, Berger S, Kouzarides T. Crosstalk between CARM1 methylation and CBP acetylation on histone H3. Curr Biol 2002;12:2090-7.
153. Zhao S, Xu W, Jiang W, *et al.* Regulation of cellular metabolism by protein lysine acetylation. Science 2010;327:1000-4.
154. Wang Q, Zhang Y, Yang C, *et al.* Acetylation of metabolic enzymes coordinates carbon source utilization and metabolic flux. Science 2010;327:1004-7.
155. Yang XJ. The diverse superfamily of lysine acetyltransferases and their roles in leukemia and other diseases. Nucleic Acids Res 2004;32:959-76.
156. Ghizzoni M, Haisma HJ, Maarsingh H, Dekker FJ. Histone acetyltransferases are crucial regulators in NF-kappaB mediated inflammation. Drug Discov Today 2011;16:504-11.
157. Suzuki T, Miyata N. Epigenetic control using natural products and synthetic molecules. Curr Med Chem 2006;13:935-58.
158. Zheng YG, Wu J, Chen Z, Goodman M. Chemical regulation of epigenetic modifications: opportunities for new cancer therapy. Med Res Rev 2008;28:645-87.
159. Sun Y, Jiang X, Chen S, Price BD. Inhibition of histone acetyltransferase activity by anacardic acid sensitizes tumor cells to ionizing radiation. FEBS Lett 2006;580:4353-6.
160. Cui L, Miao J, Furuya T, *et al.* Histone acetyltransferase inhibitor anacardic acid causes changes in global expression during in vitro *plasmodium falciparum* development. Eukaryiotic cell 2008;7:1200–1210.
161. Sbardella G, Castellano S, Vicidomini C, *et al.* Identification of long chain alkylidenemalonates as novel small molecule modulators of histone acetyltransferases. Bioorg. Med. Chem. Lett. 2008;18:2788-92.
162. Souto JA, Benedetti R, Otto K, *et al.* New anacardic acid-inspired benzamides: histone lysine acetyltransferase activators. ChemMedChem 2010;5:1530-40.
163. Altschul SF, Madden TL, Schaffer AA, *et al.* Gapped BLAST and PSI-BLAST: a new generation of protein database search programs. Nucleic Acids Res 1997;25:3389-402.
164. Dignam JD, Lebovitz RM, Roeder RG. Accurate transcription initiation by RNA polymerase II in a soluble extract from isolated mammalian nuclei. Nucleic Acids Res 1983;11:1475-89.

Acknowledgments

This thesis would not have been the same without the contribution of many people with whom I have had the privilege to share my work and life. I am really happy to have now an opportunity to express my gratitude to all of you.

First of all, I would like to acknowledge my gratitude to my promoter Prof. Hidde Haisma, who offered me a Ph.D. position in his group four years ago. Although not very frequent, our meetings have always been particularly helpful for me. And with him, I would like to thank my co-promoter Dr. Frank Dekker, who has been a constant guide during these four years. Thanks to your help, I improved my theoretical and practical skills, and I learned a lot.

Further, I am thankful to the members of the reading committee, Prof. dr. R.P.H. Bischoff, Prof. dr. R.M.J. Liskamp and Prof. dr. A.J. Minnaard, for the time and effort they invested in reviewing this thesis.

Many thanks to the people I had the pleasure to work within the Department of Pharmaceutical Gene Modulation: Anja, Anna Rita, Gera, Marije and Petra. It was curious to see how, although we worked in the same group, we had completely different backgrounds and projects. I am sorry if you had to struggle to understand my presentations during our group meetings, but I had the same problem with yours. Thanks to our secretary Janine for helping me with all kind of papers and for sending my compounds. Special thanks to Rosalina with whom I shared the experience of being a Ph.D. student and a foreigner. I wish you good luck with your own thesis.

I also would like to thank the members of the Medicinal Chemistry Department, with whom I shared not only the laboratory, but also problems, solutions and advice during the first part of my Ph.D.: Prof. Durk Dijkstra, Dr. Cor Grol, André, Jeroen and Ulrike. Thank you also for the many coffee and lunch breaks we spent together, a nice opportunity for relaxing talks.

And of course my paranymphs… Sara and Hoeke, thank you for all the trips (especially the weekends in Friesland), dinners (Sara for the pasta and Hoeke for the meat), games etc.…I enjoy very much the time we spend together and I hope we will have the possibility to do more of these things in the future. Sara, thank you also for introducing me to Groningen four years ago: through you I found friends, a house, my future wife…could you also find a job for me?

Big thanks to my friends, who made my time in Groningen enjoyable. Unfortunately, many of you have already left and I can only wish you good luck with your new life and I hope we will keep in touch. Luckily, some of you are still here and I hope we will have the possibility to continue our friendship.

I would like to acknowledge my gratitude to the Dagys family. Thanks for making my journeys to the beautiful Lithuania always interesting and enjoyable.

Special thanks to my family, mamma, papá e Clotilde per aver supportato e sopportato la mia partenza per l'Olanda e per essermi stati comunque vicini in questi anni. Grazie anche per essere venuti a trovarmi a Groningen.

Girste, the list of thanks for you would be longer than the thesis itself. Therefore, I will print it separately and give you one copy later. Meanwhile, I just say that you have been the most important person of my Ph.D. experience and I am sure you will be the most important person of the rest of my life. Thank you for existing and for being with me.

Massimo

Curriculum vitae and list of publications

Massimo Ghizzoni was born on the 25th of September 1981 in Lagonegro (PZ), a small town in Basilicata, south of Italy. He grew up in Lagonegro where he completed his pre-university education (Scientific Lyceum) in 2000. He moved then to Napoli where he studied Pharmaceutical Chemistry and Technologies at the University "Federico II". He graduated in October 2005 with a thesis entitled "Development of new peptide ligands for HER2 receptor". In December 2005, he obtained the licence for the professional qualification of pharmacist. Afterwards, he was selected for the research programme "Leonardo da Vinci – Unipharma Graduates II" and he performed an internship at Sanofi-Aventis (Frankfurt am Main, Germany) from September 2006 to March 2007, where he worked on the development of new methods for synthesizing fluorinated compounds. In January 2008 he moved to Groningen where he started his Ph.D. project, the results of which are presented in this thesis.

- **Ghizzoni M**, Haisma HJ, Dekker FJ; Reactivity of isothiazolones and isothiazolone-1-oxides in the inhibition of the PCAF histone acetyltransferase, *Eur J Med Chem* 2009, 44(12):4855-61.
- **Ghizzoni M**, Boltjes A, Graaf C, Haisma HJ, Dekker FJ; Improved inhibition of the histone acetyltransferase PCAF by an anacardic acid derivative, *Bioorg Med Chem* 2010, 18(16):5826-34.
- **Ghizzoni M**, Haisma HJ, Maarsingh H, Dekker FJ; Histone acetyltransferases are crucial regulators in NF-κB mediated inflammation, *Drug Discov Today* 2011, 16(11-12):504-11.
- Dekker FJ, **Ghizzoni M**, van der Meer N, Wisastra R, Haisma HJ; Inhibition of the PCAF histone acetyl transferase and cell proliferation by isothiazolones, *Bioorg Med Chem* 2009, 17(2):460-6.
- Wisastra R, **Ghizzoni M**, Maarsingh H, Minnaard AJ, Haisma HJ, Dekker FJ; Isothiazolones; thiolreactive inhibitors of cysteine protease cathepsin B and histone acetyltransferase PCAF, *Org Biomol Chem* 2011, 9(6):1817-22.
- **Ghizzoni M**,* Wu J,* Gao T, Haisma HJ, Dekker FJ, Zheng YG; 6-alkylsalicylates are selective Tip60 inhibitors and bind competitive to acetyl-CoA, *Submitted for publication* 2011